Doctoral Thesis
博士論文

Dependable and Energy Efficient QoS Control System
for Medical Wireless Body Area Networks
医療用無線ボディエリアネットワークのための
高信頼・エネルギー高効率な QoS 制御システム

March 24, 2017
2017 年 3 月 24 日

14SD106
Kento TAKABAYASHI
高林 健人

Supervisor: Professor Ryuji KOHNO
指導教官： 河野隆二 教授

Department of Physics, Electrical & Computer Engineering,
Graduate School of Engineering,
Yokohama National University
Kohno Laboratory
横浜国立大学大学院 工学府 物理情報工学専攻 河野研究室

Table of Contents

List of Figures

List of Tables

Acknowledgements

Abstract

The ratio between the old and young in the global population is more rapidly increasing than that in the past. This is raising concerns regarding the increasing cost of medical care. It is also thought that people will become increasingly health conscious in the future. Meanwhile, portable devices such as smart phones, tablets, and wearable devices have become widespread. Health monitoring systems employing wearable vital sensors and using wireless communication (also known as m-health or m-IoT) have received significant attention in recent years. It is expected that m-IoT will allow continuous monitoring of the user's physical condition and help preempt serious illnesses. In the field of m-IoT systems, the wireless body area networks (WBANs) is a key technology. Extensive work on the standardization of such systems has been carried out.

In a WBAN system, a wearable vital sensor node can use a range of sensor types, all of which have different data rates. The allowable communication error ratio or delay depends on the application used. IEEE Std. 802.15.6 defines eight levels of user priorities. The Quality of Service (QoS) control must ensure that different types of data can be communicated as efficiently as possible at a satisfactory quality level. The optimal QoS control of input data is therefore an important factor in sensor data transmission.

To address this requirement, we have proposed an optimal QoS control scheme employing a multiplexing layer for priority scheduling and a decomposable error control coding scheme that can adapt to varying channel conditions. The multiplexing module controls the different types of QoS requirements such as required error ratio and delay according to the following priorities by changing the number of data copies of Weldon's ARQ and combination of decomposable codes. The target WBAN is a wearable device comprising multiple sensors whose output data is transmitted using a common medium access control (MAC) and phisical (PHY) layer. Simulations are conducted to evaluate the performance of the proposed system and to compare its performance with that of a system based on IEEE 802.15.6. Then, we present a theoretical analysis and

optimization of the proposed method, and derive a lower bound on throughput and an upper bound on the residual bit error rate for both the proposed system and the standard system.

In addition, several performances of the proposed scheme are evaluated in a multiple WBANs environment, representing a more practical situation. A further study investigate the energy efficiency of the proposed scheme using computer simulations. Energy efficiency is an important factor because WBAN nodes are small and their battery capacity is limited. To complete the performance evaluation of the proposed scheme, this study quantitatively evaluate the RBER and energy efficiency of our proposed system under a WBANs channel model not only in a general case, but also in the worst-case scenario.

Furthermore, we evaluate some performances of our QoS control scheme in the case of a multi-hop WBAN based on IEEE Std. 802.15.6. IEEE Std. 802.15.6 supports a two-hop extension. Then, a WBAN extended to multihop communication is studied in order to increase the lifetime of a WBAN. However, many studies of a multihop WBAN focus on an energy-efficient MAC or routing protocol, and then they do not consider an error controlling. As a result of computer simulations, our proposed scheme has better performances than the standard scheme. Then, numeral results show both systems have the best performance in case that communication distance on the first hop is equal to that on the second hop.

Finally, we analyze and optimize performance of our QoS control scheme in a cross-layer design for WBANs. A cross-layer approach is one of the most important technique in order to optimize satisfied QoS of various types of data. In this study, we focus on cross-layer design between PHY and MAC layers. Slotted ALOHA is focused on as a random access protocol, because slotted ALOHA is adopted in UWB-PHY of IEEE802.15.6 and Smart BAN. Then, TDMA (Time Division Multiple Access) is considered as a scheduled access protocol. Numerical results show our proposed scheme has better performances than the standard scheme. Additionally, the case utilizing a schedule access protocol has basically better performances than a random access protocol except delay performance.

In the final chapter, we conclude our doctoral thesis, and then describe future work and prospects about this study and a related research field.

あらまし

　近年の先進国における高齢人口の急速な増加や生産年齢人口の減少，それに伴った医療費の高額化などが世界的な社会問題となりつつある．そのため，多くの人々が可能な限り長く健康を維持し，自立して暮らすことができ，病気になっても質の高い医療・福祉サービスを享受し，住み慣れた地域で安心して暮らすことができることに加え，経済成長をも成し遂げることができる社会の実現が重要となっている．ところで，自動車・家電・ロボット・施設などあらゆるモノがセンサと無線通信機能を搭載してインターネットにつながり，情報のやり取りをすることで，モノのデータ化やそれに基づく自動化等が進展し，新たな付加価値を生み出す「モノのインターネット」（IoT : Internet of Things）が近年大きな注目を集めている．とりわけ，上記のような社会情勢から，体内外に装着したバイタルセンサやカプセル内視鏡などの医療・ヘルスケア機器・ロボットを用いた在宅医療や遠隔医療システムを構築するための医療・ヘルスケア IoT に注目が集まっている．例えば，2012 年には医療・ヘルスケア IoT システムの一つとして知られる「無線ボディエリアネットワーク」(WBANs : Wireless Body Area Networks) の標準規格の一つである「IEEE802.15.6」が策定された．また，欧州における標準化組織である欧州電気通信標準化機構 (ETSI : European Telecommunications Standards Institute) においても，Smart Body Area Networks (Smart BAN) の標準化が進められている．これらの規格では取り扱うデータに対して数段階の優先度を設定することが可能になっている．しかしながら，これらの優先度に応じた QoS（Quality of Service）の具体的な制御手段は実装依存である．また本研究の対象としている IEEE802.15.6 の超広帯域（UWB : Ultra Wide Band）無線システムでは，物理層において二つのモード（default mode と High QoS mode）が定められているだけである．一般に，WBANs ではヘルスケアに必要なバイタルデータや医療機器の制御データといったデータの他，スポーツ用途やエンターテイメント用途，ネットワーク制御用データなどの幅広いデータを扱う．しかしながら，これらのデータに要求される QoS は各々大きく異なっており，現在の規格では十分対応しきれない．

　そこで，私は WBANs における複数データの優先度に合わせた QoS 実現手法についてこれまで研究してきた．具体的には、WBANs の国際標準規格である

IEEE802.15.6 の UWB-PHY で規定されている default mode（Hybrid ARQ を用いないモード）においても Hybrid ARQ を適用し，優先度毎に ARQ（Automatic Repeat reQuest）や FEC（Forward Error Correction）の使い方を選択できるように修正を施すことで QoS パラメータの有効活用を行えるようにした．この際，複数のデータを同時に扱えるように multiplexing layer を設け，この層に設置した MUX コントローラが事前に設定された QoS パラメータに従い誤り制御や遅延制御を行う．加えて，誤り訂正符号として Decomposable code，再送プロトコルとして Weldon's ARQ と呼ばれる手法を用いた．この提案方式では、Weldon's ARQ のデータコピーの数や Decomposable codes の組み合わせ方により，異なる QoS を持つデータが多重化して送られるシステムにおいて，必要とされる QoS の制御が可能となった．加えて，この方式の理論解析と最適化を行った．また，より現実的な環境として複数の WBANs が共存し，互いに干渉を与えてくる環境を想定した場合の評価も行った．この際，Decomposable codes の組み合わせ方を拡張してより低符号化率の誤り訂正符号を構成出来るようにしたことにより，誤り訂正能力を向上させて，より強力な干渉が与えられた場合でも高信頼性を持たせた．加えて，本 QoS 制御方式の Energy Efficiency(消費電力あたりのスループット) を幾つかの変調方式において評価した．Energy Efficiency とは，単位エネルギーに対して，どの程度の情報量を正確に送れるかを測る指標である．無線ボディエリアネットワークではノードは非常に小さく，同時にバッテリー容量も小さいことが想定される．そのため，Energy Efficiency を評価することは非常に重要である．スケジュールアクセス方式の MAC プロトコルを想定し，計算機シミュレーションにより，結果として標準規格と比較して各々の QoS を柔軟に満たすことが出来，なおかつ最悪ケースにおける特性保障が出来ることも示せた．

　また，IEEE802.15.6 で規定されている 2 ホップ通信を適用した場合の本方式の性能評価についても行った．本規格ではハブ-ノード間のシングルホップによる通信が不可能な場合に備えて，他のノードを一度だけ経由することができる．しかしながら，多くのマルチホップ WBAN の研究では，低消費電力な MAC プロトコルやルーティング手法が主な対象であり，誤り制御方式についての研究は少ない．加えて，IEEE802.15.6 を基にしたマルチホップ WBAN の性能評価も少ない．本研究では，IEEE802.15.6 に基づいた 2 ホップまで拡張された WBAN における，我々が提案してきた QoS 制御方式と標準規格の通信距離に関する性能評価を異なる優先度のデータにおいて行った．この際，提案方式においては，事前に設定されたパラメータに基づいて再送を行う方式と，プリアンブルを用いて推定したチャネル SNR を用いて各データの QoS に基づいた誤り訂正符号の符号化率を設定した場合とで比較した．計算機シミュレーションの結果，プリアンブルから推定したチャネル SNR から誤り訂正符号の符号化率を決定した方式を用い，2 ホップとも

同じ距離で通信を行った場合の特性が最も良いことが確認できた．

　最後に，本 QoS 制御方式における，異なる MAC プロトコルを適用した際のクロスレイヤでの性能解析と最適化を行った．クロスレイヤでのアプローチは，様々な種類のデータの QoS を最適化する上では重要な手法の一つである．これまでの研究ではスケジュールアクセス方式の MAC プロトコルを前提に考えてきたが，IEEE802.15.6 ではランダムアクセス方式とのハイブリッド MAC プロトコルが適用されている．そのため，各 MAC プロトコルにおける自らの提案 QoS 制御方式を物理層・MAC 層のクロスレイヤで評価・解析を行った．ランダムアクセス方式には slotted ALOHA を想定する．これは，IEEE802.15.6 の UWB-PHY や Smart BAN での適用が想定されているためである．また，スケジュールアクセス方式には解析の単純化のため TDMA を想定した．性能解析の結果，基本的にはスケジュールアクセス方式の方が良い特性が得られ，ランダムアクセス方式における限界値も確認できた．加えて，ある条件化での最大送信回数の最小値も求めることができた．

　第 1 章では本研究の背景，目的について述べた後，本論分の章構成について説明する．第 2 章では IEEE802.15.6 における，本研究との関連事項について述べる．第 3 章では本論文におけるシステムモデルについて述べる．第 4 章では，本論文における提案 QoS 制御方式について述べ，次の章でその理論解析と最適化について述べる．第 6 章ではこの方式における Decomposable codes の拡張について述べ，より現実的な環境における Energy Efficiency を含めた性能評価について述べる．さらに第 7 章は IEEE802.15.6 で規定されている 2 ホップ通信を適用した場合の本方式の性能評価について述べる．続く章では，本方式における PHY-MAC でのクロスレイヤ解析について説明する．最後に本論文をまとめ，今後の研究課題と将来への展望について述べる．

Chapter 1

Introduction

The ratio between the old and young in the global population is more rapidly increasing than that in the past. This is raising concerns regarding the increasing cost of medical care. It is also thought that people will become increasingly health conscious in the future. Meanwhile, portable devices such as smart phones, tablets, and wearable devices have become widespread. Health monitoring systems employing wearable vital sensors and using wireless communication (also known as m-health or m-IoT) have received significant attention in recent years [1]-[21]. It is expected that m-IoT will allow continuous monitoring of the user's physical condition and help preempt serious illnesses. In the field of m-IoT systems, the wireless body area network (WBAN) is a key technology [1]-[21]. Extensive work on the standardization of such systems has been carried out [22]-[24].

To realize smaller sensor devices and longer battery life, the following technical requirements should be considered.

- Ultra-low power consumption Although this has been considered in the above standards, substantially lower power-consuming media access control (MAC) and physical layer (PHY) technologies are required.

- Coexistence with other networks The 2.4 GHz industrial, scientific, and medical (ISM) band is globally assigned for common use in local area network (LAN) and personal area network (PAN) devices. This frequency band is potentially a good candidate for BANs; however, when using this band, interference from other systems must be taken into consideration.

- Optimal quality of service (QoS) control In a WBAN system, a wearable vital sensor node can use a range of sensor types, all of which have different data rates. The allowable communication error ratio or delay depends

on the application used. IEEE Std. 802.15.6 defines eight levels of user priorities, as shown in Table 1.1 [22]. QoS control must ensure that different types of data can be communicated as efficiently as possible at a satisfactory quality level. The optimal QoS control of input data is therefore an important factor in sensor data transmission.

Table 1.1   Quality of service for IEEE802.15.6.

User priority	Traffic designation	Frame type
0	Background (BK)	data
1	Best effort (BE)	data
2	Excellent effort (EE)	data
3	Video (VI)	data
4	Voice (VO)	data
5	Medical data or network control	data or management
6	High priority medical data or network control	data or management
7	Emergency or medical event report	data

To address this requirement, we have proposed an optimal QoS control scheme employing a multiplexing layer for priority scheduling and a decomposable error control coding scheme that can adapt to varying channel conditions. The multiplexing module controls the different types of QoS requirements such as required error ratio and delay according to the following priorities by changing the number of data copies of Weldon's ARQ and combination of decomposable codes. The target WBAN is a wearable device comprising multiple sensors whose output data is transmitted using a common medium access control (MAC) and phisical (PHY) layer. Simulations are conducted to evaluate the performance of the proposed system and to compare its performance with that of a system based on IEEE 802.15.6. Then, we present a theoretical analysis of the proposed method, and derive a lower bound on throughput and an upper bound on the residual bit error rate for both the proposed system and the standard system in the additive white gaussian noise (AWGN) and the Rayleigh fading channel case.

In addition, several performances of the proposed scheme are evaluated in a multiple WBANs environment, representing a more practical situation. A further study investigate the energy efficiency of the proposed scheme using computer simulations. Energy efficiency is an important factor because WBAN nodes are small and their battery capacity is limited. To complete the perfor-

mance evaluation of the proposed scheme, this study quantitatively evaluate the RBER and energy efficiency of our proposed system under a WBANs channel model not only in a general case, but also in the worst-case scenario.

Furthermore, we evaluate some performances of our QoS control scheme in the case of a multi-hop WBAN based on IEEE Std. 802.15.6. IEEE Std. 802.15.6 supports a two-hop extension. Then, a WBAN extended to multihop communication is studied in order to increase the lifetime of a WBAN. However, many studies of a multihop WBAN focus on an energy-efficient MAC or routing protocol, and then they do not consider an error controlling. As a result of computer simulations, our proposed scheme has better performances than the standard scheme. Then, numeral results show both systems have the best performance in case that communication distance on the first hop is equal to that on the second hop.

Finally, we analyze performance of our QoS control scheme in a cross-layer design for WBANs. A cross-layer approach is one of the most important technique in order to optimize satisfied QoS of various types of data. In this study, we focus on cross-layer design between PHY and MAC layers. Slotted ALOHA is focused on as a random access protocol, because slotted ALOHA is adopted in UWB-PHY of IEEE802.15.6 and Smart BAN. Then, TDMA (Time Division Multiple Access) is considered as a scheduled access protocol. Numerical results show our proposed scheme has better performances than the standard scheme. Additionally, the case utilizing a schedule access protocol has basically better performances than a random access protocol.

This remainder of this thisis is organized as follows. In Chapter 2, we introduce descriptions related to the thesis in IEEE Std. 802.15.6. In Chapter 3, the system model of our proposed scheme is given. Chapter 4 explains our decomposable error correction codes and the working process of our proposed system. In the next chapter, the theoretical analysis and optimization of our proposed scheme under the AWGN channel and the Rayleigh fading channel is also described. The structure of extended decomposable codes and the results of performance evaluations including an energy efficiency using computer simulation in a multiple WBANs environment are given in Chapter 6. Chapter 7 describes a model of a two-hop extension case and the performance evaluation. And then, the cross-layer design and optimization of our proposed scheme and the performacne analysis are explained in the eighth chapter. Finally, we conclude our thesis and provide directions for future work in Chapter 9. The
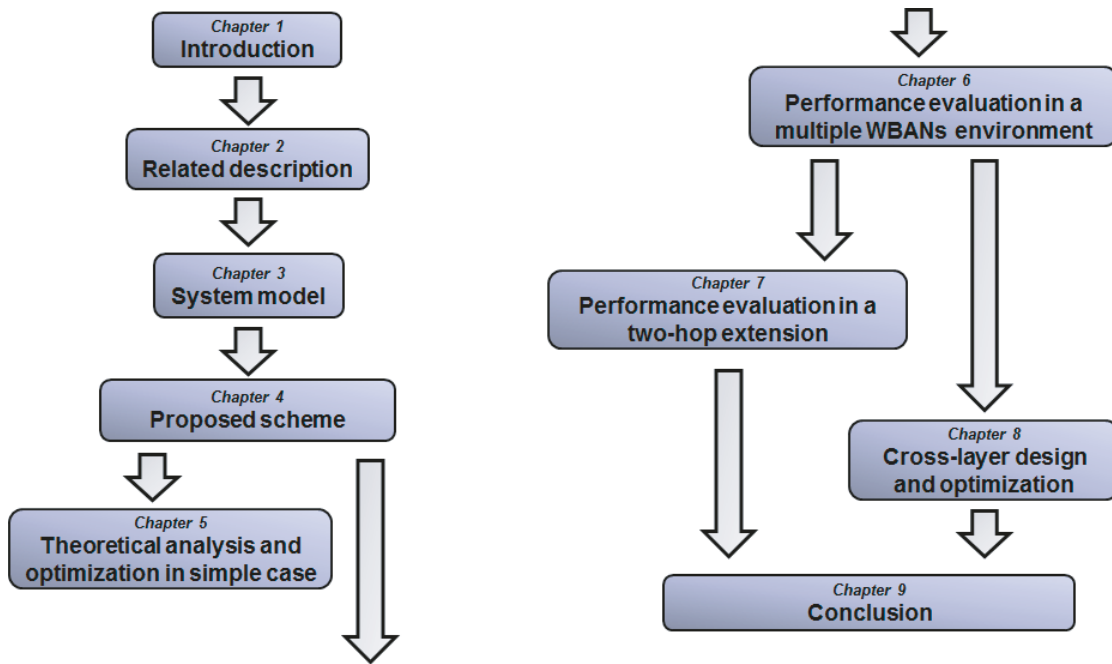
Figure 1.1   The flow chart of this thesis

relations of these chapters can be found in Fig.1.1

Chapter 2

Related descriptions

In this chapter, we describe the relevant parts of IEEE 802.15.6. A more detailed account of IEEE 802.15.6 is presented in [22].

2.1 PHY layer in IEEE802.15.6

The 15.6 Std. defines three PHY layers: narrowband (NB), ultra-wideband (UWB), and human body communications (HBC) like Fig.2.1 [18], [20]-[22].

- NB PHY: In NB communication, multiple nodes are on the body to communicate with other on-body and in-body nodes. NB PHY supports ISM band (863-870 MHz, 902-968 MHz, 950-958 MHz, 2400-2483.5 MHz), Medical Implant Communications Service (MICS) band (402-405 MHz), Wireless Medical Telemetry System (WMTS) band (420-450 MHz, 900 MHz) and Medical Body Area Network (MBAN) band (2360-2400 MHz). Depending on a frequency band, each data rate is different. In order to achieve low power consumption and complexity, three types of differential phase shift keying (DBPSK, DQPSK and D8PSK) and a simple BCH code are applied.

- HBC PHY: The primary technology is electric field coupling which includes capacitive coupling and galvanic coupling. The HBC channel of the capacitive coupling type is developed based on the near electric field around the human body, which is induced by a transmitter terminal, and a receiver terminal is used to detect the weak coupling changes of the near electric field along the body channel. In HBC, the communication range is short and the transmission power is low. However, there are concerns that HBC affects other devices in and out of body. The HBC PHY has a bandwidth of 4 MHz and operates in two frequency bands centered at 16 MHz and 27 MHz.

- UWB PHY: The UWB physical layer is used for communication between on-body devices and for communication between on-body and off-body devices. Transceivers in a UWB PHY generate similar signal power levels to that used in the MICS band and also allow low implementation complexity. In this band the frequency range varies between 3.1GHz and 10.6GHz. Two frequency bands exist in the UWB PHY: high band and low band; each of which are divided into channels with a bandwidth of 499.2 MHz. The low band only has 3 channels: (1-3). Channel 2 is considered as a mandatory channel with the central frequency of 3993.6 MHz. The high band has eight channels: (4-11). Channel seven is considered as a mandatory channel with the central frequency of 7987.2 MHz. All other channels are considered to be optional. At least one of the mandatory channels has to be supported by a UWB device.

In this study, we focused on an impulse radio ultra-wideband PHY layer (IR-UWB-PHY) which offers high data rate transmission, low energy consumption, and good coexistence with other wireless communication systems. In addition, this PHY can support an error correcting code which has various coding rates because of the very wide frequency band. In the UWB-PHY of IEEE 802.15.6, there are two modes of operation: default mode and high QoS mode. The default mode can be used in both medical and non-medical applications. The high QoS mode is for use in medical applications which have a user priority of six.
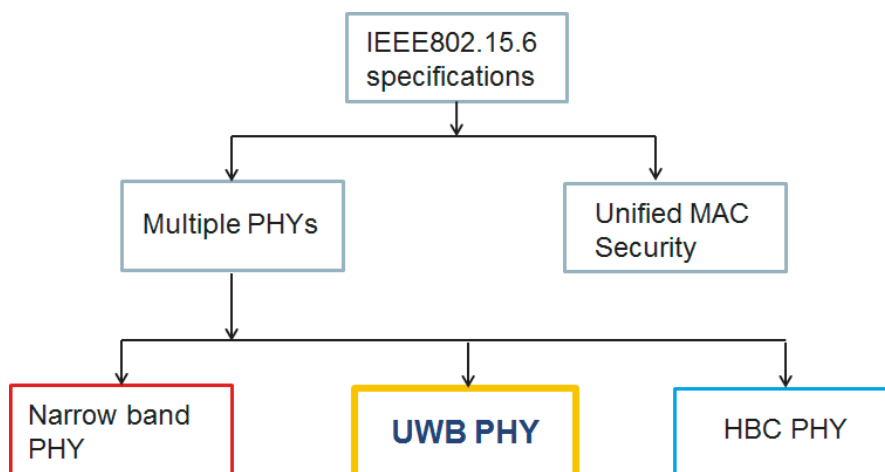
Figure 2.1 PHY layer in 15.6 Std. [22].

2.2 UWB PHY frame format

The UWB PHY frame format is formed by the synchronization header (SHR), the physical layer header (PHR), and the physical layer service data unit (PSDU), respectively, as shown in Figure 2.1 [22]. The PSDU contains the MAC protocol data unit (MPDU) and the BCH parity bits in default mode, while the PSDU contains either the MPDU or BCH parity bits in high QoS mode. The PSDU can therefore be regarded as the payload. The information contained by the PHR includes the data rate of the PSDU and the length of the MAC frame body, and the SHR contains the preamble used for timing synchronization, packet detection and other purposes, and the start-of-frame delimiter (SFD) for frame synchronization. In this research we focused mainly on the performance of the payload (PSDU).
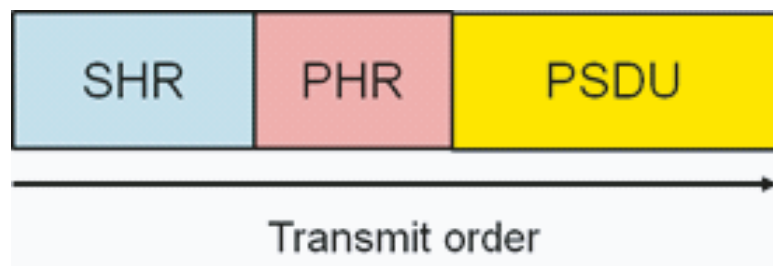
Figure 2.2 UWB PHY frame structure [22].

2.3 Error control scheme for the UWB-PHY

In these modes of operation, the channel codes applied to the PSDU are (63, 51) BCH code in the default mode defined in UWB-PHY and NB-PHY and (126, 63) shortened BCH code in the high QoS mode defined in UWB-PHY. In the high QoS mode, the (126, 63) shortened BCH encoder uses the hybrid ARQ mechanism and the (126, 63) shortened BCH code is derived from the mother code (127, 64) BCH. Hybrid ARQ is defined as the joint use of ARQ and forward error coding (FEC) at the transmitter and/or receiver [25]-[28]. Basically, hybrid ARQ is classified into two types as follows:

- Type I (Chase Combining, CC): This scheme is to send a number of repeats of coded data and decoders combine multiple coded packets before de-

coding. In CC, the same coded packet is retransmitted while the receiver combines several copies to improve the quality of the decoding.

- Type II (Incremental Redundancy, IR): This scheme is to transmit additional redundant information in each retransmission and receiver decode on each retransmission. IR schemes consist to encode the first transmission with a high coding-rate while the following transmissions consist of additional redundancy in order to decrease the code rate seen by the receiver.

The type II hybrid ARQ scheme is used in the high QoS mode. The process can be summarized as follows:

(1) A packet D is encoded with the (126, 63) shortened BCH code. The output of the encoder consists of parity bits P and systematic bits D of the same length. Both D and P are stored at the transmitter, but only D is transmitted. If such a transmitted packet is detected in error by the CRC-16-CCITT code, D is not discarded but is stored at the receiver.

(2) Upon No acknowledgment (N-ACK) at the transmitter, P is transmitted and the information bits are recovered by (126, 63) BCH decoding with the stored D and received P.

(3) If the (126, 63) BCH decoding fails, the D stored at the receiver is discarded and P is stored instead. Upon N-ACK at the transmitter, the previously stored D at the transmitter is sent again.

(4) If such a retransmitted D is detected in error, (126, 63) BCH decoding is applied to the received D and the stored P. If (126, 63) BCH decoding fails and the maximum number of retransmissions has not been reached, the stored P is discarded, the received D is stored, and P is retransmitted upon N-ACK at the transmitter.

(5) This process is repeated until D is successfully received or the maximum number of retransmissions is reached. The maximum number of retransmissions for the hybrid ARQ is set to four.

IEEE 802.15.6 defines such an error control method. However, in the default mode, the error correction capacity is increased by repeated retransmission, as

only a single BCH code is used. This limits the error correcting capacity of the high QoS mode because both the maximum number of retransmissions and the coding rate of the error correcting code are fixed. The error control scheme of the standard cannot therefore meet the various QoS requirements for WBANs data.

Chapter 3

System model

Figure 3.1 shows the overall concept of our proposed system. In general, different types of data are input and multiplexed at a single sensor device [16]. Here we assume that the different types of data input and multiplexed have potentially different QoS requirements. Given the varying QoS requirements, the different types of data have different priorities. These data are multiplexed and transmitted from a sensor (i.e., a wireless body area network (WBAN) node) to a WBAN hub.
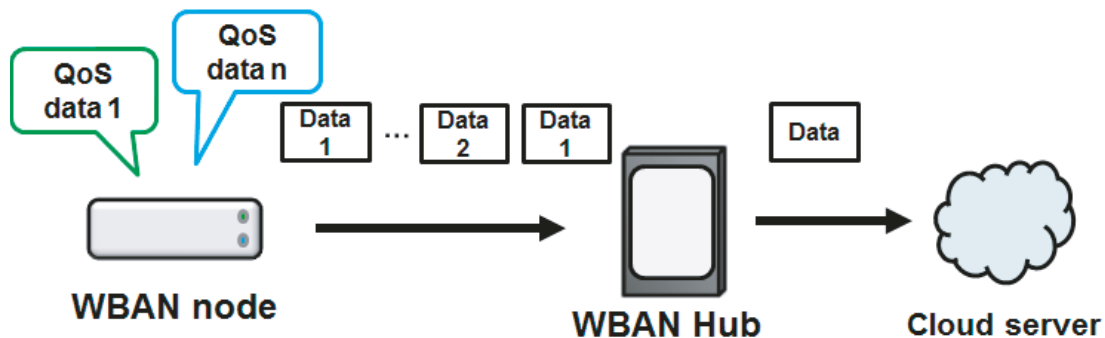
Figure 3.1 System concept.

Figure 3.2 shows the system model. The transmitter consists of a multiplexing module, a MAC module, and a PHY module. The multiplexing module controls the different types of QoS requirements according to the following priorities. First, several data are added to user priorities. Then, the header, which includes user priority information (e.g., latency, rate of error control coding, the number of repetitions in ARQ, etc.), is added to the user priorities in the multiplexing layer. Next, the multiplexer (MUX) controller in the multiplexing layer provides instructions to each data depending on predefined parameters. According to the QoS control signal, the multiplexing layer performs error and delay control.

Finally, data with different user priorities are multiplexed and sent to the MAC layer.
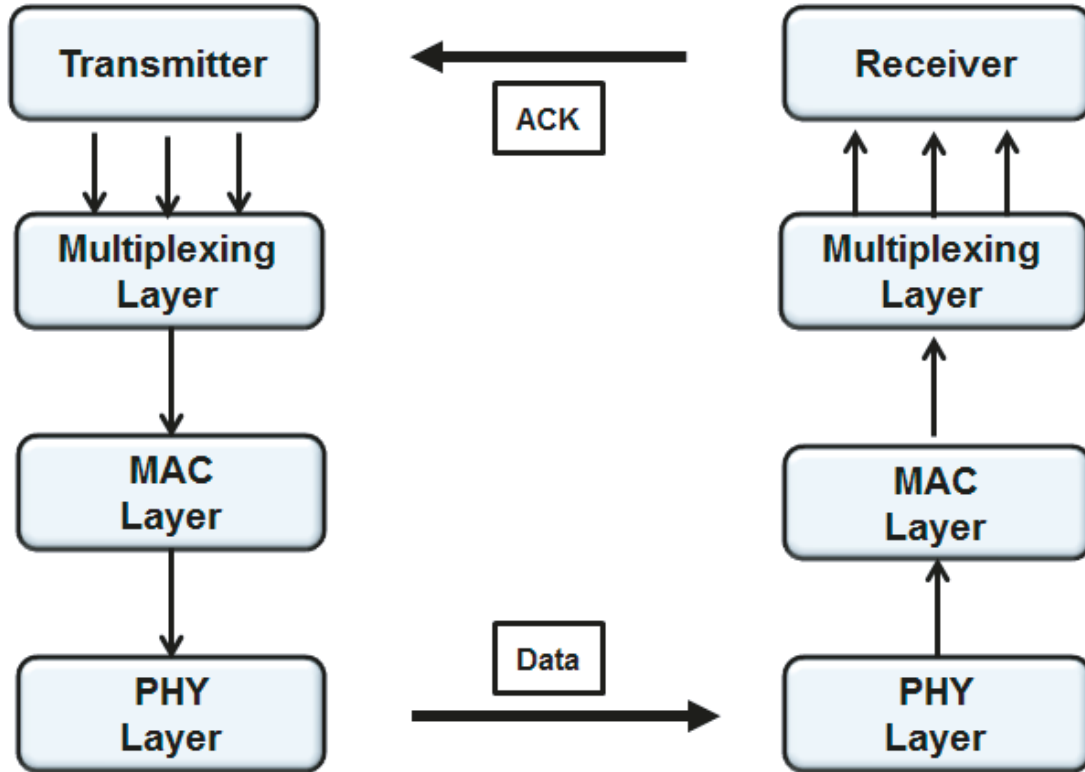
Figure 3.2 System model of the proposed scheme.

In the MAC module, the error control process is performed according to the instructions from the multiplexing module. In the PHY module, this multiplexed data is modulated. In Chapter 4, coherent phase shift keying (PSK) is used for basic analysis. Then, differentially encoded phase-shift keying (DPSK) is considered after Chapter 5, because DPSK modulation has higher robustness against errors than OOK, and this modulation scheme can also be more easily simulated. In particular, DBPSK and DQPSK modulation in the IEEE 802.15.6 definitions are assumed. The DPSK transmitting symbols are given by following equation:

$$c_m = c_{m-1} \exp(j\varphi_m) \tag{3-1}$$

where c_m is the mth encoded DBPSK or DQPSK symbol, $m = (0, 1, \ldots, N)$, N gives the number of symbols, $c_{-1} = 1$, and φ_0 is an arbitrary phase. The
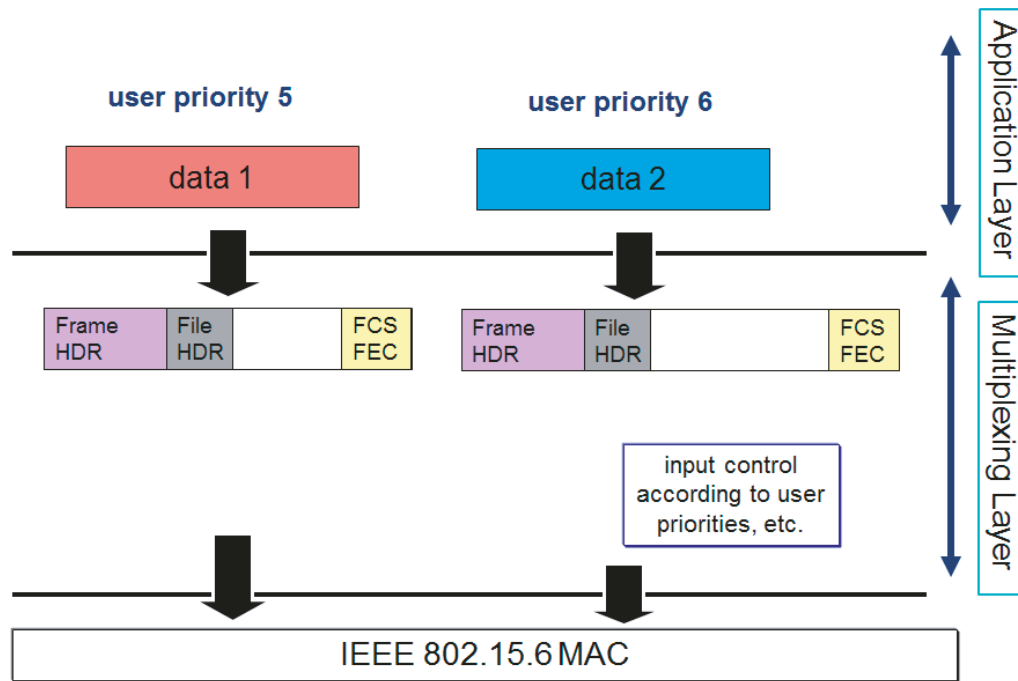
Figure 3.3 Example of multiplexing layer.

symbol c_m carries either one (DBPSK) or two (DQPSK) bits of information. The mapping of information bits onto φ_m is given in Tables 3.1 and 3.2.

Table 3.1 Mapping of information bits onto φ_m for DBPSK.

g_m	φ_m
0	0
1	π

Table 3.2 Mapping of information bits onto φ_m for DQPSK.

g_{2m}	g_{2m+1}	φ_m
1	1	$\pi/2$
0	1	π
0	0	$-\pi/2$
1	0	0

In addition, direct sequence spread spectrum (DSSS) can be applied to increase robustness against multipath fading and multiuser interference.

At the receiver, the transmission operation is processed in the reverse order. Finally, after the process at the demultiplexing module is complete, error detection is performed on the data.

In the MAC layer, this study assumed a beacon mode with super frames, following [22]. In this mode, a hub sets the access phase, such as an exclusive access phase (EAP), random access phase (RAP), managed access phase (MAP), or contention access phase (CAP). This is illustrated in Figure 4. A hub may set the length of any of these access phases to zero. In this study, only MAP is used, except Chapter 7, in order to reflect the requirement for medical data to be transmitted more reliably than non-medical data. A hub and nodes may send data by using scheduled allocations, preventing collisions from occurring in the same WBAN. If a random access protocol is also used, the required delay, energy consumption, or number of retransmissions will increase because of packet collisions. These factors cannot then be guaranteed, and their dependability is reduced. Some ACK policies, including I-ACK and G-ACK and so on, are defined in IEEE 802.15.6 [22]. In this research we assumed that I-ACK was sent immediately if the packet was sent successfully, while N-ACK was sent if the packet transmission failed.
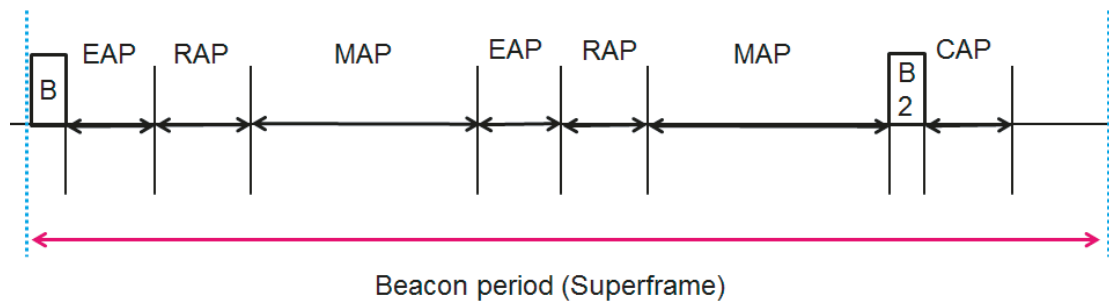
Figure 3.4 Beacon mode with superframes (mode I) [22].

Chapter 4

Proposed scheme

In our proposed scheme, Weldon's ARQ [30] is employed rather than selective repeat ARQ, and decomposable code is employed as error-correction code for Hybrid ARQ. The proposed scheme can provide an error control method that satisfies various QoS requirements by coordinating the number of data copies and changing how the decomposable code is combined.

Figure 4.1 shows a relationship in the proposed scheme. In this chapter, a simple version of our decomposable code is explained, and then the extended version is described in Chapter 6.
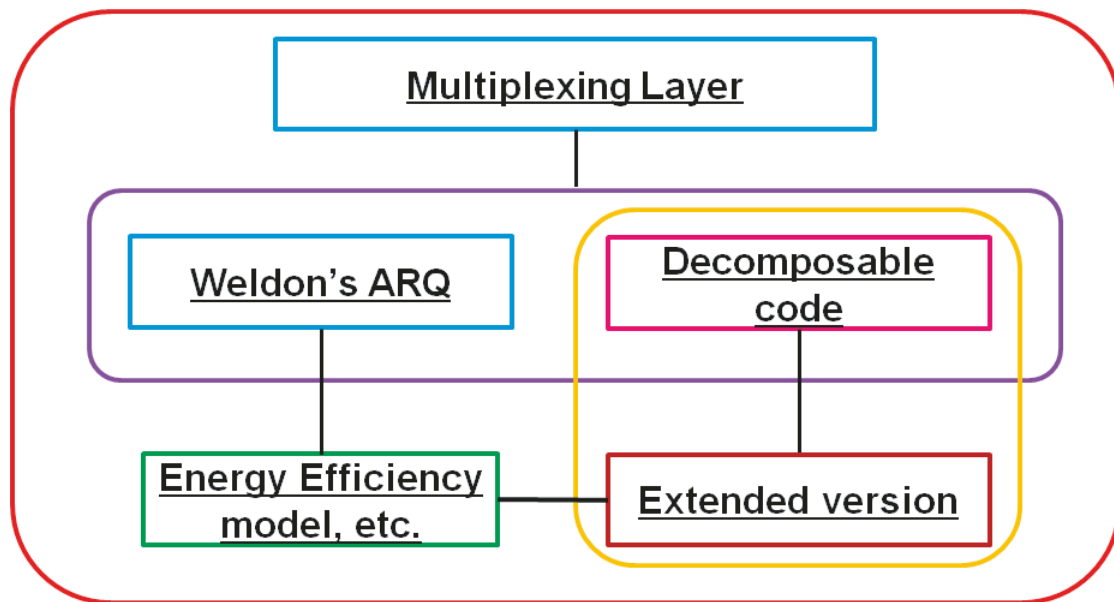
Figure 4.1   Relationship in the proposed scheme.

4.1 Weldon's ARQ

Fig.4.2 illustrates an example of the working process of Weldon's ARQ. This ARQ method cascades several n_i copies of the original data at each retransmission if N-ACK is received. The block is repeated n_i times until even one block is successful or the maximum number of transmission q is reached
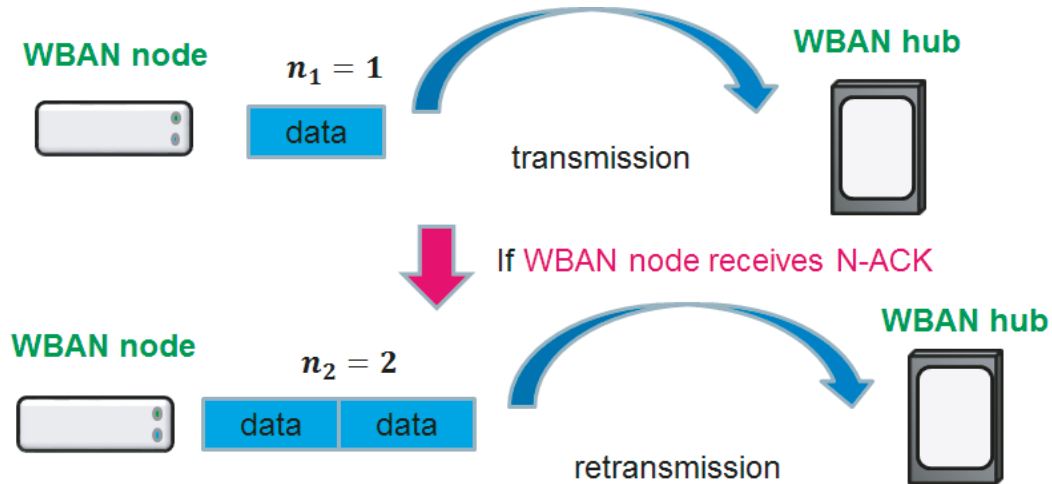
Figure 4.2 Weldon's ARQ.

4.2 Decomposable error control coding

As an example of decomposable code, a punctured convolutional code with constraint length K set to 3 and coding rates 8/9, 4/5, 2/3, and 1/2 is used. Punctured matrices which we select in this thesis are quite simple and can be analyzed more easily. The punctured convolutional code is generated based on the convolutional code with a generator polynomial of [7,5] and coding rate $r = 1/2$. The punctured matrix of $r = 8/9$ is shown in Fig.4.3. The two patterns of the $r = 8/9$ punctured codes (codeword 1 and codeword 1') can be generated using this punctured matrix. More specifically, at the first transmission, codeword 1 is sent; then, to increment the code rate of the punctured code, a part of codeword 1' is sent as the second transmission. Figure 4.4 illustrates how to increment redundancies and send the sub-codewords except u_{11} and u_{21} from the first transmission to the fourth transmission. As shown in the figure, these punctured matrices consist of a subset that is a part of the next punctured matrix.

In general, at the ith transmission, reconstructed codewords are decoded as error correction codes with a coding rate set as follows:

$$r_i = \begin{cases} 8/9 & (i = 1) \\ 4/5 & (i = 2) \\ 2/3 & (i = 3) \\ 1/2 & (i \geq 4) \end{cases} . \tag{4--1}$$

information m	m_1	m_2	m_3	m_4	m_5	m_6	m_7	m_8
output u_1	u_{11}	u_{12}	u_{13}	u_{14}	u_{15}	u_{16}	u_{17}	u_{18}
output u_2	u_{21}	u_{22}	u_{23}	u_{24}	u_{25}	u_{26}	u_{27}	u_{28}

punctured matrix

$$\begin{bmatrix} 1 & 1 & 0 & 1 & 0 & 1 & 0 & 1 \\ 1 & 0 & 1 & 0 & 1 & 0 & 1 & 0 \end{bmatrix}$$

information m	m_1	m_2	m_3	m_4	m_5	m_6	m_7	m_8
output u_1	u_{11}	u_{12}	$\times$	u_{14}	$\times$	u_{16}	$\times$	u_{18}
output u_2	u_{21}	$\times$	u_{23}	$\times$	u_{25}	$\times$	u_{27}	$\times$

codeword 1

$$\begin{bmatrix} u_{11} & u_{12} & u_{14} & u_{16} & u_{18} \\ u_{21} & u_{23} & u_{25} & u_{27} & \times \end{bmatrix}$$

codeword 1'

$$\begin{bmatrix} u_{11} & u_{13} & u_{15} & u_{17} & \times \\ u_{21} & u_{22} & u_{24} & u_{26} & u_{28} \end{bmatrix}$$

Figure 4.3   Punctured convolutional code $r = 8/9$.

It can be said that this scheme is a kind of the type II hybrid ARQ.

4.3   Procedure of the proposed scheme

Figure 4.5 shows a flowchart of the protocol for our proposed scheme. In the proposed method, retransmission is performed as follows. First, information m is encoded via the punctured convolutional code whose $r_1 = 8/9$; then codeword 1 in Fig.4.4 is transmitted. If errors are detected, the receiver stores
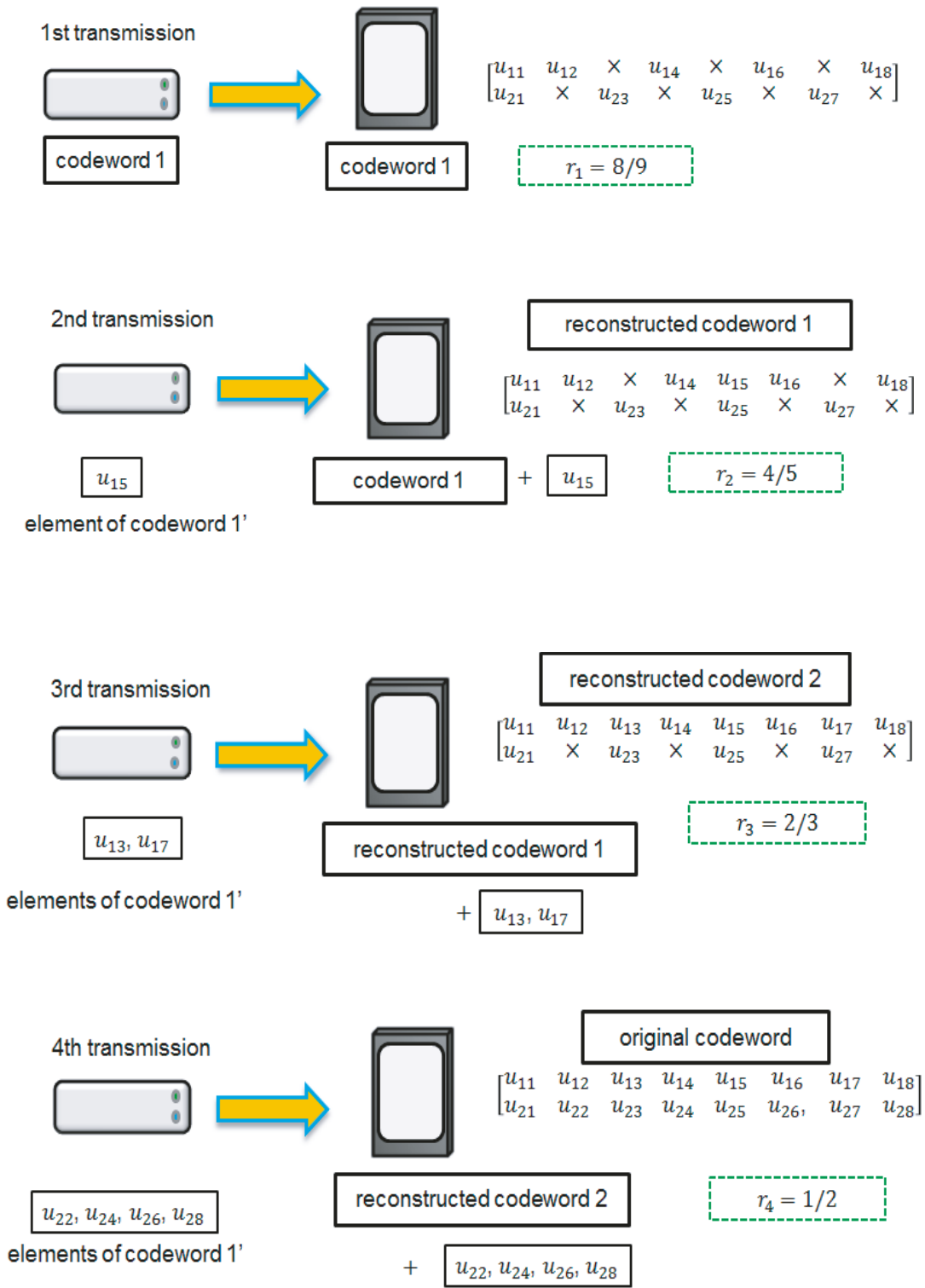
Figure 4.4 Reconstructing punctured convolutional codes $8/9 \leq r \leq 1/2$.

the transmitted codeword 1 and the transmitter re-sends the sub-codeword of codeword 1' n_i times in the case $2 \leq i \leq 4$. At the receiver, a received sub-codeword and stored codeword are combined (Fig.4.4) and the reconstructed codeword is decoded. After the third retransmission, codeword 1 is sent n_5 times and combined with a buffered codeword. If errors are detected, one of n_5 codeword 1 is buffered in the receiver and codeword 1' is transmitted n_6 times and combined with a stored codeword. After that, codeword 1 and codeword 1' are sent alternately n_i times and stored. When codeword 1 or codeword 1' is buffered, the first one among n_i copies is stored. The transmitter repeats these operations until the data is received correctly or the number of retransmissions reaches the predefined maximum number of transmissions q.

Figure 4.5 Flowchart of the proposed ARQ protocol.

Chapter 5

Theoretical analysis

In this chapter, the theoretical analysis and optimization of our proposed scheme in a simple case is described. Then, the AWGN channel and the Rayleigh fading channel is assumed as a channel model.

5.1   Theoretical analysis

5.1.1   Theoretical analysis

We define normalized throughput $\eta = k_0/T_{bit}$ as the number of total communicated bits and uncoded bits k_0. The number of total communicated bits T_{bit} is determined as follows:

$$T \simeq \sum_{i=1}^{q} \prod_{j=1}^{i} P_{j-1}^{n_{j-1}} \left(1 - P_i^{n_i}\right) \left(\sum_{k=0}^{i} n_k m_k\right) + \left(\sum_{j=1}^{q} n_j m_j\right) \prod_{j=1}^{q} P_j^{n_j} \quad \text{(5–1)}$$
$$\left(* P_0 \equiv 1, \ n_0 \equiv 0\right).$$

Here, P_i is the packet error ratio (PER), m_i is the number of transmitted bits, and n_i is the number of copy blocks of Weldon's ARQ at the ith transmission. Then, P_i changes in stages because the received data is decoded by decomposable codes with coding rates varying in order of equation 4–1. Note that throughput η is described as the above approximate equation due to the maximum transmission limit.

Next, we consider the upper bounds on error probability of the punctured convolutional codes used by the proposed scheme to obtain P_i. These bounds are obtained from the transfer function $T(D, N)$ of the code, which describes the weight distribution or weight spectrum of the incorrect codewords and

the number of bit errors on these paths [31]. The transfer function $T(D, N)$ is expressed as follows:

$$T(D, N)|_{N=1} = \sum_{d=d_{free}}^{\infty} a_d D^d \tag{5-2}$$

$$\frac{dT(D, N)}{dN}\bigg|_{N=1} = \sum_{d=d_{free}}^{\infty} c_d D^d. \tag{5-3}$$

Here, d_{free} is the free distance of the code, and a_d is the number of incorrect paths or adversaries of the Hamming weight d, $d \leq d_{free}$. In addition, c_d is the total number of information bit errors produced by the incorrect paths of the Hamming weight.

Using $T(D, N)$, the upper bounds on the event error probability P_E and the bit error probability P_B of a code with rate $r_i = k/v$ are given as follows:

$$P_E \leq \sum_{d=d_{free}}^{\infty} a_d P_d \tag{5-4}$$

$$P_B \leq \frac{1}{k} \sum_{d=d_{free}}^{\infty} c_d P_d. \tag{5-5}$$

Here,

$$P_d = Q(\sqrt{2dRE_b/N_0}) \tag{5-6}$$

$$Q(x) = \int_x^{\infty} \frac{1}{2\pi} \exp(-\frac{1}{2}z^2) dz. \tag{5-7}$$

Here, E_b/N_0 is the energy per bit-to-noise density ratio and P_d is the error probability in the case of PSK modulation and unquantized AWGN channels [32]. Then, in case of the Rayleigh fading channel, P_d is expressed as follows [33]:

$$P_d = (P_e)^d \sum_t^{d-1} {}_{d-1-t}C_t (1 - P_e)^t \tag{5-8}$$

$$P_e = 1 - \sqrt{\frac{\gamma_b r_i}{1 + \gamma_b r_i}}. \tag{5-9}$$

where γ_b is the average of E_b/N_0.

Further, P_i is determined using P_B from the following equation:

$$P_i = 1 - (1 - P_B)^{L_{info}}. \tag{5–10}$$

Here, L_{info} is the number of information bits. In addition, the upper bound of the residual bit error ratio (RBER) is obtained by the following equation:

$$RBER \leq r_{B,q} \prod_{i=0}^{q-1} P_i. \tag{5–11}$$

Here, $r_{B,q}$ is P_B in the case of a code with rate r_q.

The transfer function $T(D, N)$ changes according to the punctured matrices. Further details of the transfer function $T(D, N)$ are provided in the next subsection.

5.1.2   Transfer function

To obtain P_E and P_B, we derive the transfer function $T(D, N)$ from the state diagram using the transfer function technique [31],[32]. Figure 5.1 shows the state diagram for the punctured convolutional codes.

Here, X_a and X_b express state zero, and the remaining states are arbitrarily labeled X_1, X_2, and X_3. The exponent of N indicates the number of information bits set to " 1 " that cause the transition to occur, and the exponent of D indicates the Hamming weight on the transition. From Fig. 5.1, the matrix equation of coding rate 4/5 is given as follows:
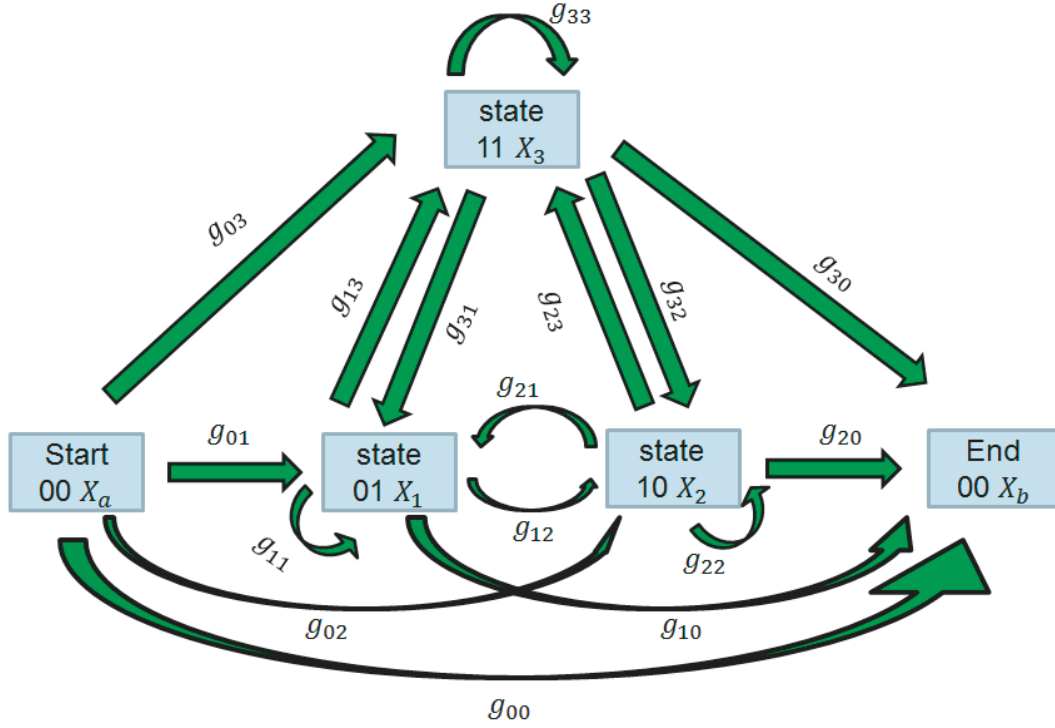
Figure 5.1 State diagram of punctured convolutional codes.

$$
\begin{bmatrix} X_1 \\ X_2 \\ X_3 \end{bmatrix} = \begin{bmatrix} g_{11} & g_{12} & g_{13} \\ g_{21} & g_{22} & g_{23} \\ g_{31} & g_{32} & g_{33} \end{bmatrix} \begin{bmatrix} X_1 \\ X_2 \\ X_3 \end{bmatrix}
$$

$$
+ \begin{bmatrix} (N^3 + N^2 + N)D^2 + N^2 D^4 \\ (N^2 + N)D + N^3 D^3 + N^2 D^5 \\ N^2 D + (N^4 + 2N^3)D^3 \end{bmatrix} X_a \tag{5-12}
$$

$$
\begin{cases}
g_{11} = N^3 + N^2 D^2 + (N^2 + N)D^4 \\
g_{12} = (N^3 + 2N^2)D^2 + ND^4 \\
g_{13} = (N^3 + 2N^2)D^2 + ND^4 \\
g_{21} = N^3 D + (2N^2 + N)D^3 \\
g_{22} = N^2 D + (N^3 + N^2 + N)D^3 \\
g_{23} = N^2 D + (N^3 + N^2 + N)D^3 \\
g_{31} = N^7 D + N^2 D^5 + N^3 D^3 \\
g_{32} = N^3 D + (N^4 + N^3 + N^2)D^3 \\
g_{33} = N^2 D + (N^3 + N^2 + N)D^3
\end{cases} \tag{5-13}
$$

$$
\mathbf{X} = \mathbf{A}\mathbf{X} + \mathbf{F}X_a \tag{5-14}
$$

$$X_b = \begin{bmatrix} (N^2 + N + 1)D^2 + ND^4 \\ (2N + 1)D^2 + N^2 D^4 \\ (2N + 1)D^2 + N^2 D^4 \end{bmatrix}^T \begin{bmatrix} X_1 \\ X_2 \\ X_3 \end{bmatrix}$$
$$+ (ND^2 + (N^2 + N)D^4)X_a \qquad (5\text{--}15)$$

$$X_b = \mathbf{G}\mathbf{X} + hX_a. \qquad (5\text{--}16)$$

As above, the transfer function is given as follows:

$$T(D, N) = \frac{X_a}{X_b} = \mathbf{G}\left[\mathbf{I} - \mathbf{A}\right]^{-1} \mathbf{F} + h$$
$$= h + \mathbf{G}\mathbf{F} + \mathbf{G}\mathbf{A}\mathbf{F} + \mathbf{G}\mathbf{A}^2\mathbf{F} + \mathbf{G}\mathbf{A}^3\mathbf{F} + \cdots . \qquad (5\text{--}17)$$

Thus, coefficient c_d is given as follows:

$$\left.\frac{dT(D, N)}{dN}\right|_{N=1} = \sum_{d=d_{free}}^{\infty} c_d D^d$$
$$= D^2 + 21D^3 + 1872D^4 + 9127D^5 + 40922D^6 + 206380D^7$$
$$+ 871148D^8 + 3372445D^9 + 12553649D^{10} + 43727850D^{11} + \cdots . \qquad (5\text{--}18)$$

For coding rate 8/9, we obtain its transfer function using the same procedure:

$$\begin{cases} h = g_{00} \\ \mathbf{G} = \begin{bmatrix} g_{01} & g_{02} & g_{03} \end{bmatrix} \\ \mathbf{F} = \begin{bmatrix} g_{10} \\ g_{20} \\ g_{30} \end{bmatrix} \\ \mathbf{A} = \begin{bmatrix} g_{11} & g_{12} & g_{13} \\ g_{21} & g_{22} & g_{23} \\ g_{31} & g_{32} & g_{33} \end{bmatrix} \end{cases} \qquad (5\text{--}19)$$

$$
\left\{
\begin{aligned}
g_{00} =\ & N^4 D^9 + (N^5 + N^4 + 4N^3 + N^2)D^7 \\
& + (N^6 + 2N^5 + N^4 + 3N^3 + 2N^2)D^6 \\
& + (N^5 + 6N^4 + 4N^3 + 3N^2)D^5 + (2N^5 + 6N^4 + 3N^3 + 3N^2)D^4 \\
& + (3N^3 + 2N^2 + N)D^3 + (2N^3 + N^2 + N)D^2 \\
g_{01} =\ & N^3 D^8 + (2N^5 + 5N^4 + 2N^3)D^7 + (4N^4 + 2N^3)D^6 \\
& + (2N^6 + 5N^5 + 3N^4 + 4N^3 + N^2)D^5 \\
& + (N^7 + 3N^6 + 5N^5 + N^4 + 3N^3 + N^2)D^4 \\
& + (N^5 + 3N^4)D^3 + (N^6 + 2N^5 + 3N^4)D^2 \\
g_{02} =\ & (N^5 + 2N^4 + N^3)D^8 + (N^4 + N^3)D^7 + (N^6 + 3N^5 + 4N^4 + 2N^3)D^6 \\
& + (N^7 + 3N^6 + 4N^5 + 4N^4 + 3N^3)D^5 + (N^6 + 4N^5 + 4N^4 + 3N^3 + N^2)D^4 \\
& + (N^6 + 3N^5 + 2N^4 + 2N^3 + N^2)D^3 + N^4 D^2 + N^4 D \\
g_{03} =\ & (N^6 + N^5)D^8 + (2N^5 + 2N^4)D^7 + (2N^7 + 5N^6 + 6N^5 + 3N^4)D^6 \\
& + (N^8 + 2N^7 + 2N^6 + 2N^5 + 2N^4)D^5 + (2N^6 + 3N^5 + 3N^4 + N^3)D^4 \\
& + (2N^7 + 5N^6 + 3N^5 + 2N^4 + N^3)D^3 + N^5 D^2 + N^5 D
\end{aligned}
\right.
\tag{5–20}
$$

$$
\left\{
\begin{aligned}
g_{10} =\ & N^5 D^8 + (3N^4 + 4N^3 + 2N^2)D^7 + (3N^4 + 2N^3 + 2N^2)D^6 \\
& + (N^5 + N^4 + 6N^3 + 5N^2 + 2N)D^5 + (N^6 + N^5 + N^4 + 5N^3 + 4N^2 + 3N)D^4 \\
& + (N^5 + 4N^4 + N^3 + N^2)D^3 + (2N^5 + 3N^4 + N^3 + N^2)D^2 + N^3 D \\
g_{11} =\ & N^4 D^9 + (N^5 + N^4 + 4N^3 + N^2)D^7 + (N^6 + N^5 + N^4 + 4N^3 + 2N^2)D^6 \\
& + (3N^5 + 8N^4 + 3N^3 + N^2)D^5 + (2N^5 + 7N^4 + 3N^3 + N^2)D^4 \\
& + (2N^6 + 4N^5 + 2N^4 + N^3)D^3 + (N^7 + 2N^6 + 4N^5)D^2 + N^6 \\
g_{12} =\ & (N^4 + N^3)D^8 + (N^6 + N^5 + N^4 + N^3)D^7 + (3N^5 + 6N^4 + 5N^3 + 2N^2)D^6 \\
& + (2N^5 + 3N^4 + 3N^3 + 2N^2)D^5 + (N^6 + 3N^5 + 4N^4 + 2N^3)D^4 \\
& + (N^7 + 2N^6 + 3N^5 + 4N^4 + 3N^3 + N^2)D^3 + (N^6 + 2N^5 + N^4)D^2 + (N^6 + N^5)D \\
g_{13} =\ & (N^6 + 2N^5 + N^4)D^8 + (N^7 + N^4)D^7 + (2N^6 + 4N^5 + 3N^4 + N^3)D^6 \\
& + (3N^6 + 5N^5 + 5N^4 + 3N^3)D^5 + (2N^7 + 4N^6 + 5N^5 + 4N^4 + N^3)D^4 \\
& + (N^8 + N^7 + 2N^6 + 3N^5 + N^4)D^3 + (N^6 + N^5)D^2 + (2N^7 + 2N^6)D
\end{aligned}
\right.
\tag{5–21}
$$

$$
\left\{
\begin{aligned}
g_{20} =\ & (N^5 + 2N^4 + 2N^3 + N^2)D^7 + (N^6 + N^5 + N^4 + 2N^3 + N^2)D^6 \\
& + (N^5 + 5N^4 + 7N^3 + 5N^2 + 2N)D^5 + (3N^5 + 5N^4 + 5N^3 + 5N^2 + 2N)D^4 \\
& + (N^4 + 3N^3 + 2N^2)D^3 + (N^4 + N^3 + N^2 + N)D^2 \\
g_{21} =\ & (N^5 + 2N^4 + 2N^3 + N^2)D^7 + (2N^4 + 3N^3 + N^2)D^6 \\
& + (2N^6 + 5N^5 + 7N^4 + 5N^3 + N^2)D^5 + (N^7 + 2N^6 + 4N^5 + 5N^4 + 4N^3 + 2N^2)D^4 \\
& + (2N^5 + 3N^4 + N^3)D^3 + (2N^6 + 3N^5 + N^4)D^2 \\
g_{22} =\ & N^4 D^8 + N^3 D^7 + (N^6 + 4N^5 + 3N^4 + 5N^3 + 2N^2)D^6 \\
& + (N^7 + 2N^6 + 3N^5 + 6N^4 + 2N^3 + N^2)D^5 + (N^6 + 3N^5 + 8N^4 + 3N^3)D^4 \\
& + (2N^6 + 4N^5 + N^4 + 4N^3 + 2N^2)D^3 + N^5 D^2 + N^4 D \\
g_{23} =\ & N^4 D^8 + N^5 D^7 + (2N^7 + 5N^6 + 6N^5 + N^4 + N^3)D^6 \\
& + (N^8 + N^7 + 2N^6 + 3N^5 + 6N^4 + 2N^3)D^5 + (3N^6 + 5N^5 + 6N^4 + N^3)D^4 \\
& + (3N^7 + 4N^6 + 4N^5 + N^4 + N^3)D^3 + N^5 D^2 + N^6 D
\end{aligned}
\right.
\tag{5–22}
$$

$$
\begin{cases}
g_{30}=(N^5+2N^4+2N^3+N^2)D^7+(N^6+N^5+N^4+2N^3+N^2)D^6 \\
\quad+(N^5+5N^4+7N^3+5N^2+2N)D^5+(3N^5+5N^4+5N^3+5N^2+2N)D^4 \\
\quad+(N^4+3N^3+2N^2)D^3+(N^4+N^3+N^2+N)D^2 \\
g_{31}=(N^5+2N^4+2N^3+N^2)D^7+(2N^4+3N^3+N^2)D^6 \\
\quad+(2N^6+5N^5+7N^4+5N^3+N^2)D^5+(N^7+2N^6+4N^5+5N^4+4N^3+2N^2)D^4 \\
\quad+(2N^5+3N^4+N^3)D^3+(2N^6+3N^5+N^4)D^2 \\
g_{32}=N^4D^8+N^3D^7+(N^6+4N^5+3N^4+5N^3+2N^2)D^6 \\
\quad+(N^7+2N^6+3N^5+6N^4+2N^3+N^2)D^5+(N^6+3N^5+8N^4+3N^3)D^4 \\
\quad+(2N^6+4N^5+N^4+4N^3+2N^2)D^3+N^5D^2+N^4D \\
g_{33}=N^4D^8+N^5D^7+(2N^7+5N^6+6N^5+N^4+N^3)D^6 \\
\quad+(N^8+N^7+2N^6+3N^5+6N^4+2N^3)D^5+(3N^6+5N^5+6N^4+N^3)D^4 \\
\quad+(3N^7+4N^6+4N^5+N^4+N^3)D^3+N^5D^2+N^6D
\end{cases}
\tag{5--23}
$$

From the matrices, c_d is given in the same way as follows:

$$
\left.\frac{dT(D,N)}{dN}\right|_{N=1} = \sum_{d=d_{free}}^{\infty} c_d D^d
$$
$$
= 9D^2 + 1780D^3 + 17036D^4 + 164093D^5 + 1463387D^6 + 11239801D^7
$$
$$
+80280102D^8 + 535025955D^9 + 3323529844D^{10} + 19393645707D^{11}
$$
$$
+\cdots. \tag{5--24}
$$

For coding rates 1/2 and 2/3, we use the transfer functions in reference [32] because their coefficients are the same in the case of ideal punctured matrices. Here, $r = 1/2$ is enumerated as follows:

$$
\left.\frac{dT(D,N)}{dN}\right|_{N=1} = \sum_{d=d_{free}}^{\infty} c_d D^d
$$
$$
= \sum_{d=d_{free}}^{\infty} (d - d_{free} + 1)2^{d-d_{free}} D^d. \tag{5--25}
$$

And $r = 2/3$ is represented as follows:

$$
\left.\frac{dT(D,N)}{dN}\right|_{N=1} = \sum_{d=d_{free}}^{\infty} c_d D^d
$$
$$
= D^3 + 10D^4 + 54D^5 + 226D^6 + 856D^7 + 3072D^8
$$
$$
+10647D^9 + 35998D^{10} + 119478D^{11} \cdots. \tag{5--26}
$$

5.2   Performance analysis

5.2.1   Simulation condition

In this subsection, we evaluate our proposed scheme by theoretical analysis and simulations. To analyze our proposed scheme, we set two patterns under the AWGN channel and the Rayleigh fading channel, as shown in Table 5.1 and 5.2 respectively. A coding rate of a decomposable code r_i is determined according to the order of equation 4–1. Then, r_i is a coding rate after reconstructing a decomposable code. For the required QoS, the residual BER of pattern 2 is more important than its latency, and the latency and throughput of pattern 1 are more important than its residual BER. The number of copies of pattern 1 can achieve the maximum throughput in a high or middle E_s/N_0 area from our theoretical formulae. For pattern 2, the number of copies n_i is large because the latency is allowed; however, the residual BER and throughput performance must be significantly improved. Also, pattern 2 is fixed, as the throughput of pattern 2 is higher than that of the high QoS mode defined in IEEE 802.15.6 (hereinafter called the conventional scheme).

Table 5.1   Number of copies n_i for each pattern under AWGN channel.

i	1	2	3	4	5	$q=6$
Pattern 1, n_i	1	1	1	1	2	4
Pattern 2, n_i	1	2	2	4	4	6
r_i	8/9	4/5	2/3	1/2	1/2	1/2

Table 5.2   Number of copies n_i for each pattern under Rayleigh fading channel.

i	1	2	3	4	5	$q=6$
Pattern 1, n_i	1	1	1	1	1	3
Pattern 2, n_i	1	3	4	4	5	5
r_i	8/9	4/5	2/3	1/2	1/2	1/2

Note that another channel model is assumed to be Rayleigh fading channel, which is one of the channel models for wearable WBANs [34]. The data rate is referenced from the IEEE802.15.6 standard [22] and the roundtrip time is set based on the data rate and twice the maximum packet length defined in IEEE802.15.6. Simulation parameters are summarized in Table 5.3.

Table 5.3 Simulation parameters

Parameter	Detail
Channel model	AWGN
	Rayleigh fading
Modulation	BPSK
FEC	r_i=8/9, 4/5, 2/3 and 1/2
	K=3 convolutional codes
Decoding	Soft decision
	Viterbi decoding
ARQ protocol	Weldon's ARQ
L_{info}	504 bits
Data rate	487 kbps
Roundtrip Time	9.84 ms

5.2.2 Numerical results

Figure 5.2 shows the bit error probability of the punctured convolutional codes under the AWGN channel. Our proposed punctured convolutional codes with coding rates of 4/5 and 8/9 have a different upper bound than that of the ideal matrix; however, these differences do not significantly influence the performance of our proposed scheme. Relative to the simulation, the performance of the modified punctured convolutional codes is the same as that of the ideal punctured matrices, unlike results of the upper bound. This occurs because the number of trials in the simulation is not large enough. Further, the difference between the error-correcting capacity of the ideal matrix and that of the modified one is very small in the simulation. Hence, the difference does not clearly emerge in the graph without the huge number of trials. The difference between the upper bound and the simulation becomes greater as E_s/N_0 decreases.

Table 5.4 shows examples of the optimal number of copies n_i for the minimum latency while satisfying PER $\leq 10^{-5}$ by a full search under the AWGN channel. Table 5.5 shows examples of the optimal number of copies n_i for the maximum throughput while meeting the same condition. Figure 5.3 and 5.4 show the theoretical PER and throughput, respectively, according to parameters of Table 5.4 and 5.5. The parameters of Table 5.4 satisfy the condition that PER $\leq 10^{-5}$ by a smaller delay than Table 5.5 in Figure 5.3, whereas those of Table 5.5 achieve a larger throughput than Table 5.4 even though a large delay is expected in Figure 5.4. In other words, performance with non-optimal parameters in each policy can be considered same as that of sub-optimal parameters.
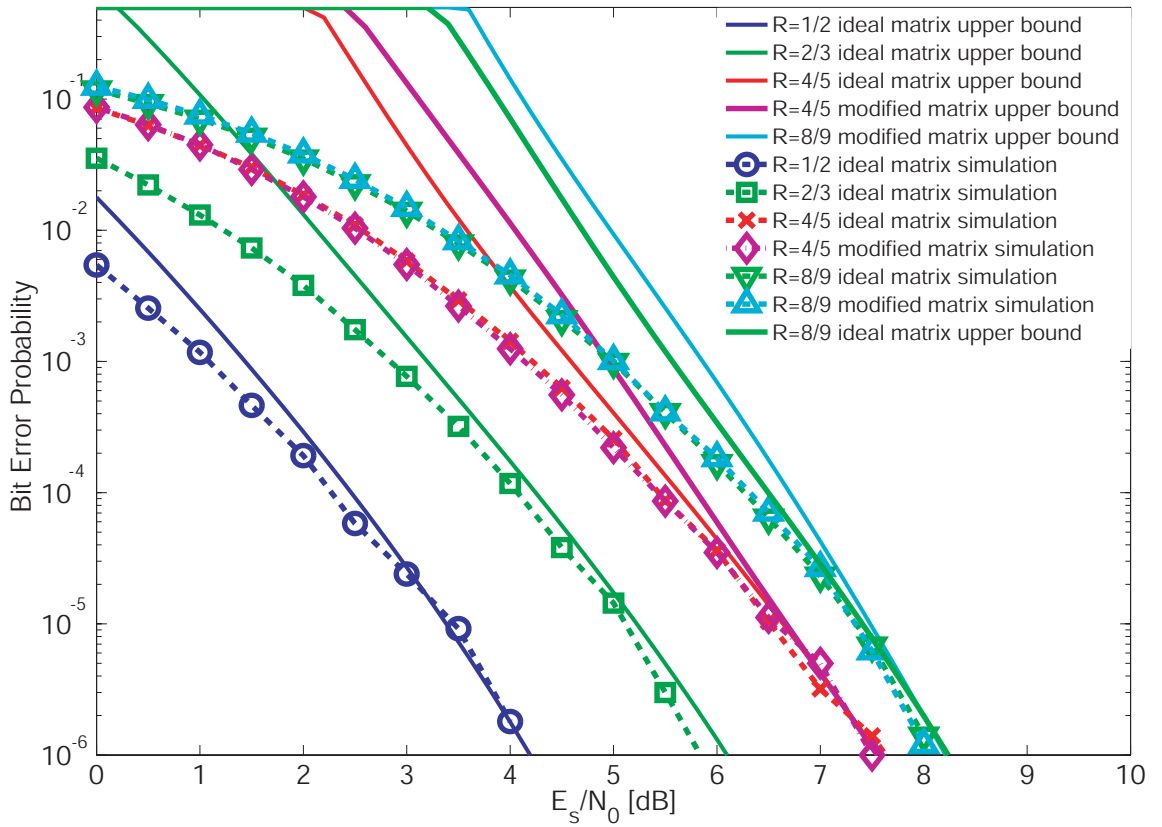
Figure 5.2   Bit error probability of punctured convolutional codes under AWGN channel.

Table 5.4   Optimal number of copies n_i for minimum latency while satisfying PER $\leq 10^{-5}$ under AWGN channel.

E_s/N_0	n_1	n_2	n_3	n_4
3 dB	1	1	10	-
			i=q	
5 dB	1	7	-	-
		i=q		
6 dB	1	4	-	-
		i=q		
r_i	8/9	4/5	2/3	1/2

Figures 5.5 and 5.6 show the throughput and residual BER performance, respectively, for patterns 1 and 2 of our proposed scheme and the conventional scheme under the AWGN channel. Overall, the residual BER performance of our proposed scheme is better than that of the conventional scheme. The throughput

Table 5.5 Optimal number of copies n_i for maximum throughput while satisfying PER $\leq 10^{-5}$ under AWGN channel.

E_s/N_0	n_1	n_2	n_3	n_4
3 dB	1	1	1	3
				i=q
5 dB	1	1	2	-
			i=q	
6 dB	1	1	1	-
			i=q	
r_i	8/9	4/5	2/3	1/2

Figure 5.3 PER performance with optimal and sub-optimal parameters under AWGN channel. Parameters of Table 5.4 are optimal.

of our proposed scheme is also better than that of the conventional scheme. The throughput and residual BER performances of pattern 1 are opposite to those of pattern 2 because of the parameter settings shown in Table 5.1. Note that

Figure 5.4 Throughput performance with optimal and sub-optimal parameters under AWGN channel. Parameters of Table 5.5 are optimal.

simulation results differ from bounds shown in Figure 5.2.

Table 5.6 shows examples of the optimal number of copies n_i for the minimum latency while satisfying PER $\leq 10^{-5}$ by a full search under the Rayleigh fading channel. And then, Table 5.7 shows examples of the optimal number of copies n_i for the maximum throughput while meeting the same condition. Figure 5.7 and 5.8 express the theoretical PER and throughput, respectively, depending on parameters of Table 5.6 and 5.7. Selected E_s/N_0 is higher than that in case of the AWGN channel. The reason is that the performance in case of the Rayleigh fading channel is worse than that of the AWGN case. The parameters of Table 5.6 achieve the condition that PER $\leq 10^{-5}$ by a smaller delay than Table 5.7 in Figure 5.7, whereas those of Table 5.7 satisfy a larger throughput than Table 5.6 even though a large delay is needed in Figure 5.8. Then, as the case of the
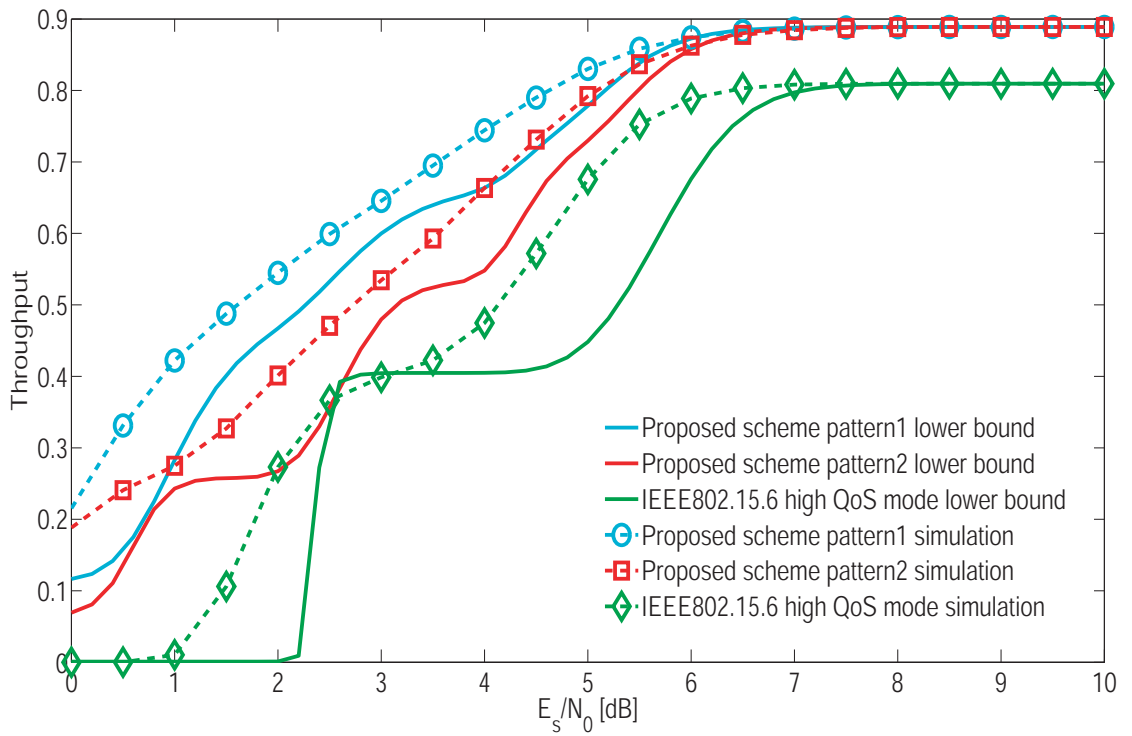
Figure 5.5 Throughput performance in the proposed method and conventional schemes under AWGN channel.

AWGN channel, performance with non-optimal parameters in each policy can be regarded as that of sub-optimal parameters.

Table 5.6 Optimal number of copies n_i for minimum latency while satisfying PER $\leq 10^{-5}$ under Rayleigh fading channel.

E_s/N_0	n_1	n_2	n_3	n_4	n_5	n_6
8 dB	1	1	1	3	-	-
			i=q			
11 dB	1	1	4	-	-	-
		i=q				
14 dB	1	7	-	-	-	-
		i=q				
r_i	8/9	4/5	2/3	1/2	1/2	1/2

Figures 5.9 and 5.10 present the throughput and residual BER performance, respectively, for patterns 1 and 2 of our proposed scheme and the conventional scheme under the Rayleigh fading channel. On the whole, our proposed scheme has better residual BER performance than the conventional scheme. In the
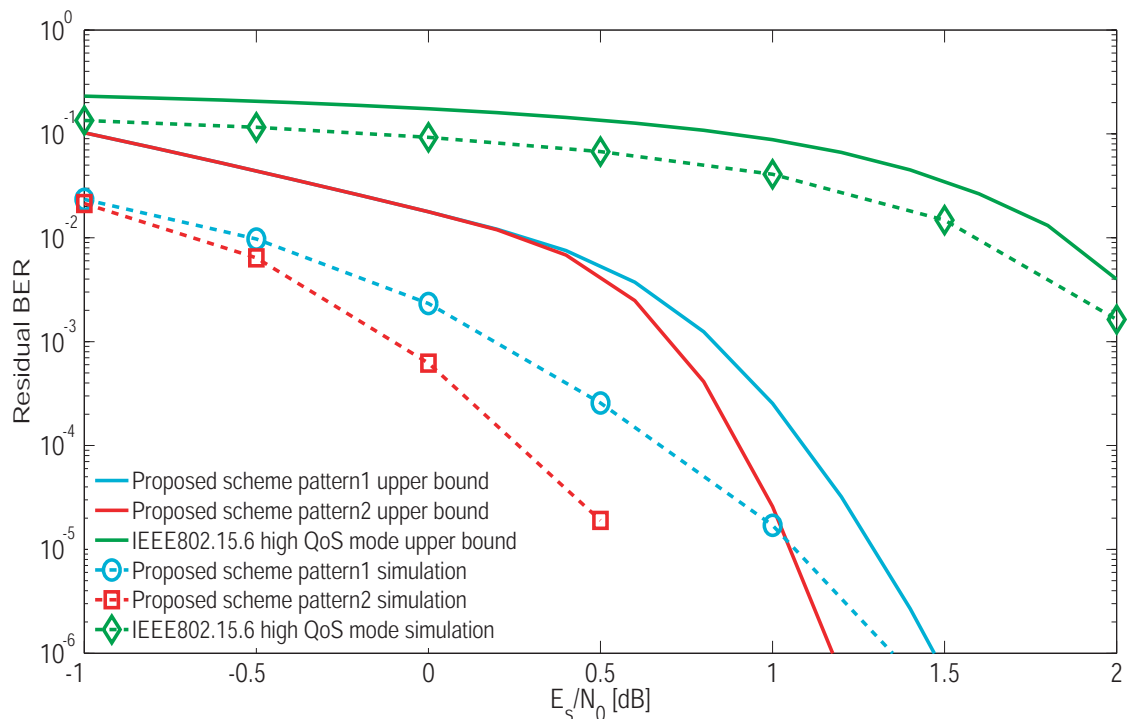
Figure 5.6 Residual BER performance in the proposed and conventional schemes under AWGN channel.

Table 5.7 Optimal number of copies n_i for maximum throughput while satisfying PER $\leq 10^{-5}$ under Rayleigh fading channel.

E_s/N_0	n_1	n_2	n_3	n_4	n_5	n_6
8 dB	1	1	1	1	1	1
						i=q
11 dB	1	1	1	1	1	-
					i=q	
14 dB	1	1	1	1	-	-
				i=q		
r_i	8/9	4/5	2/3	1/2	1/2	1/2

optional pattern, the proposed system obtains over 4.2dB gain than the standard system. The throughput of our proposed scheme is also better than that of the conventional scheme. Then, the gain of the proposed scheme is over 4.5dB gain than that of IEEE802.15.6 in the optional pattern. The throughput and residual BER performances of pattern 1 are also opposite to those of pattern 2 because of the parameter settings shown in Table 5.2 like the AWGN case. Note that simulation results are different from bounds for the same reason as the case of
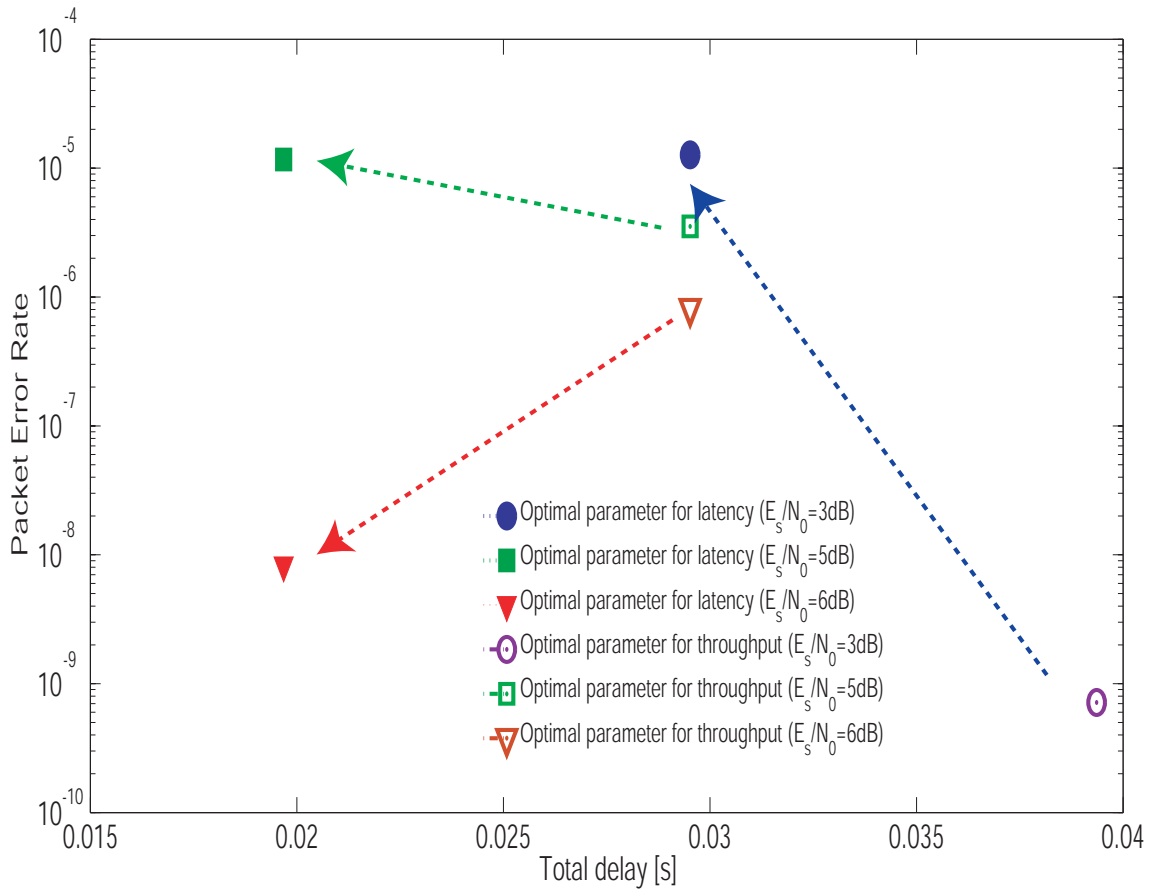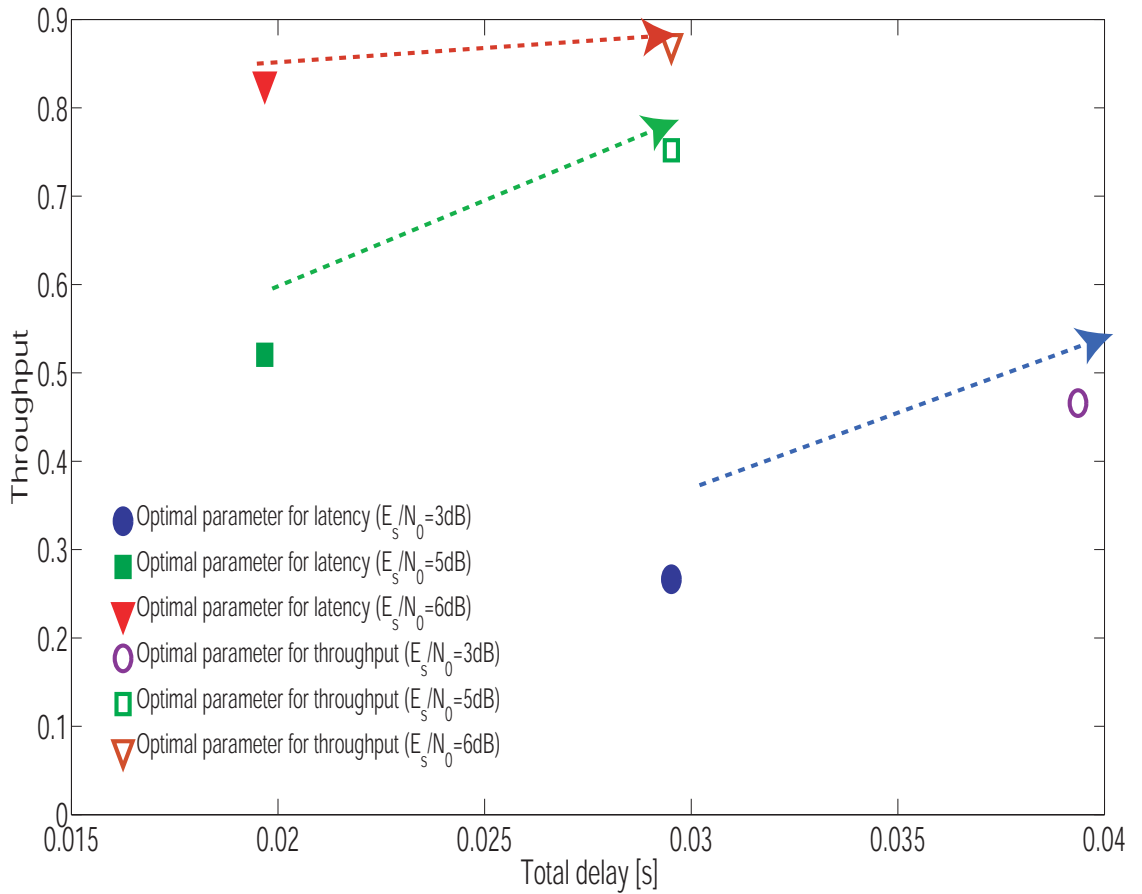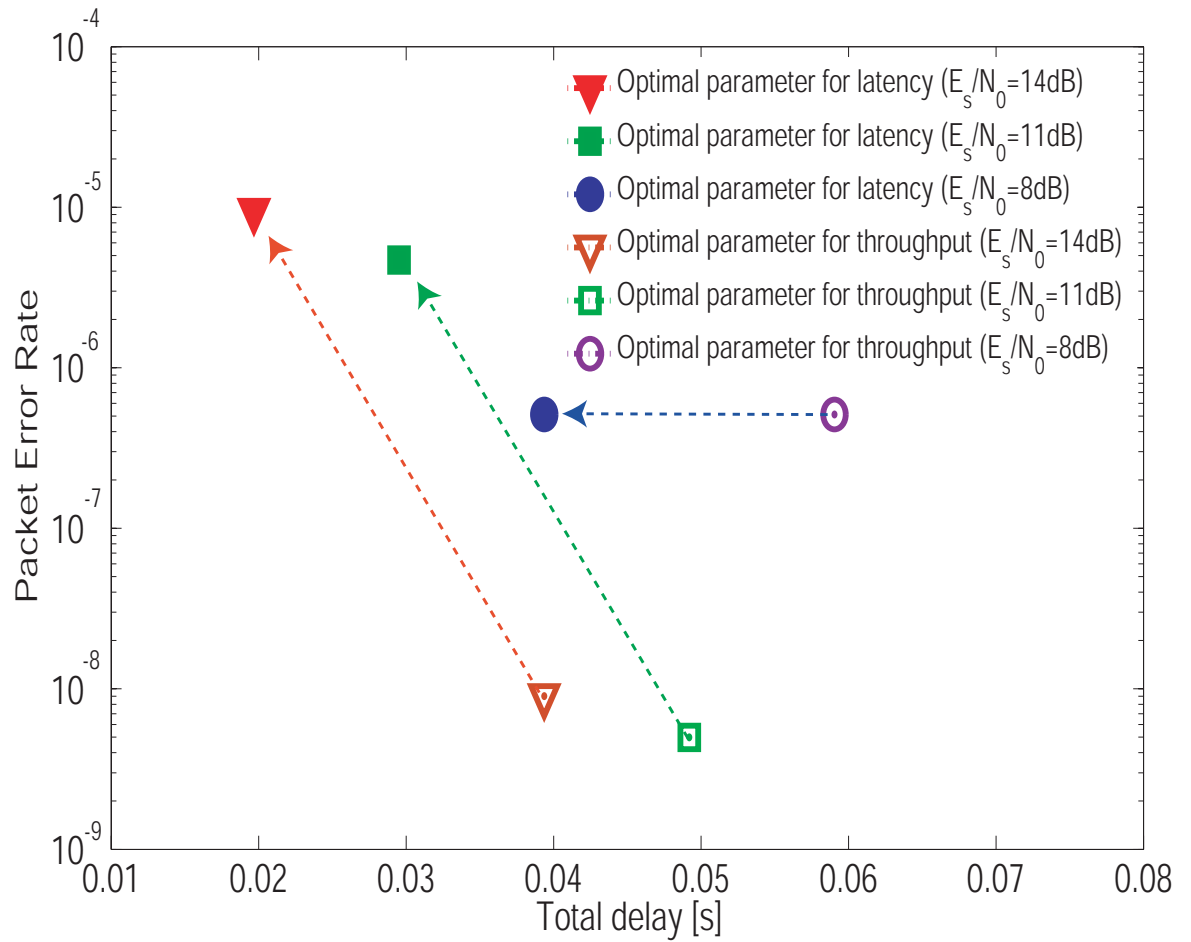
Figure 5.7 PER performance with optimal and sub-optimal parameters under Rayleigh fading channel. Parameters of Table 5.6 are optimal.

the AWGN channel.
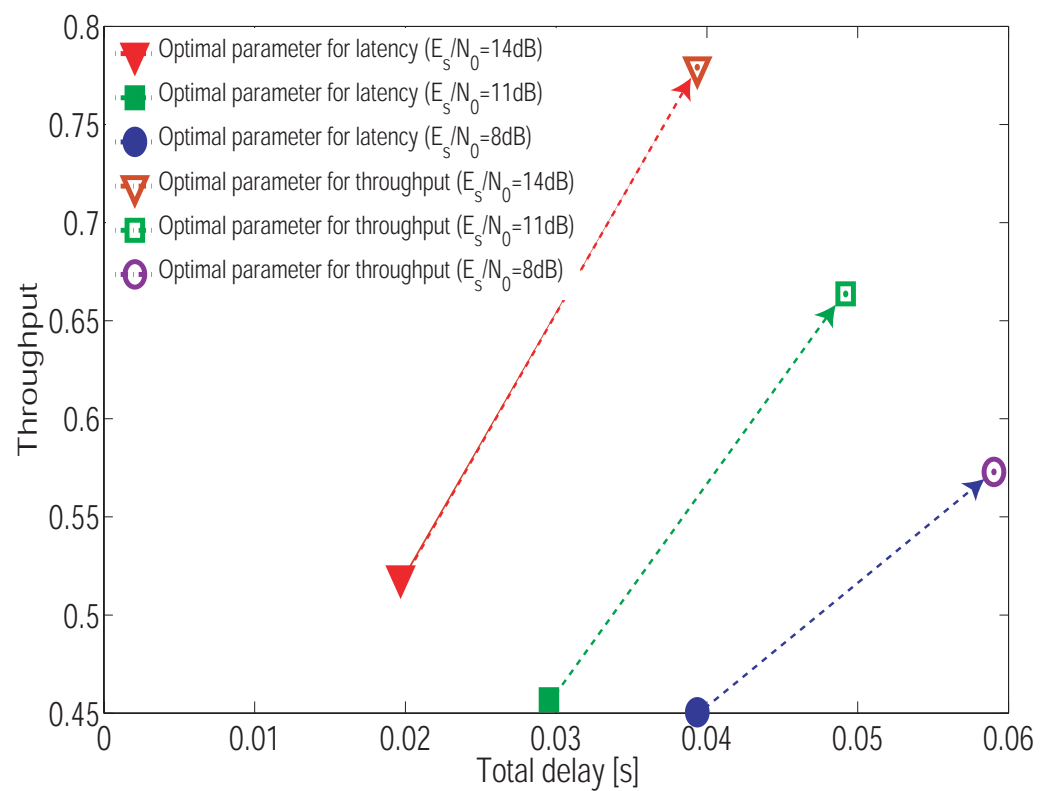
Figure 5.8 Throughput performance with optimal and sub-optimal parameters under Rayleigh fading channel. Parameters of Table 5.7 are optimal.
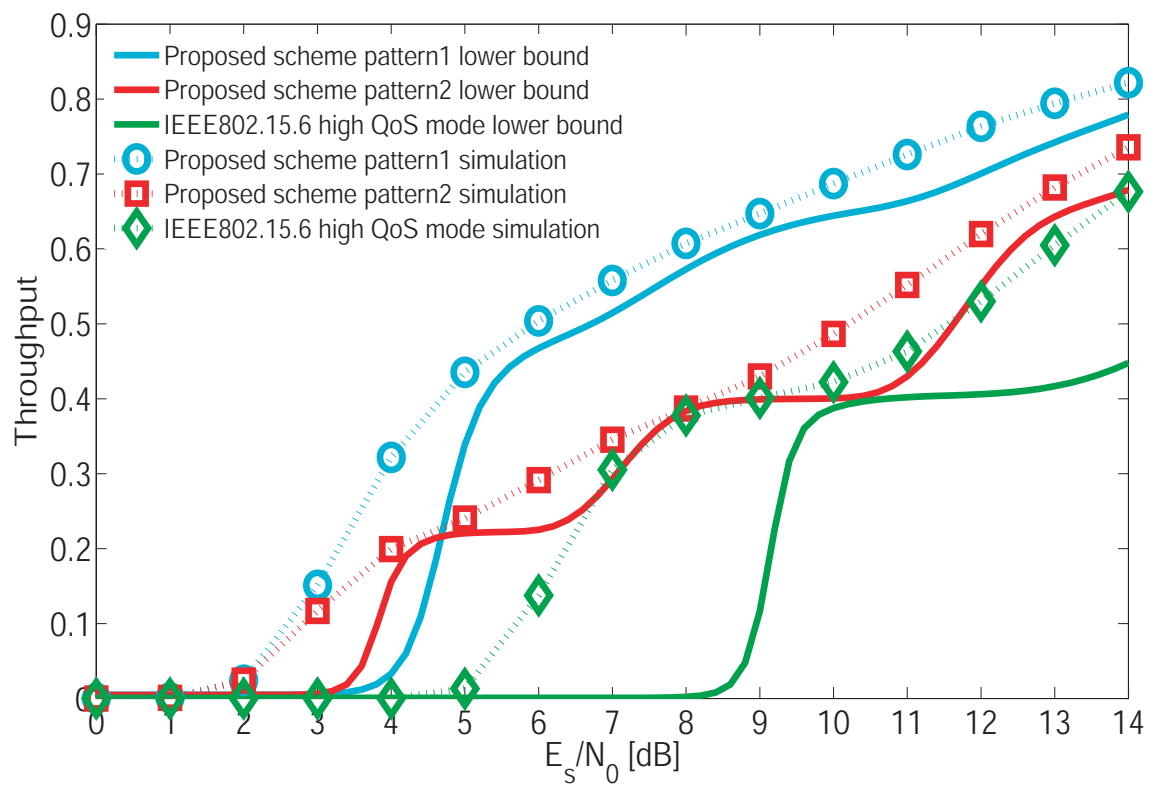
Figure 5.9 Throughput performance in the proposed method and conventional schemes under Rayleigh fading channel.
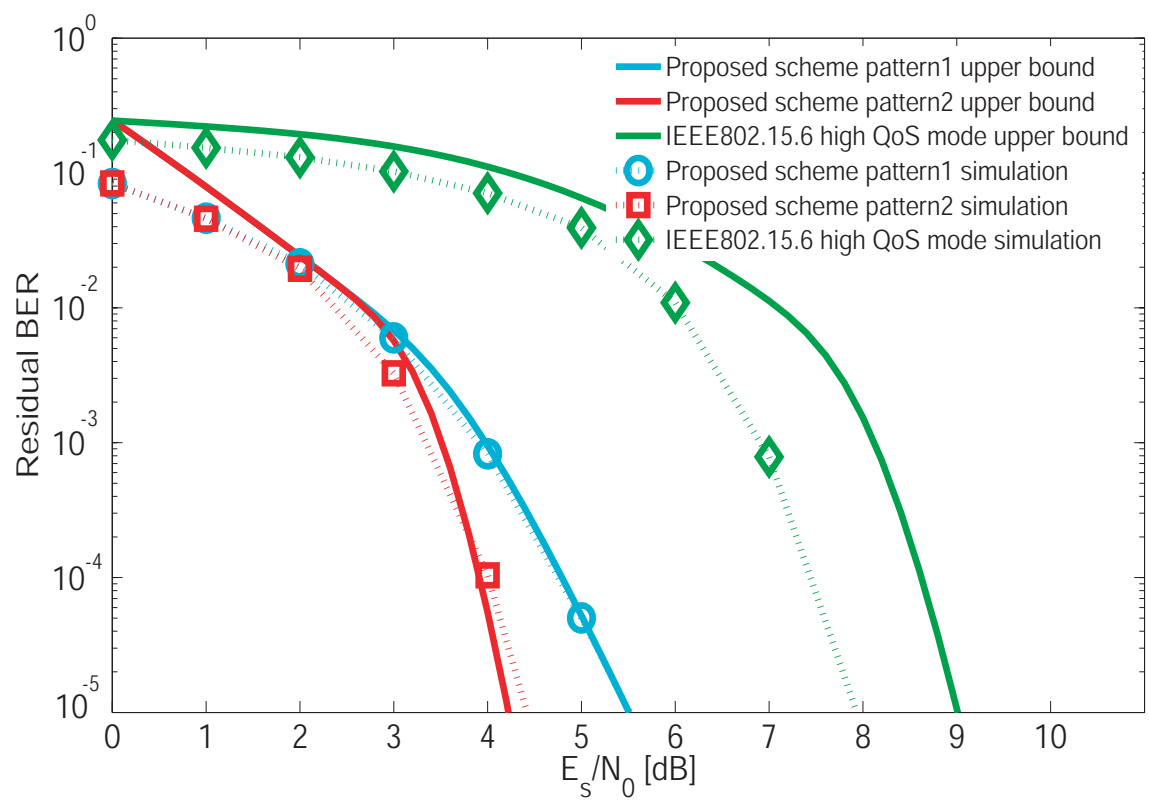
Figure 5.10 Residual BER performance in the proposed and conventional schemes under Rayleigh fading channel.

Chapter 6

Performance Evaluation in Multiple-WBANs Environment

In this chapter, several performances of the proposed scheme are evaluated in a multiple WBANs environment, representing a more practical situation. At first, we extend the error correcting capability of our decomposable codes in order to increase the robustness. A further study investigate the energy efficiency of the proposed scheme using computer simulations. Energy efficiency is an important factor because WBAN nodes are small and their battery capacity is limited. To complete the performance evaluation of the proposed scheme, this study quantitatively evaluate the RBER and energy efficiency of our proposed system under a WBANs channel model not only in a general case, but also in the worst-case scenario.

6.1   Extended decomposable code

In the previous chapter, as an example of a decomposable code, a punctured convolutional code with a constraint length $K = 3$ and coding rates of 8/9 1/2 was used. However, in cane of a multiple WBANs environment, it can not be said that the robustness of the previous structure against strong interference is enough. So, the coding rate is extended to 1/16 in order to increase the dependability in this thesis.

The procedure is the same as that of Chapter 4 until $i = 4$. Figure 6.1 illustrates how to increment the redundancies and how to send the elements in case of $i > 4$. After reconstructing the half rate convolutional code, codeword 1 and codeword 1′ are transmitted alternately like figure 6.1. Then, a receiver reconstructs and decodes any low-rate decomposable code by changing the number of data copies in Weldon's ARQ protocol. At that time, a buffured old codeword is updated

to a transmittied new codeword. The low-rate decomposable code is based on reference [35]. Figure 6.2 shows the flowchart of the protocol of the proposed scheme. The operation is continued until no errors are detected or the muximum number of transmissions q is achieved.

5th transmission

codeword 1

codeword 1

$n_5 = 2$

Original codeword $+$ codeword 1

codeword 1

$$\begin{bmatrix} u_{11} & u_{12} & u_{13} & u_{14} & u_{15} & u_{16} & u_{17} & u_{18} \\ u_{21} & u_{22} & u_{23} & u_{24} & u_{25} & u_{26} & u_{27} & u_{28} \\ u_{11} & u_{12} & X & u_{14} & X & u_{16} & X & u_{18} \\ u_{21} & X & u_{23} & X & u_{25} & X & u_{27} & X \end{bmatrix}$$

reconstructed codeword $r_5 \cong 1/3$

6th transmission

codeword 1'

codeword 1'

$n_6 = 2$

reconstructed codeword $r_5 \cong 1/3$

$+$

codeword 1'   codeword 1'

$$\begin{bmatrix} u_{11} & u_{12} & u_{13} & u_{14} & u_{15} & u_{16} & u_{17} & u_{18} \\ u_{21} & u_{22} & u_{23} & u_{24} & u_{25} & u_{26} & u_{27} & u_{28} \\ u_{11} & u_{12} & u_{13} & u_{14} & u_{15} & u_{16} & u_{17} & u_{18} \\ u_{21} & u_{22} & u_{23} & u_{24} & u_{25} & u_{26} & u_{27} & u_{28} \end{bmatrix}$$

reconstructed codeword $r_6 = 1/4$

Figure 6.1   Example of method of reconstructing decomposable codes $1/2 < r_i$.
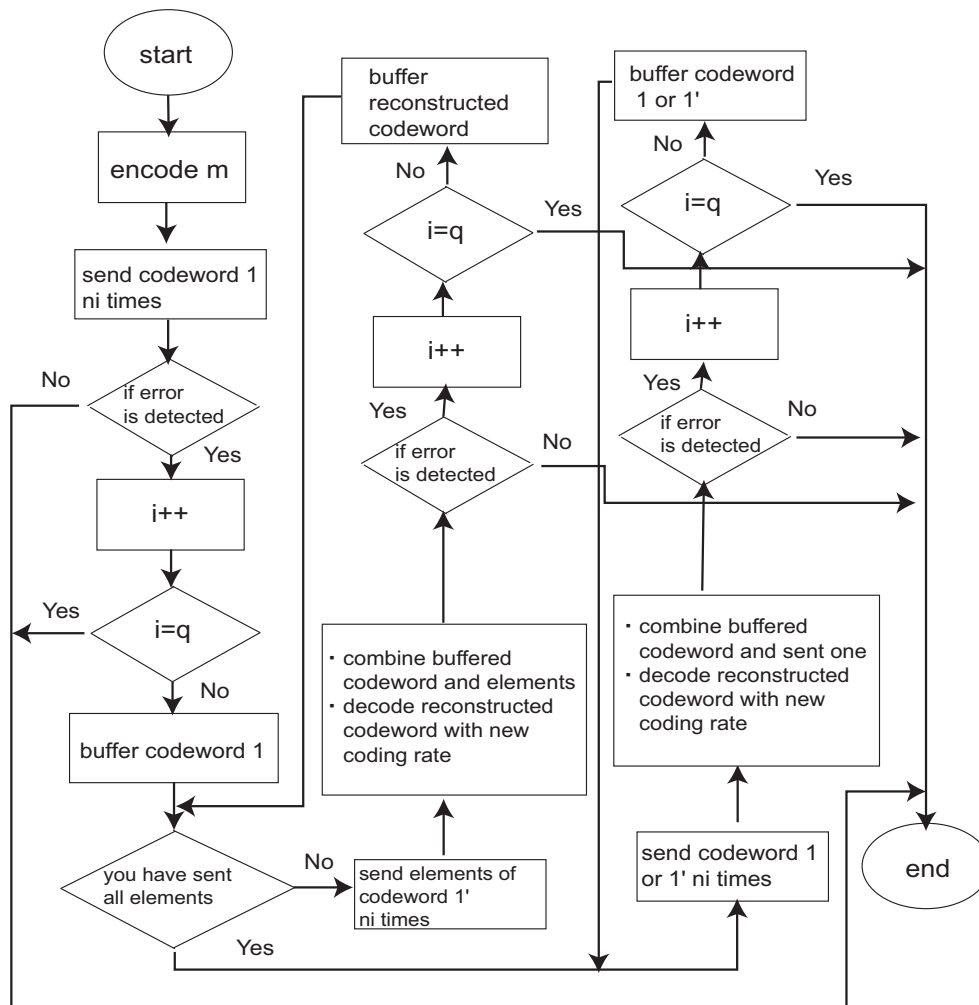
Figure 6.2 Flowchart of the proposed ARQ protocol utilizing extended decomposable codes.

It can be said that this extended scheme is similar to the type I hybrid ARQ.

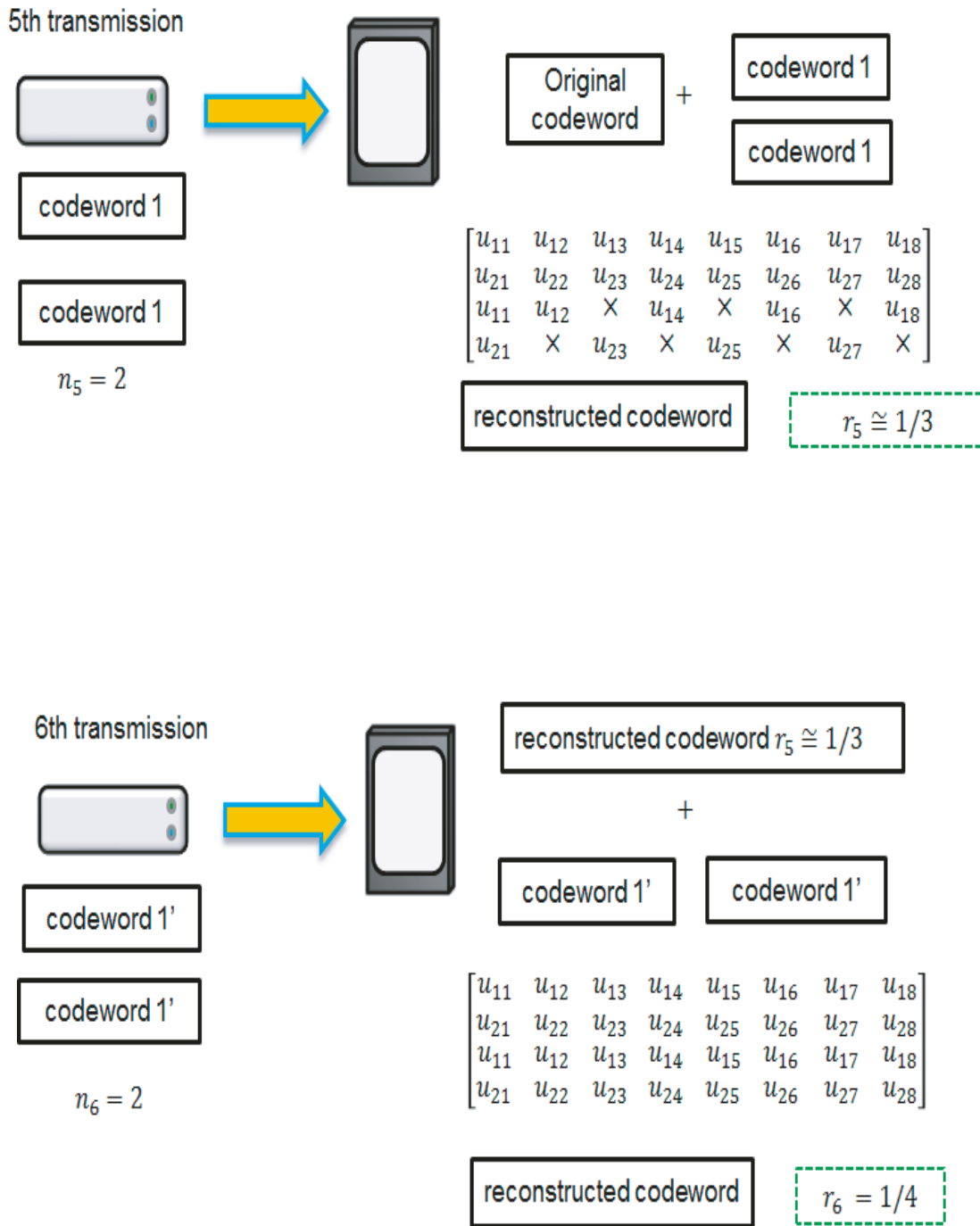## 6.2 Energy efficiency model

The energy consumption modeling of our proposed scheme is based on [36] and is calculated as

$$E_{link} = (T_{TOT} + N_{tx}T_{ACK})(P_{tx,RF} + P_{tx,circ} + P_{rx}) + N_{tx}(\epsilon_{enc} + \epsilon_{dec}) \quad \text{(6–1)}$$

$$T_{TOT} = \sum_{i=1}^{N_{tx}} \frac{L_{packet,i}}{R} \quad \text{(6–2)}$$

$$L_{packet,i} = L_{PHR} + L_{SHR} + L_{PSDU,i} \quad \text{(6–3)}$$

$$L_{PSDU,i} = n_{block,i}m_{tbit,i} \quad \text{(6–4)}$$

$$T_{ACK} = \frac{L_{ACK}}{R}, \quad \text{(6–5)}$$

where L_{ACK} is ACK packet length, R is data rate, L_{PHR} is length of physical layer header (PHR), L_{SHR} is length of synchronization header (SHR), $L_{PSDU,i}$ is length of physical layer service data unit (PSDU) for i_{th} transmission, $L_{packet,i}$ is length of i_{th} transmission, N_{tx} is the number of transmissions, T_{TOT} is duration of N_{tx} transmissions, $P_{tx,RF}$ is transmitter RF power consumption, $P_{tx,circ}$ is transmitter circuitry power consumption, P_{rx} is receiver power consumption, ϵ_{enc} and ϵ_{dec} are the encoding and decoding energies, $m_{tbit,i}$ is the number of transmitted bits and $n_{block,i}$ is the number of copy blocks of Weldon's ARQ at the i_{th} transmission. PSDU length is changed in every retransmission according to the used decomposable error crrecting codes method.

Then, ϵ_{enc} and ϵ_{dec} for the decomposable coding are calculated as [37]

$$\epsilon_{enc} = \frac{P_{convenc}}{R} L_{info}^2 \quad \text{(6–6)}$$

$$\epsilon_{dec} = \frac{P_{vitdec}}{R} L_{info}^2, \quad \text{(6–7)}$$

where $P_{convenc}$ [nW/bit] is the encoding power of a convolutional code, P_{vitdec} [nW/bit] is the decoding power of viterbi decoding and L_{info} is the number of information bits in a code word. Values of $P_{convenc}$ and P_{vitdec} are referred from [37]. Finally, energy efficiency is defined as

$$\eta \triangleq \frac{\lambda}{E_{link}} \quad \text{(6–8)}$$

$$\lambda \triangleq P_{succ}L_{info} \quad \text{(6–9)}$$

where λ is the number of successfully received information bits and P_{succ} is the probability of successful transmission.

6.3   Performance evaluations

6.3.1   Simulation conditions

In this section, the simulation model developed for the performance evaluation of the proposed scheme is described.

At the beginning, two data types (Data A and Data B) with different applicable QoS standards are considered. Low RBER is required for Data A, while low redundancy is needed for Data B, to maximize energy efficiency and reduce latency. Data A is assumed to be a physiological parameter with a low data rate, for example blood pressure, SpO2, or temperature, and Data B to be a waveform such as an ECG output. The transmission order and error control processes of different types of data packet depend on the QoS level required. Table 6.1 summarizes the characteristics of the different data types. The required data rates are taken from [38]. RBER is the ratio of bit errors when the maximum number of retransmissions has been reached. The parameters of Weldon 's ARQ protocol were set as shown in Table 6.2.

Table 6.1   Characteristics of different data types.

Data Types	Data A	Data B
User priority	5	6
RBER	restricted $< 10^{-6}$	allowable $< 10^{-2}$
Redundancy	allowable	restricted
The maximum number of transmissions, q	11	5
Required data rate	160 bps	2.4 kbps

Table 6.2   The number of data copies in Weldon's ARQ n_i.

i	0	1	2	3	4	5	6	7	8	9	10
Data A, n_i	1	4	4	5	5	6	6	8	8	8	8
Data B, n_i	1	1	2	3	4	-	-	-	-	-	-

Two types of situation are considered, as shown in Figure 6.3. Here, d_j means the distance from the jth other WBAN of an objective WBAN. In Case 1, a general case, other WBANs follow a uniform distribution within three meters of the objective WBAN. A path loss of transmission power from the other WBANs

is treated as a free space propagation loss. IEEE802.15.6 CM4 [34] is applied to the channel model from the other WBANs. IEEE802.15.6 CM4 defines a channel model between a WBAN node or hub and an external device. In Case 2, the other WBANs are placed more closely to the objective WBAN. This case applies IEEE802.15.6 CM3 [34], which is a channel model for a wearable WBAN under interference from other WBANs. In this scenario, the other WBANs are not regarded as external devices but as an asynchronous wearable WBAN node. This constitutes the worst-case scenario. With respect to the objective WBAN, IEEE802.15.6 CM3 is adopted. These channel models are derived experimentally [34]. IEEE Std. 802.15.6 allows beacon shifting or channel hopping to be utilized to allow coexistence with other WBANs. This scheme is not considered in the current study, as we wish to test the robustness of our approach and the standard approach against interference from other WBANs. To do this, we investigate whether each scheme could achieve high levels of dependability under poor conditions, such as the presence of significant interference.

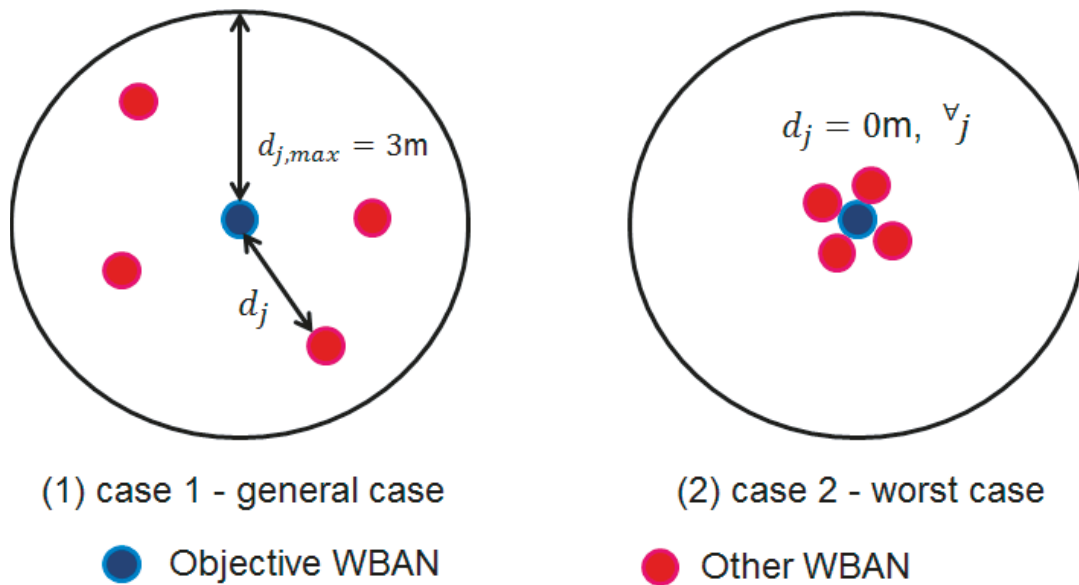**Figure 6.3** Two types of cases in computer simulations. (1) and (2) present case 1 (general case) and case 2 (worst case), respectively.

The main simulation parameters are listed in Table 6.3. The power consumption parameters for the transceivers are based on [36], [39], and [40]. In the simulations, we compare our proposed scheme with both the modes defined in the IR-UWB PHY specifications of IEEE 802.15.6 [22]: default mode with

optional modulation and high QoS mode with mandatory modulation. DBPSK and DQPSK modulation are therefore utilized. In the simulations of the standard scheme, Data A is transmitted using the default mode with ordinary ARQ, whereas Data B is transmitted using the high QoS mode with hybrid ARQ. If errors are detected, the system retransmit until the maximum number of retransmissions is reached. The spreading factor N_s is then changed based on the modulation scheme, as the data rate is fixed. For DBPSK, N_s=7, while for DQPSK, N_s=15. As our main focus is on the performance of the payload (PSDU), we assume that the control process is completed in a time slot, and the signaling or control overhead is not considered in the simulations.

Table 6.3   Simulation parameters

Parameter	Detail
Channel model	IEEE802.15.6 CM3, CM4
Bandwidth	499.2MHz
Central frequency	3.99GHz
Modulation	DBPSK, DQPSK
FEC	R=8/9 $\sim$ 1/16, K=3 convolutional codes
Decoding	Soft decision Viterbi decoding
ARQ protocol	Weldon's ARQ
Spreading sequence	Gold sequence
Spreading Factor, N_s	7, 15
Pulse shape	Gaussian monopulse
The number of other WBANs	0 $\sim$ 14
d_j	0 $\sim$ 3m
L_{info}	306 bits
L_{ACK}	7 bytes
R	0.557 Mbps
Time slot length	1.5ms
Superframe length	115.5ms

6.3.2   Numerical results

Figures 6.4-6.7 show the RBER, and energy efficiency of the proposed scheme with each mode defined in IEEE 802.15.6 as a function of the energy per symbol to noise power spectral density (E_s/N_0). The number of other WBANs is set at five. In Case 1, the proposed scheme satisfies each QoS level under lower E_s/N_0

conditions, whereas the standard approach does not. The RBER performance of our proposed scheme is clearly better than that of the standard scheme. For Data A, the difference between the proposed scheme and the standard scheme is approximately 8.5-10 dB. For Data B, our proposed scheme more successfully mitigates the RBER the high QoS mode. The energy efficiency of IEEE.15.6 is 1.5-3 [information bit/μJ] greater than that of our proposed scheme under high SNR conditions. Our proposed scheme needs retransmissions to reach the required error correction capacity, and therefore larger power consumption. However, this higher performance can be achieved under a range of SNRs. The standard scheme needs fewer transmissions under high SNR conditions as sufficient errors were removed in the first transmission. This meant that the standard does not have large power consumption due to retransmissions under high SNR conditions. However, it is unable to achieve this high performance under low or middle SNR conditions, even though the power consumption is high. The performances in Case 2 are worse than those in Case 1, especially when using the standard method. However, our proposed scheme is able to satisfy the required QoSs in the worst-case scenario under lower SNR conditions than the standard scheme. Under high SNR conditions in Case 2, the energy efficiency of our proposed scheme is better by 1.5-2.5 [information bit/μJ] than that of IEEE 802.15.6. This is due to the error correction of the standard scheme. For our system, the energy efficiency is better for Data A than for Data B under low SNR conditions in both Cases 1 and 2. This is because the error correction capacity for Data B was insufficient, and bit errors can not be sufficiently reduced under these conditions. Table 6.4 shows the average difference in performance between Cases 1 and 2. The difference achieved by our proposed scheme is 4-71 % smaller than that of IEEE 802.15.6. The proposed method was shown to achieve a good performance in the worst case, suggesting that it is more dependable than IEEE 802.15.6. It can be seen from Table 6.4 that the difference in RBER for Data B of the standard scheme is smaller than that of the proposed scheme in the DQPSK modulation. This reflects the poor RBER performance of the standard scheme under low and middle SNR conditions.

Figures 6.8-6.11 show the energy efficiency, and RBER performance of the proposed scheme at each mode defined in IEEE802.15.6 as a function of the number of other WBANs. E_s/N_0 is set to 5 dB in the DBPSK modulation and 8dB in the DQPSK modulation, respectively. The results mirror those presented in Figures 6.4-6.7. In Figure 6.8, the RBER of Data A is not plotted

Figure 6.4 RBER performance as a function of E_s/N_0 in DBPSK modulation. The number of other WBANs is five.

Table 6.4 Average difference of each performance as a function of E_s/N_0 between Case 1 and Case 2. The number of other WBANs is five.

	Proposal Data A	Proposal Data B	Standard Data A	Standard Data B
log_{10}(RBER) DBPSK	0.7645	2.4947	2.5945	2.7468
log_{10}(RBER) DQPSK	0.7800	2.1679	1.5146	1.7875
Energy efficiency (bit/μJ) DBPSK	3.486	4.160	5.147	5.599
Energy efficiency (bit/μJ) DQPSK	1.535	2.010	2.336	3.044

because all errors are removed by the large error correcting capacity. As the number of other WBANs increases, the performance deteriorate. However, the

Figure 6.5   RBER performance as a function of E_s/N_0 in DQPSK modulation. The number of other WBANs is five.

proposed scheme satisfies the QoSs for two data sets. In contrast, the standard perform very poorly, especially in Case 2. This suggests that the standard scheme is not robust against strong interference from other WBANs. In Case 1, the energy efficiency performance of the high QoS mode is inferior to those for Data A of the proposed scheme, with a maximum difference in energy efficiency of 2 [information bit/μJ]. The standard scheme has a poor RBER performance under small interference conditions in both modulation cases, whereas the RBER performance of our scheme under the same conditions is good. The superior performance of our scheme reflects the previous analysis. In these simulations, parameters such as E_s/N_0 are taken from these references. Table 6.5 summarizes the difference in performance between Cases 1 and 2. The difference for Data A in IEEE 802.15.6 for both modulation cases is very small because of the very poor performance in both Cases 1 and 2. Then, the difference for Data B of IEEE 802.15.6 is smaller than that of our system in the DQPSK modulation, because of its poor performance in the worst case.
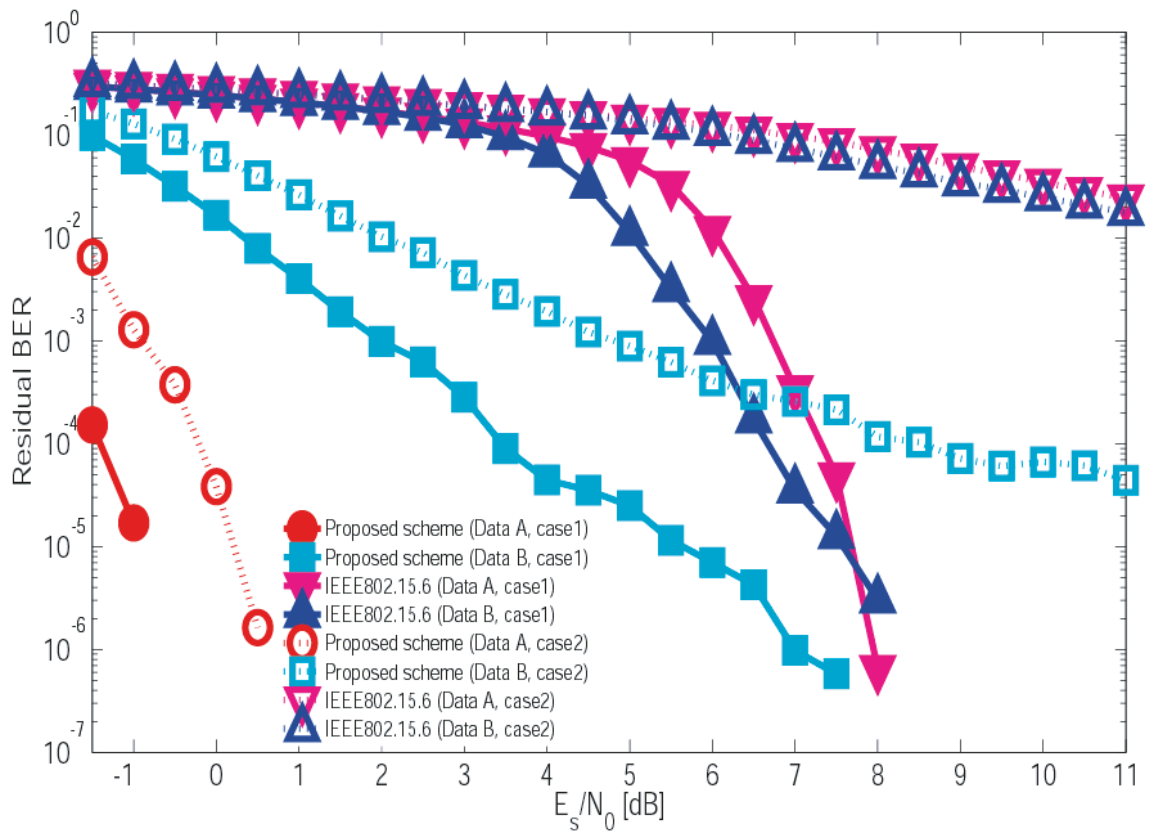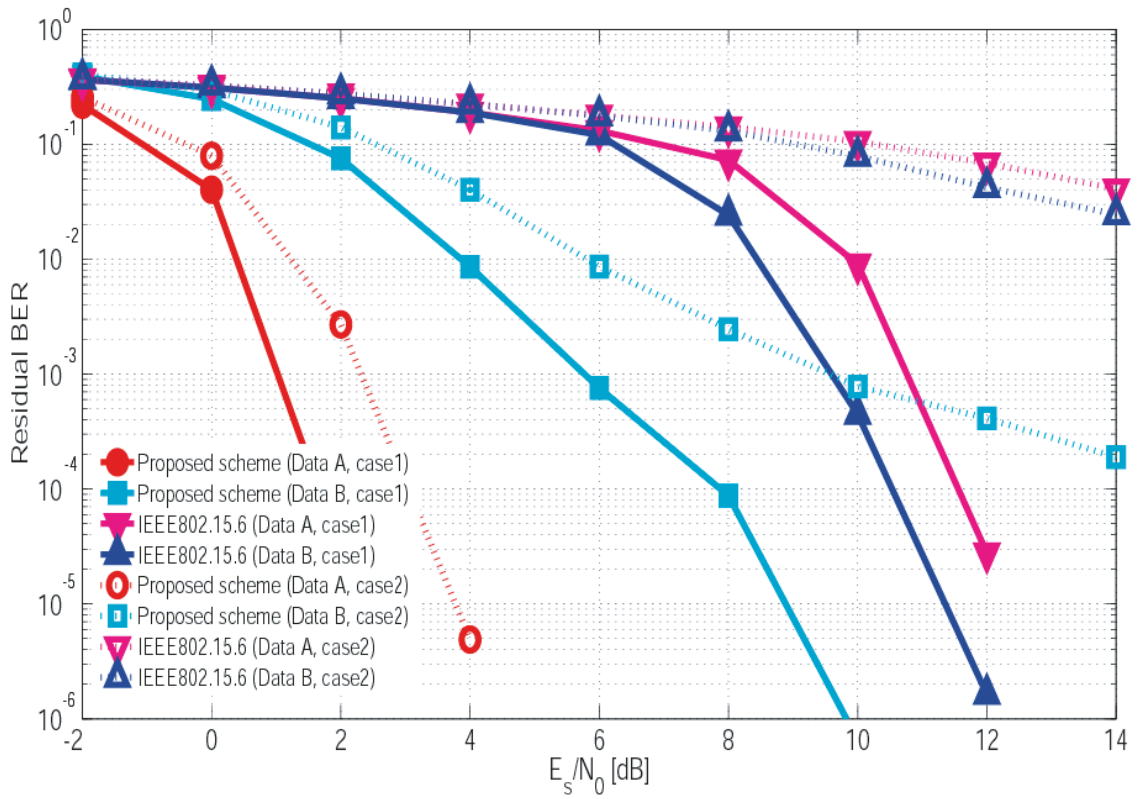
Figure 6.6 Energy efficiency performance as a function of E_s/N_0 in DBPSK modulation. The number of other WBANs is five.

Table 6.5 Average difference of each performance as a function of the number of other WBANs between Case 1 and Case 2. E_s/N_0=5dB (DBPSK) and 8dB (DQPSK).

	Proposal Data A	Proposal Data B	Standard Data A	Standard Data B
log_{10}(RBER) DBPSK	0	1.7269	0.3428	0.8721
log_{10}(RBER) DQPSK	0.4989	1.5683	0.2628	0.5891
Energy efficiency (bit/μJ) DBPSK	1.517	2.256	0.2595	2.695
Energy efficiency (bit/μJ) DQPSK	1.320	2.080	0.106	1.556

Figures 6.12-6.15 show the performance as a function of allowed delay with E_s/N_0= 5 dB and E_s/N_0= 8 dB using DBPSK modulation. The allowed delay
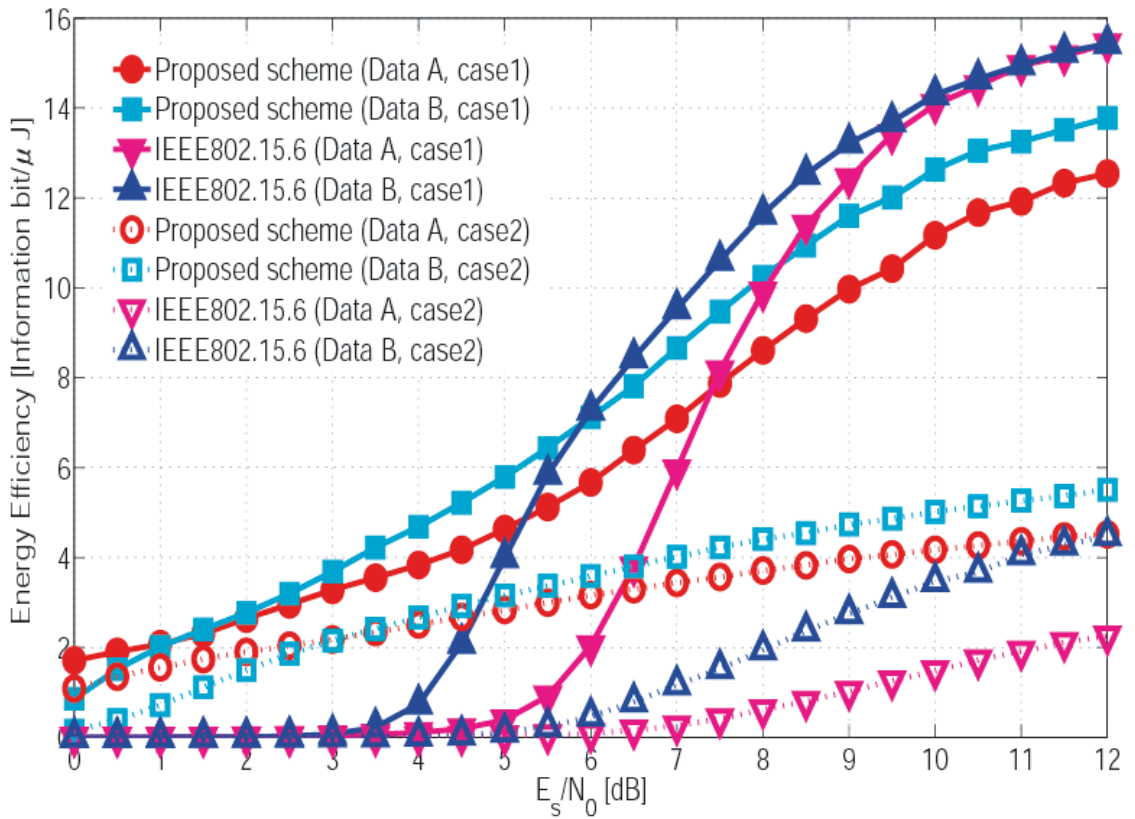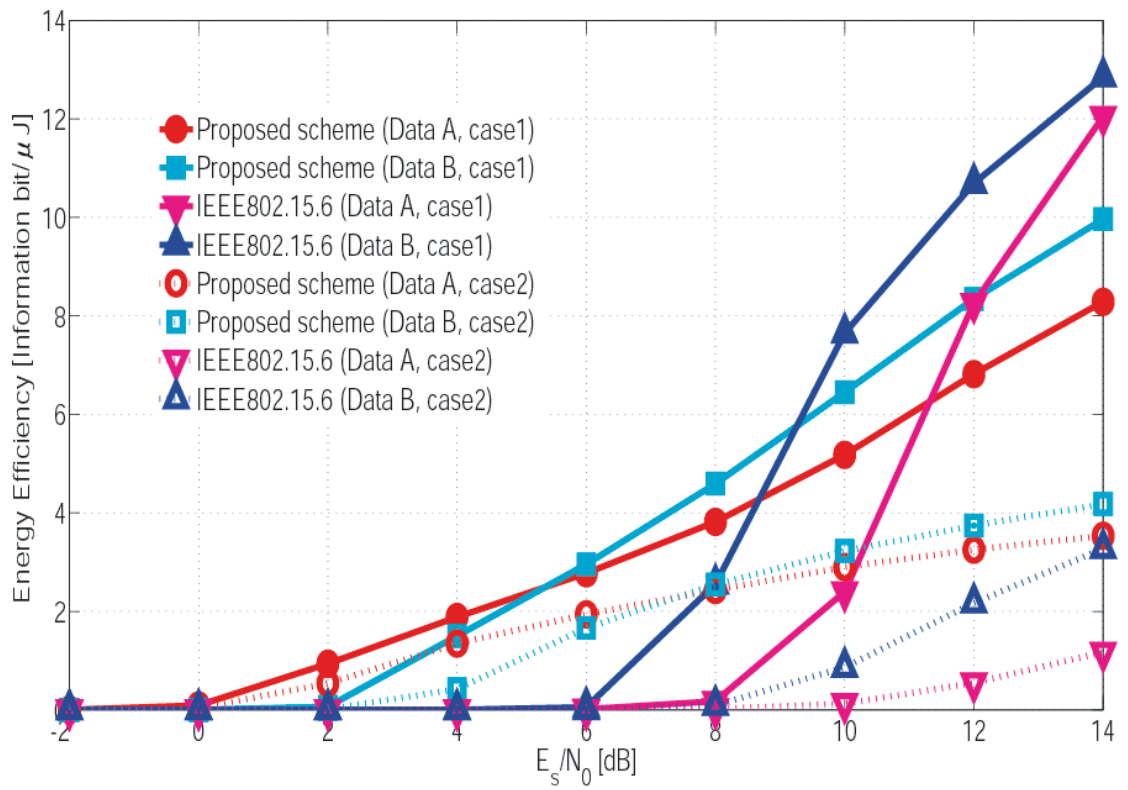
Figure 6.7 Energy efficiency performance as a function of E_s/N_0 in DQPSK modulation. The number of other WBANs is five.

affects the number of retransmissions that can be performed within the latency requirements for the particular data type. It can be seen that as the allowed delay became longer, the performance of the proposed scheme improves. This is especially true under poor channel conditions such as those shown in Figures 6.12-6.15, because the error correction for each retransmission is increased. These delays are acceptable for the target applications. In contrast, the performance of the standard method does not improve at low SNRs, even when the allowed delay is increased. This is because error correction does not increase with retransmission. In Case 1, the maximum energy efficiency of our proposed scheme is 2.5 [Information bit/μJ] higher than that of the standard scheme for Data B, and approximately 4.5 [Information bit/μJ] greater than the standard for Data A. In Case 2, the maximum energy efficiency is approximately 3 [Information bit/μJ] higher than that of IEEE 802.15.6 for both Data A and Data B. Under high SNR conditions, the standard has a better performance at smaller allowed delay times than the proposed scheme in the general case. This is
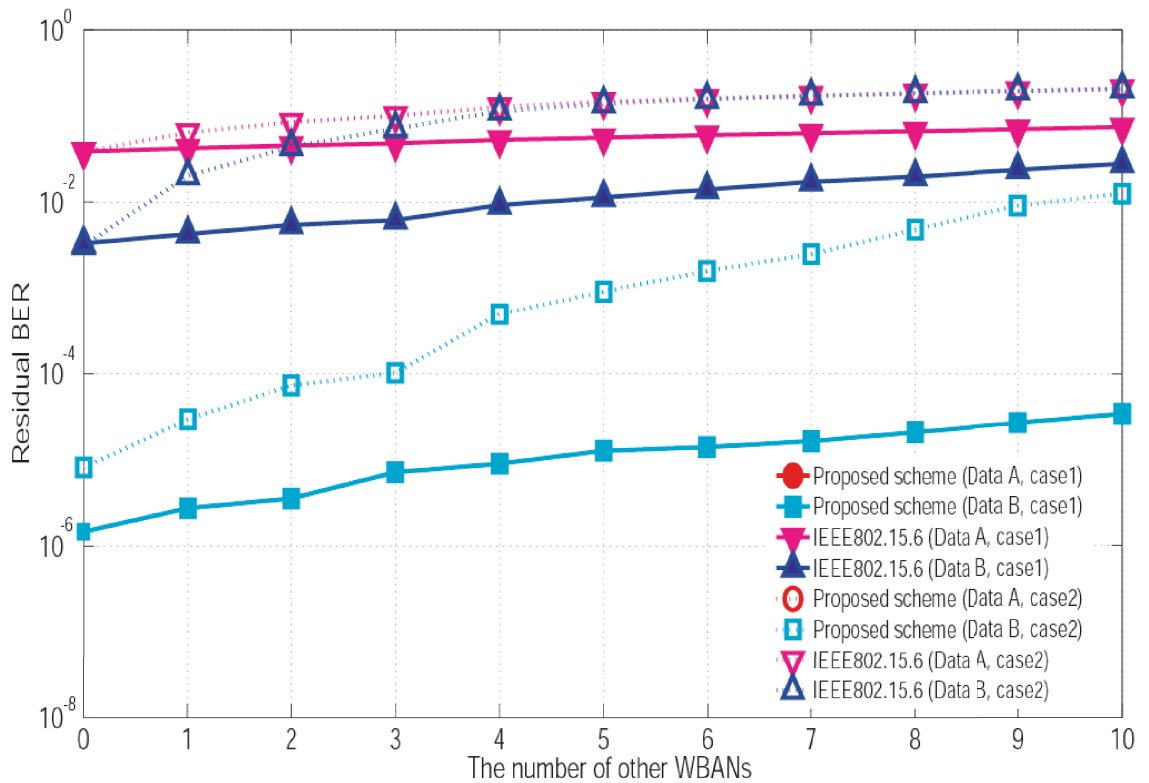
Figure 6.8 RBER performance as a function of the number of other WBANs in DBPSK modulation. E_s/N_0=5dB.

because the error correction of the standard is sufficient to remove errors at the first transmission. The maximum energy efficiency of the standard was 0.2 [Information bit/μJ] greater than that of the proposed system for both Data A and Data B. However, this difference is very small. In contrast, the performance of our proposed scheme is superior to that of IEEE 802.15.6 in the worst case, because the error correction of the standard scheme is insufficient in this case and the standard scheme is unable to increase the error correction at each retransmission. The maximum energy efficiency of our proposed method is 3.5 [Information bit/μJ] larger than that of IEEE 802.15.6 for Data A. Tables 6.6 shows the difference in performance as a function of the allowed delay between Cases 1 and 2. As can be seen from Table 6.6, the standard scheme has a smaller difference for Data A, since the performance is poor in both cases. In terms of energy efficiency, our proposed scheme is able to reduce the difference more successfully than IEEE 802.15.6 because of its superior error correction. Table 6.6 also shows a larger difference under the high SNR condition. Especially, the
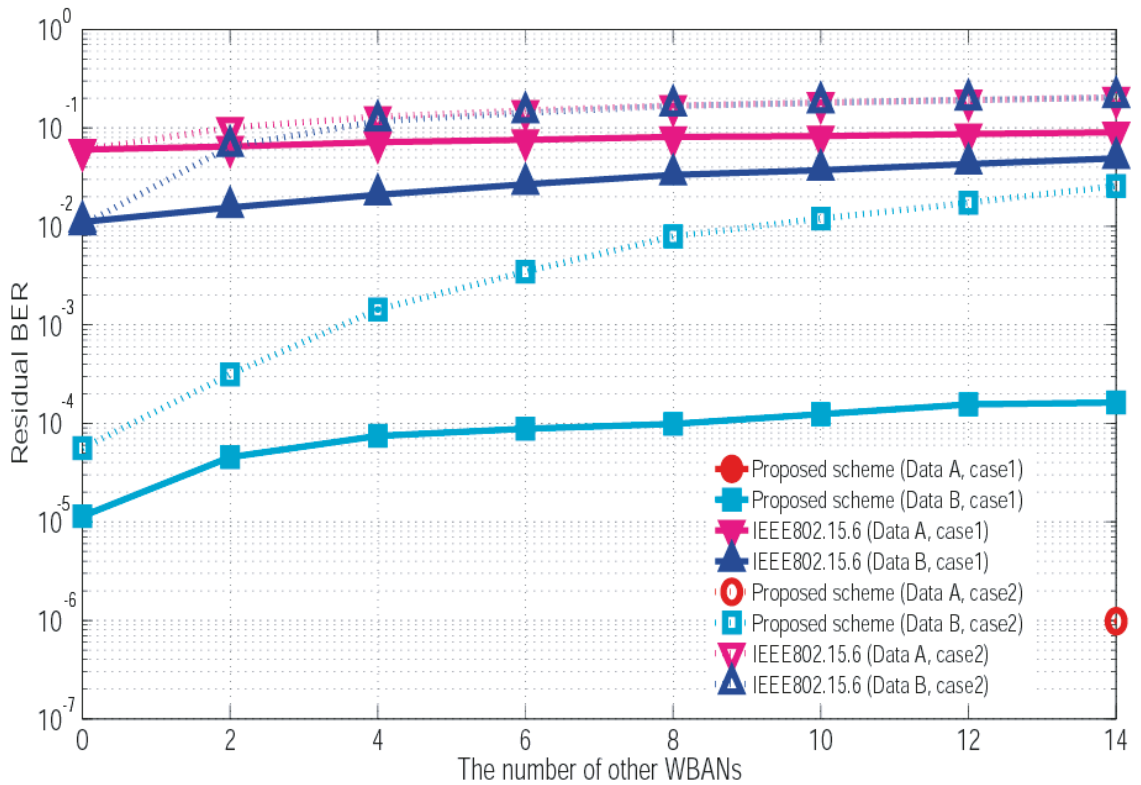
Figure 6.9 RBER performance as a function of the number of other WBANs in DQPSK modulation. E_s/N_0=8dB.

standard scheme has larger difference because it is not robust against the strong interference in the worst case scenario. Our scheme achieves a difference 4-57% smaller than that of the standard scheme. Figures 6.16-6.19 and Table 6.7 show the results as a function of the allowed delay with E_s/N_0= 8 and 12 dB using DQPSK modulation. The results mirror those for DBPSK modulation.

Finally, as an additional consideration, the computational complexity of the two schemes is summarized in Table 6.8. Here, t_{ec} is the maximum number of correctable error bits. The complexity of our proposed scheme is much less than that of the (126, 63) BCH code and almost the same as that of the (63,51) BCH code.

These results demonstrate that our proposed scheme achieved high performance with a low computational complexity in a multiple WBAN environment. It can be further observed that IEEE 802.15.6 fails to achieve a satisfactory performance under the worst-case scenario, while our proposed scheme is able to do so under both scenarios

Figure 6.10 Energy efficiency performance as a function of the number of other WBANs in DBPSK modulation. E_s/N_0=5dB.

Table 6.6 Average difference of each performance as a function of an allowed delay in DBPSK modulation between Case 1 and Case 2. The number of other WBANs is five.

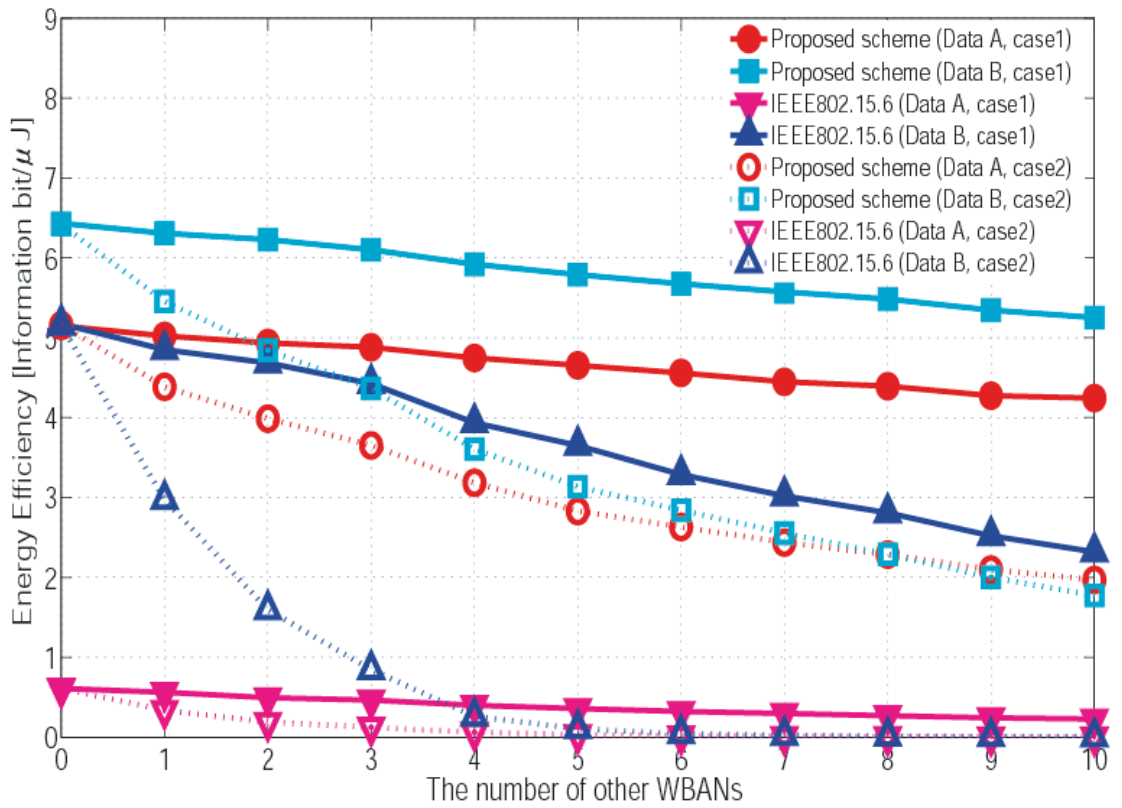|	Proposal Data A	Proposal Data B	Standard Data A	Standard Data B
log_{10}(RBER) E_s/N_0=5dB	1.3006	0.8380	0.3643	0.7374
log_{10}(RBER) E_s/N_0=8dB	1.2948	2.0552	3.0389	2.1378
Energy efficiency (bit/μJ) E_s/N_0=5dB	1.668	2.010	0.3237	2.685
Energy efficiency (bit/μJ) E_s/N_0=8dB	5.426	6.868	8.480	8.757
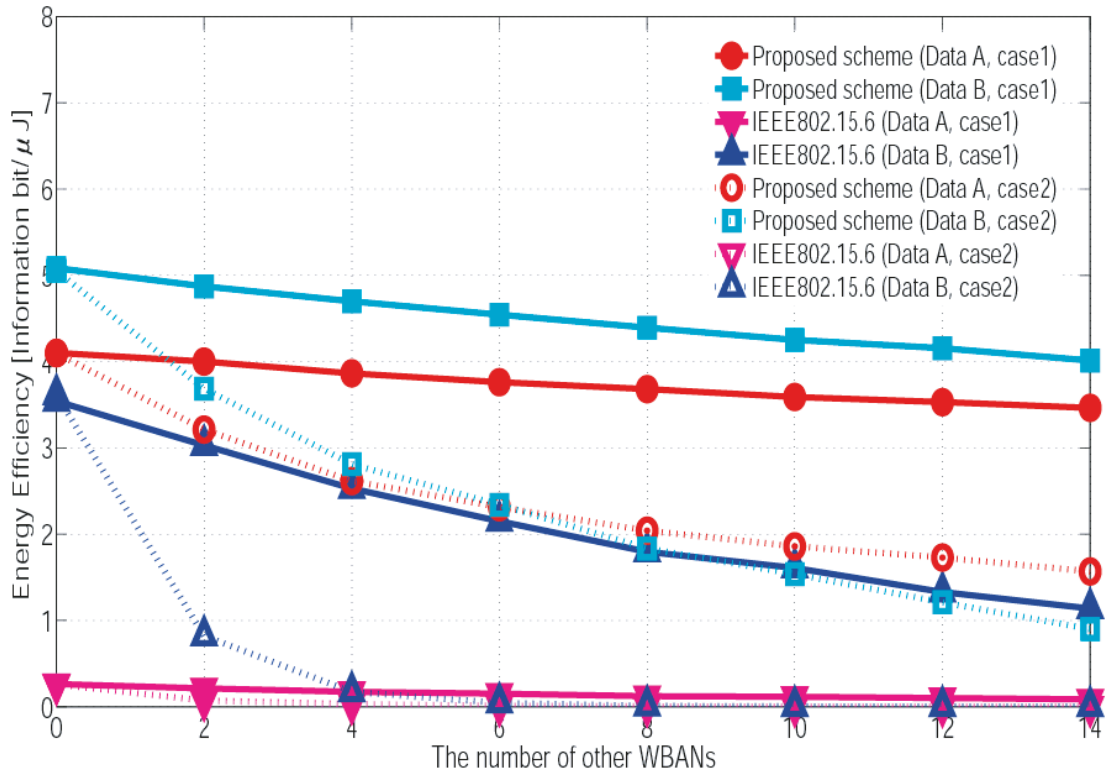
Figure 6.11 Energy efficiency performance as a function of the number of other WBANs in DQPSK modulation. E_s/N_0=8dB.

Table 6.7 Average difference of each performance as a function of an allowed delay in DQPSK modulation between Case 1 and Case 2. The number of other WBANs is five.

	Proposal Data A	Proposal Data B	Standard Data A	Standard Data B
log_{10}(RBER) E_s/N_0=8dB	1.3684	0.6987	0.2646	0.5324
log_{10}(RBER) E_s/N_0=12dB	0.8575	1.0078	2.0877	1.9898
Energy efficiency (bit/μJ) E_s/N_0=8dB	1.193	1.316	1.465	1.677
Energy efficiency (bit/μJ) E_s/N_0=12dB	3.817	4.949	7.067	7.677

Figure 6.12 RBER performance as a function of an allowed delay in DBPSK modulation. The number of other WBANs is five and E_s/N_0=5dB.

Table 6.8 Computational complexity of both schemes.

	Proposed scheme $O(2^K)$	IEEE802.15.6 (63,51)BCH $O(t_{ec}^2)$	IEEE802.15.6 (126,63)BCH $O(t_{ec}^2)$
Computational complexity	8	4	100

Figure 6.13 RBER performance as a function of an allowed delay in DBPSK modulation. The number of other WBANs is five and E_s/N_0=8dB.

Figure 6.14 Energy efficiency performance as a function of an allowed delay in DBPSK modulation. The number of other WBANs is five and E_s/N_0=5dB.

Figure 6.15   Energy efficiency performance as a function of an allowed delay in DBPSK modulation. The number of other WBANs is five and E_s/N_0=8dB.
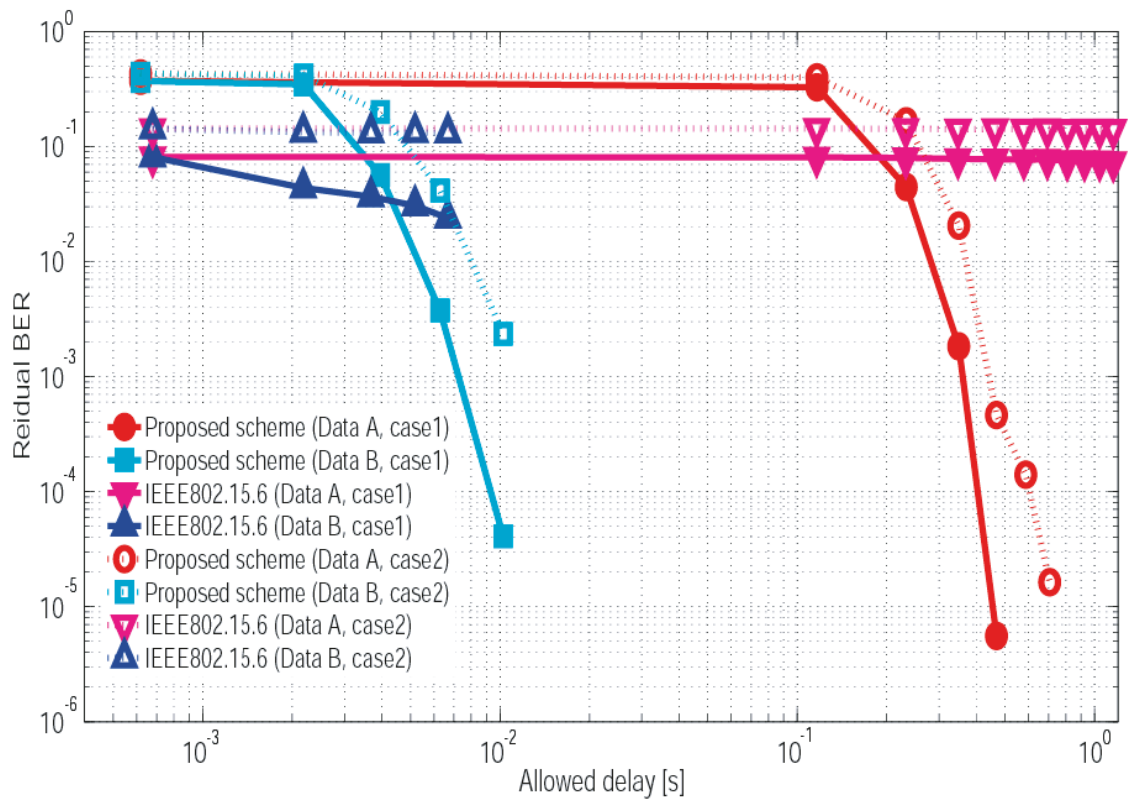
Figure 6.16 RBER performance as a function of an allowed delay in DQPSK modulation. The number of other WBANs is five and E_s/N_0=8dB.

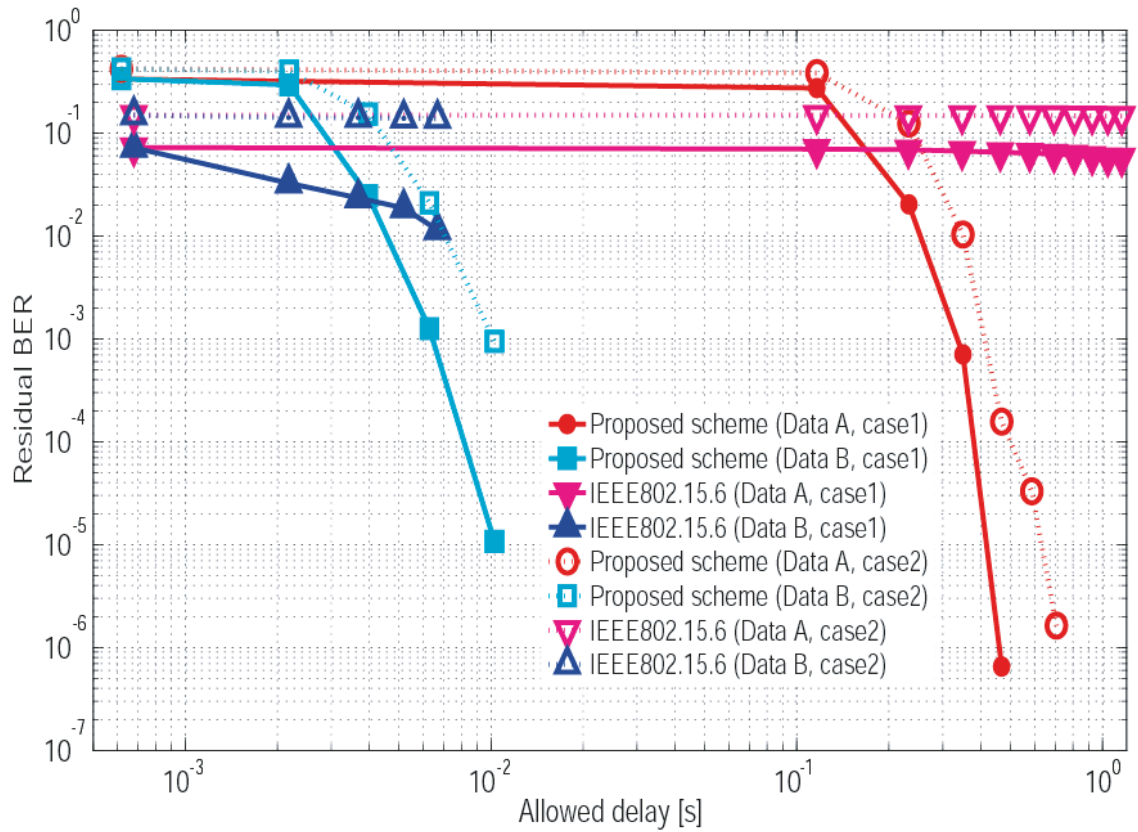**Figure 6.17** RBER performance as a function of an allowed delay in DQPSK modulation. The number of other WBANs is five and E_s/N_0=12dB.
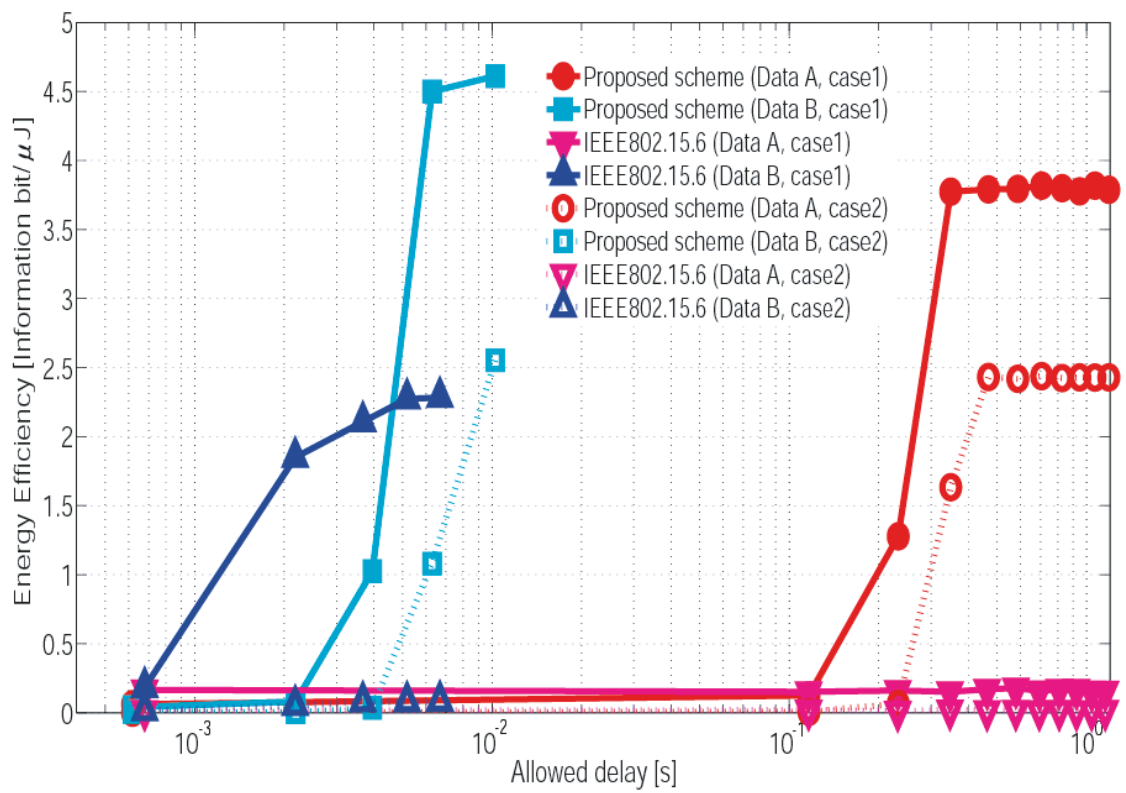
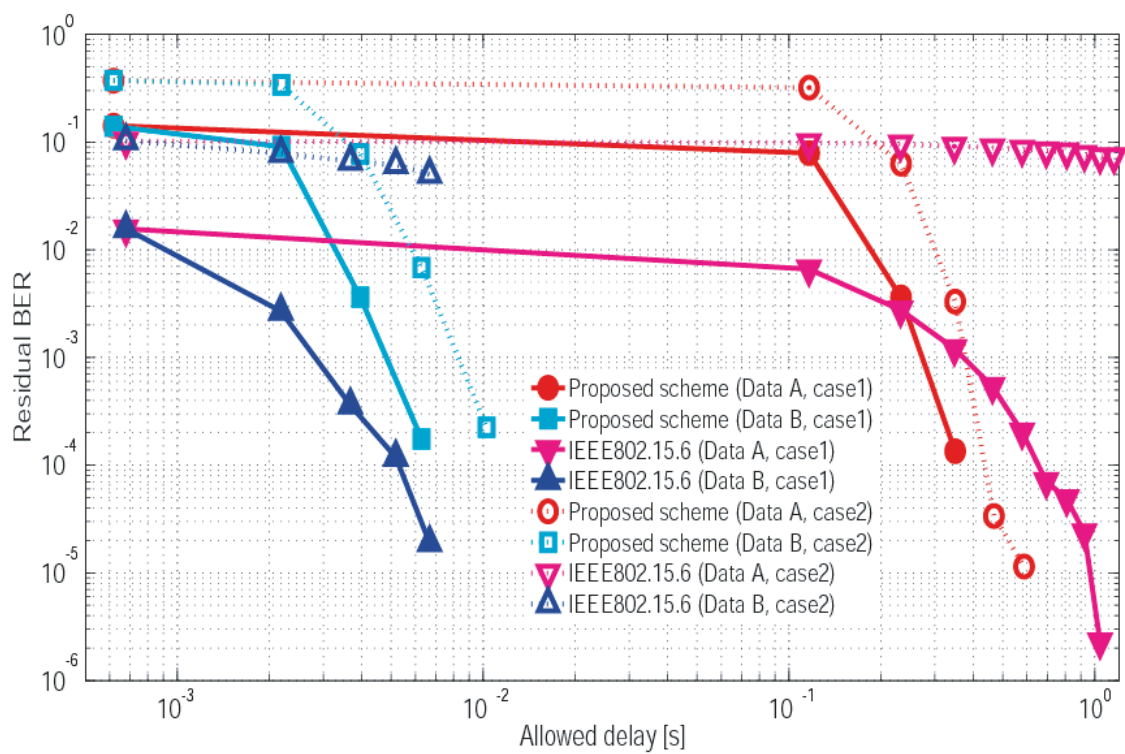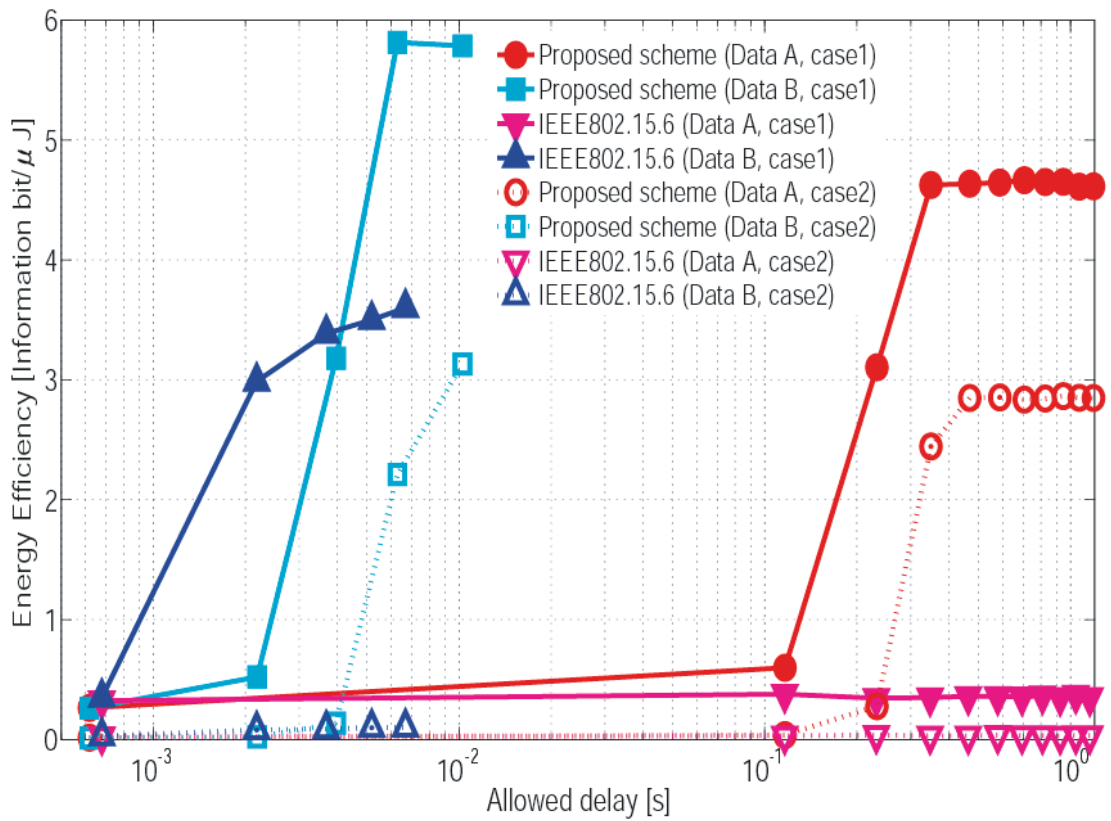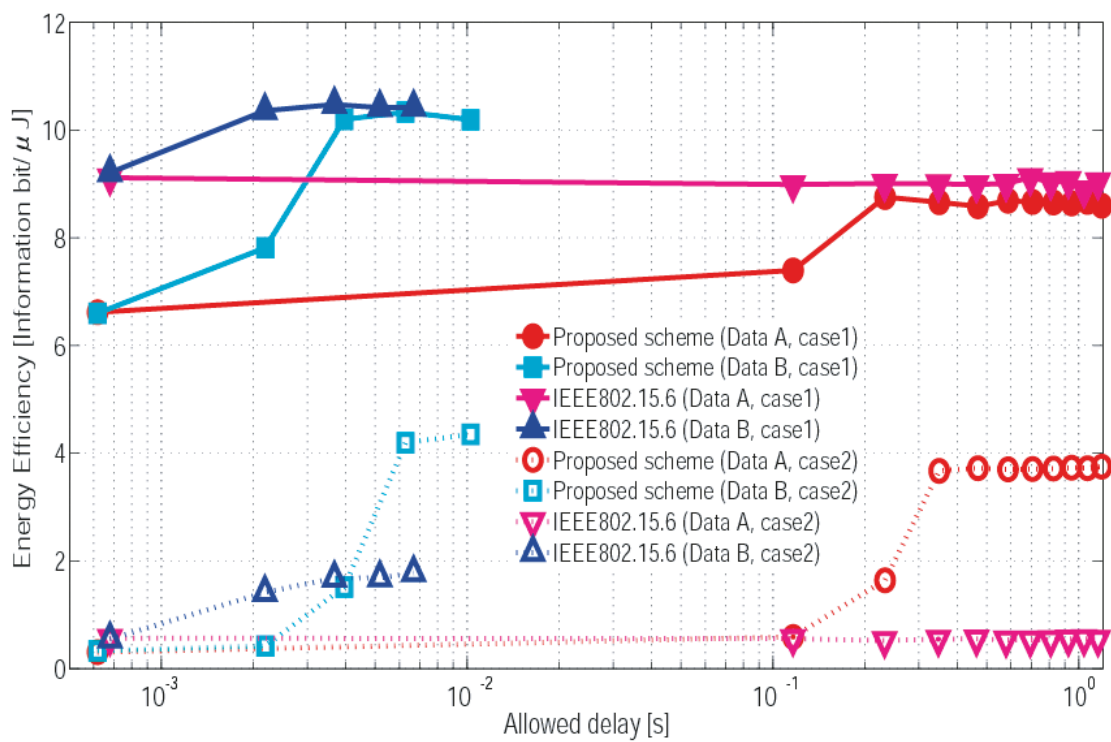**Figure 6.18** Energy efficiency performance as a function of an allowed delay in DQPSK modulation. The number of other WBANs is five and E_s/N_0=8dB.
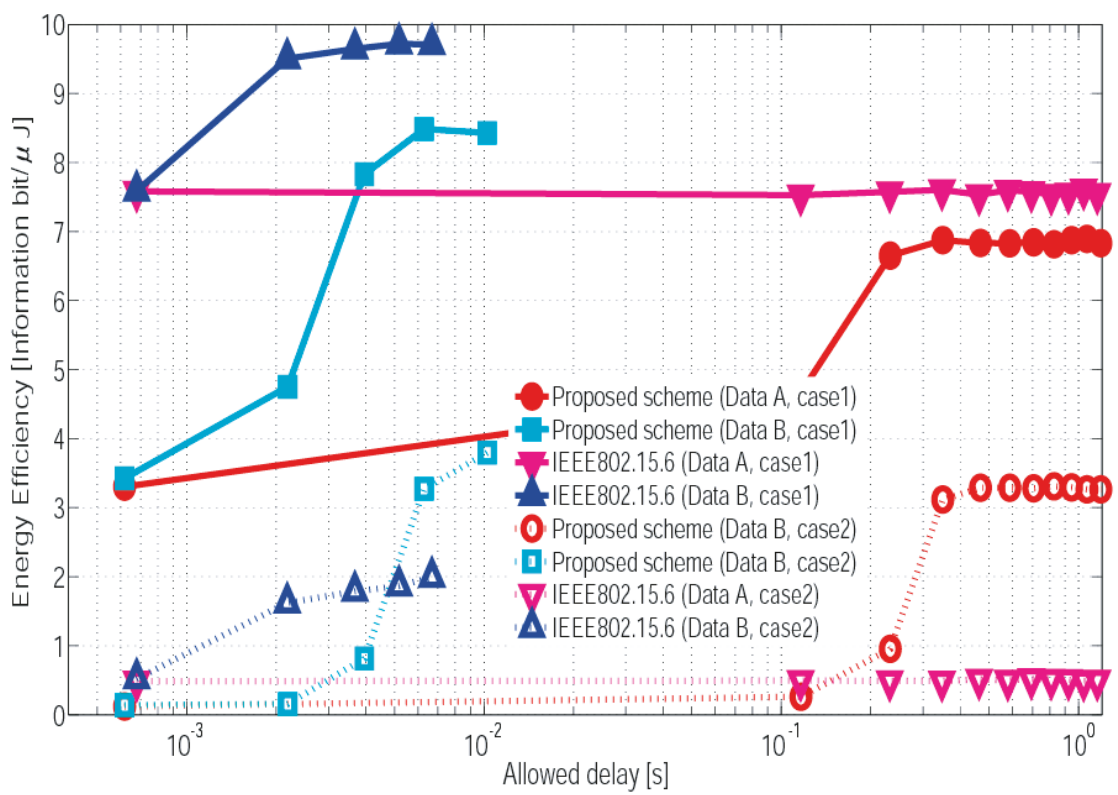
Figure 6.19   Energy efficiency performance as a function of an allowed delay in DQPSK modulation. The number of other WBANs is five and E_s/N_0=12dB.

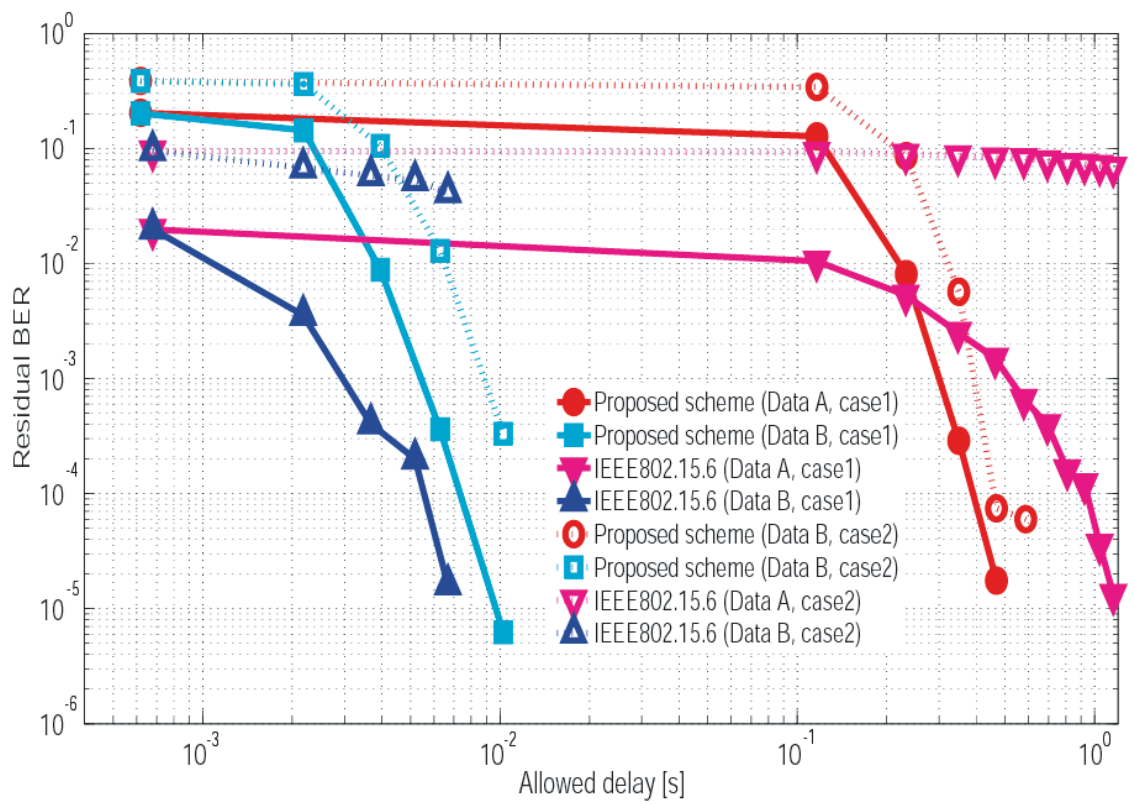# Chapter 7

Performance Evaluation in Multi-hop WBAN Based on IEEE802.15.6

In this chapter, we evaluate some performances of our QoS control scheme in the case of a multi-hop WBAN based on IEEE Std. 802.15.6. IEEE Std. 802.15.6 supports a two-hop extension [22]. Then, a WBAN extended to multihop communication is studied in order to increase the lifetime of a WBAN [41]-[42]. However, many studies of a multihop WBAN focus on an energy-efficient MAC or routing protocol, and then they do not consider an error controlling. Specifically, packet error ratio (PER), the number of transmissions and energy efficiency of our QoS control scheme proposed and IEEE Std. 802.15.6 are evaluated in the case of a two-hop extension.

7.1   Two-hop extension in IEEE Std. 802.15.6

In IEEE Std. 802.15.6, a node and a hub can utilize a two-hop extension to exchange frames through another node except in the medical implant communications service (MICS) band [22].

Figure 7.1 illustrates an example of a two-hop extended star network topology. In this figure, the terminal, intermediate nodes and the hub are turned into the relayed nodes, relaying nodes and the target hub of the relayed node, respectively. Either the relayed node or the target hub can start a two-hop extension at times determined fit by the initiator. The relaying node can also exchange its own frames with the hub directly.

A relayed node shall not send its frames to the relaying node in contended allocations provided by the target hub. Hence, a scheduled access phase can
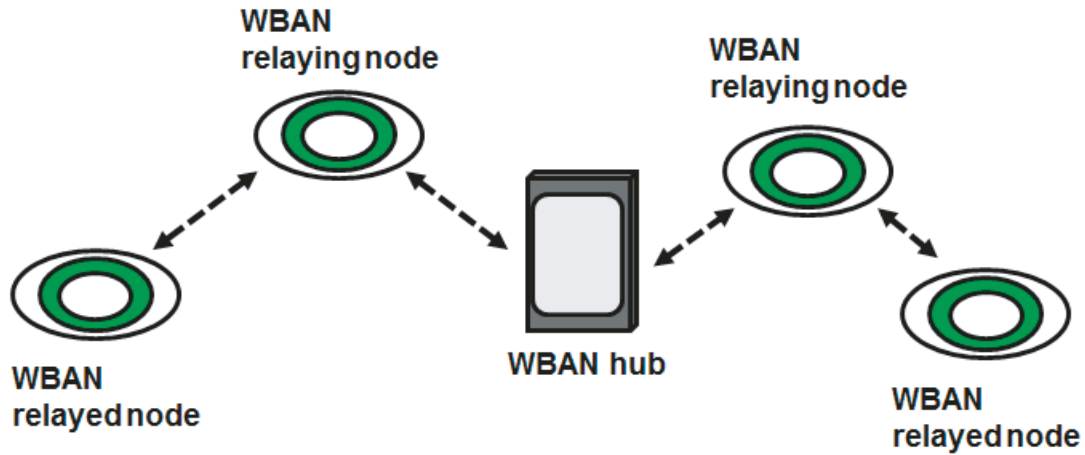
Figure 7.1 Two-hop extended star network topology [22].

only be utilized in the case of a two-hop extension. So, we assume that managed access phase (MAP) defined in IEEE Std. 802.15.6 is only utilized in this chapter.

7.2 System model in a two-hop case

It is assumed that a sensor node (N1) includes multiple sensors which produce different types of data to be transmitted through the relaying node (N2) to the target hub (H) as illustrated in Figure 7.2. The maximum number of transmissions in a two-hop extension q_{max} is expressed as follows:

$$q_{max} = q_{N1 \to N2} + q_{N2 \to H}$$
$$\geq tr_{N1 \to N2} + tr_{N2 \to H}. \tag{7–1}$$

Here, $tr_{A \to B}$ is the number of transmissions from node A to node B and $q_{A \to B}$ is the maximum number of transmissions from node A to node B. If errors are detected, the system retransmits until the maximum number of retransmissions is reached. Then, the transmission is regarded as failure if data from a sensor node does not reach the target hub.

In this chapter, two data (Data A and Data B) with different types of QoS are also considered as the previous chapter. Those QoSs and parameters of Weldon's ARQ protocol are the same as those of the previous one. Then, each q_{max} and $q_{A \to B}$ are set as shown in Table 7.1. The maximum number of retransmissions is defined as four in high QoS mode in the IR-UWB PHY of the standard. However,
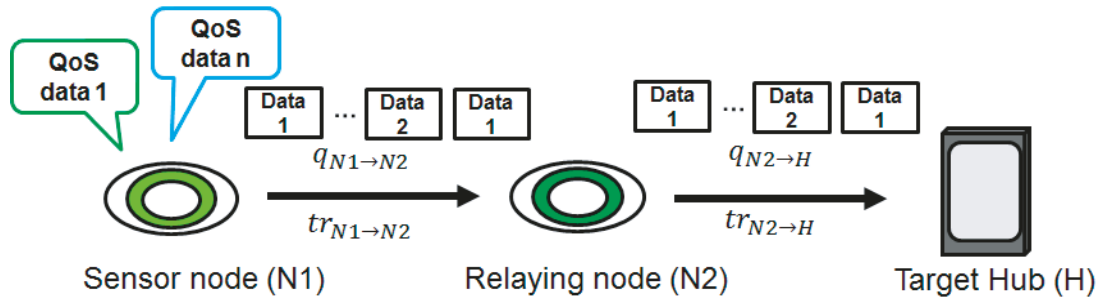
Figure 7.2 System concept in a two-hop case.

default mode in the IR-UWB PHY, the narrowband PHY and the HBC (Human Body Communication) PHY in IEEE Std. 802.15.6 do not define it. So, the parameter is set up according to the QoS of data in our previous work and is also followed in this chapter.

Table 7.1 The maximum number of transmissions.

q	$q_{N1 \to N2}$	$q_{N2 \to H}$	q_{max}
Data A	$tr_{N1 \to N2}$ $(\leq q_{max})$	q_{max} $-tr_{N1 \to N2}$	11
Data B	5	5	10

7.3 Performance evaluation

In this section, the proposed scheme and the standard scheme in a two-hop extension are evaluated by computer simulations. The main simulation parameters are listed in Table 7.2. In this simulation, a hospital room case in IEEE model CM3 is utilized as a path loss model [34].

In this performance evaluation, two proposed schemes are considered; in the first scheme (Scheme 1), data is transmitted according to a preset paramter, and then in the second one (Scheme 2), a coding rate is changed with SNR estimated by using a preamble signal according to each QoS. A channel SNR is estimated by the following equation;

$$\Gamma = \frac{|\rho|^2}{1-|\rho|^2} \tag{7-2}$$

$$\rho = \frac{\mathbf{x}^H \mathbf{r}}{\sqrt{\mathbf{x}^H \mathbf{x}} \sqrt{\mathbf{r}^H \mathbf{r}}} \tag{7-3}$$

$$0 \leq \rho \leq 1. \tag{7-4}$$

Table 7.2 Simulation parameters

Parameter	Detail
Channel model	AWGN
Path loss model	IEEE model CM3
Bandwidth (BW)	499.2 MHz
Central frequency	3993.6 MHz
Pulse shape	Gaussian mono pulse
Modulation	DBPSK
FEC	r_c=8/9～1/16
	K=3 convolutional codes
Decoding	Soft decision
	Viterbi decoding
ARQ protocol	Weldon's ARQ
Power spectral density (P_{sd})	-41.3 dBm/MHz
Thermal noise density (N_0)	-174 dBm/Hz
Implementation losses (I)	3 dB
Receiver noise figure (NF)	5 dB
Number of pulses per bit (N_{cpb})	2
Data rate (R)	7.8 Mbps
Information bit length (L_{info})	306 bits
ACK length (L_{ACK})	7 bytes

Here, Γ is an estimated SNR, ρ is a correlation coefficient, **x** is a preamble signal with noise and **r** is a preamble signal without noise or interference. Then, in Scheme 2, the criterion for determining the coding rate is as follows;

$$BER = \frac{1}{10^y} \tag{7–5}$$

$$y = \lceil \log_{10} L_{ACK} \rceil + \alpha. \tag{7–6}$$

Here, α is set as Table 7.3.

In addition, each case of the proposed scheme in each hop is summarized as Table 7.4.

Figs.7.3-7.5 show results of each performance in case that a distance of the first hop d_{1st} is changed from 10cm to 3m and a distance of the second hop d_{2nd}

Table 7.3 α of each data.

	α
Data A	3
Data B	0

Table 7.4   Case of the proposed scheme in each hop.

	N1 $\rightarrow$ N2	N2 $\rightarrow$ H
Case 1	Scheme 1	Scheme 1
Case 2	Scheme 1	Scheme 2
Case 3	Scheme 2	Scheme 2

is constant (d_{2nd}=40cm). From these graphs, our proposed scheme satisfies QoS of each data, while the standard scheme does not. Then, Case 2 and Case 3 has better energy efficiency and the average number of transmission performances than Case 1. The reason is that a coding rate is set appropriately for a channel SNR and the number of retransmissions can be reduced by utilizing the scheme. However, there is not large difference between Case 2 and Case 3. This is because d_{2nd} is a short range and the error correcting capability of coding rate $r_c = 8/9$ at the first transmission can reduce errors enough.

Figures 7.6-7.8 show results of each performance in case that a distance in two hops $d_{1st} + d_{2nd}$ is fixed to 1.5m and d_{1st} and d_{2nd} are changed. In the case that d_{1st}=1.5m, data is transmitted by only one hop. It can also be said that our proposed scheme satisfies QoS of each data, while the standard scheme does not. Then, Case 3 has the best performance. Additionally, both systems have the best performance in case that communication distance on the first hop is equal to that on the second hop. This is because d_{1st} or d_{2nd} becomes long unlike the previous condition, and then the long distance communication has an influence on performances in other cases.

Figure 7.3 PER performance in case of a constant d_{2nd}.

Figure 7.4 Energy efficiency performance in case of a constant d_{2nd}.

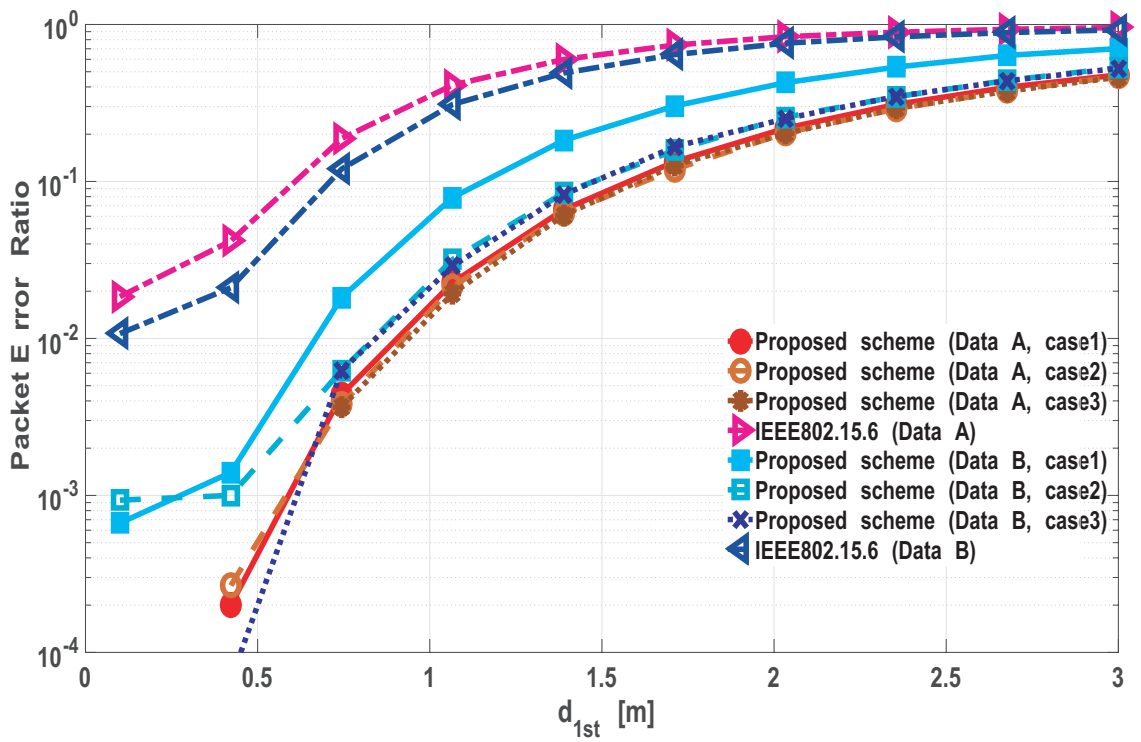**Figure 7.5** The average number of transmission in case of a constant d_{2nd}.
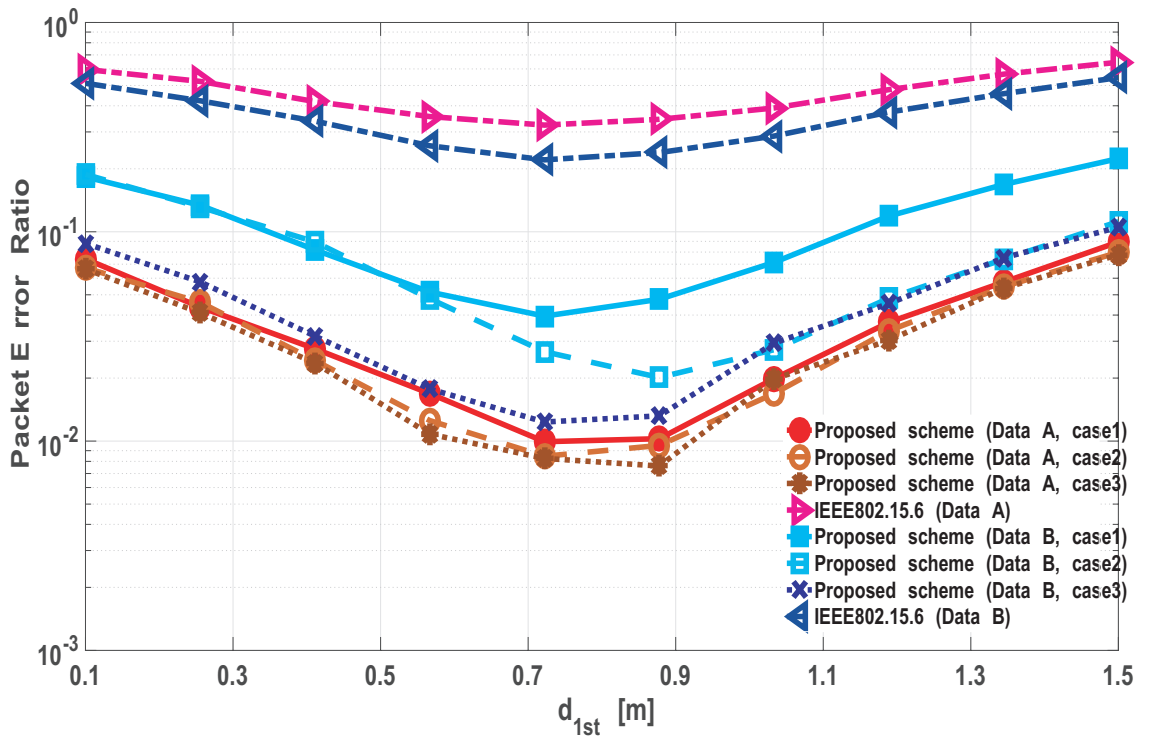
Figure 7.6   PER performance in case of a constant d_{2nd}.
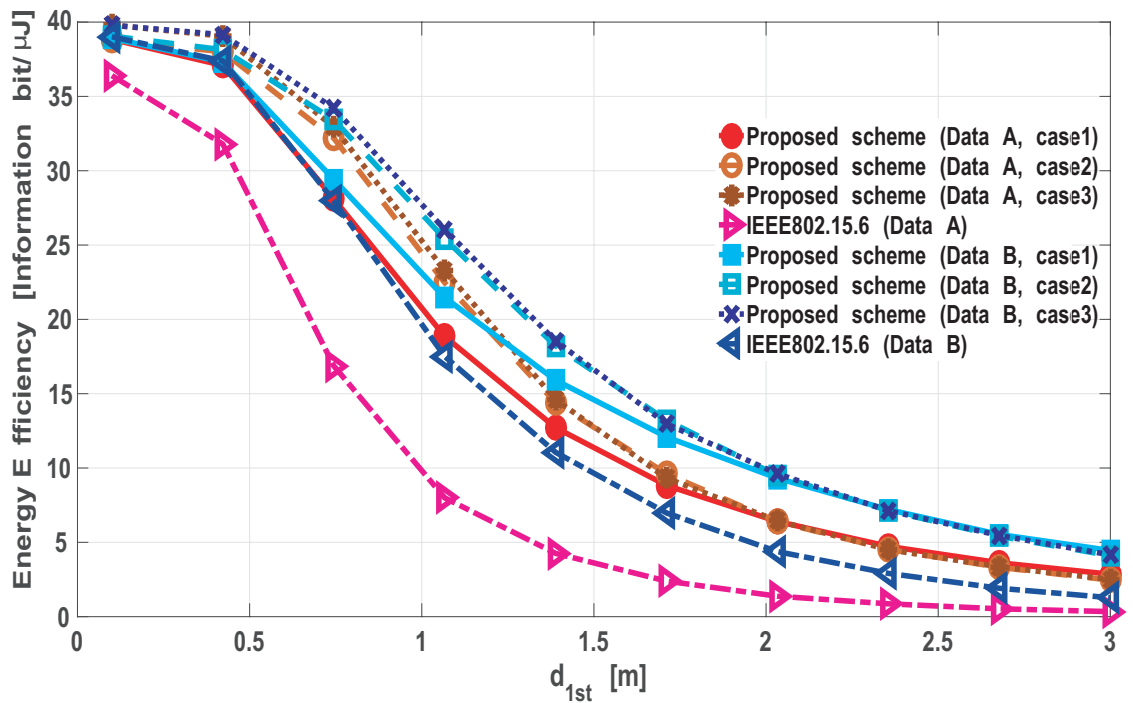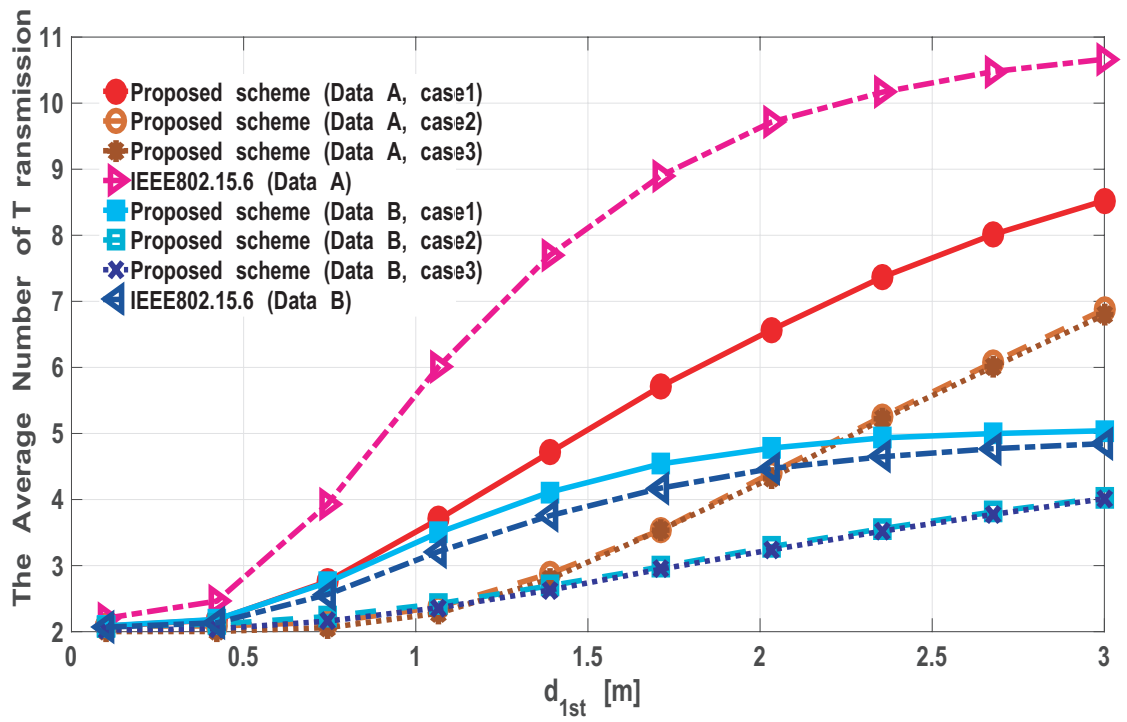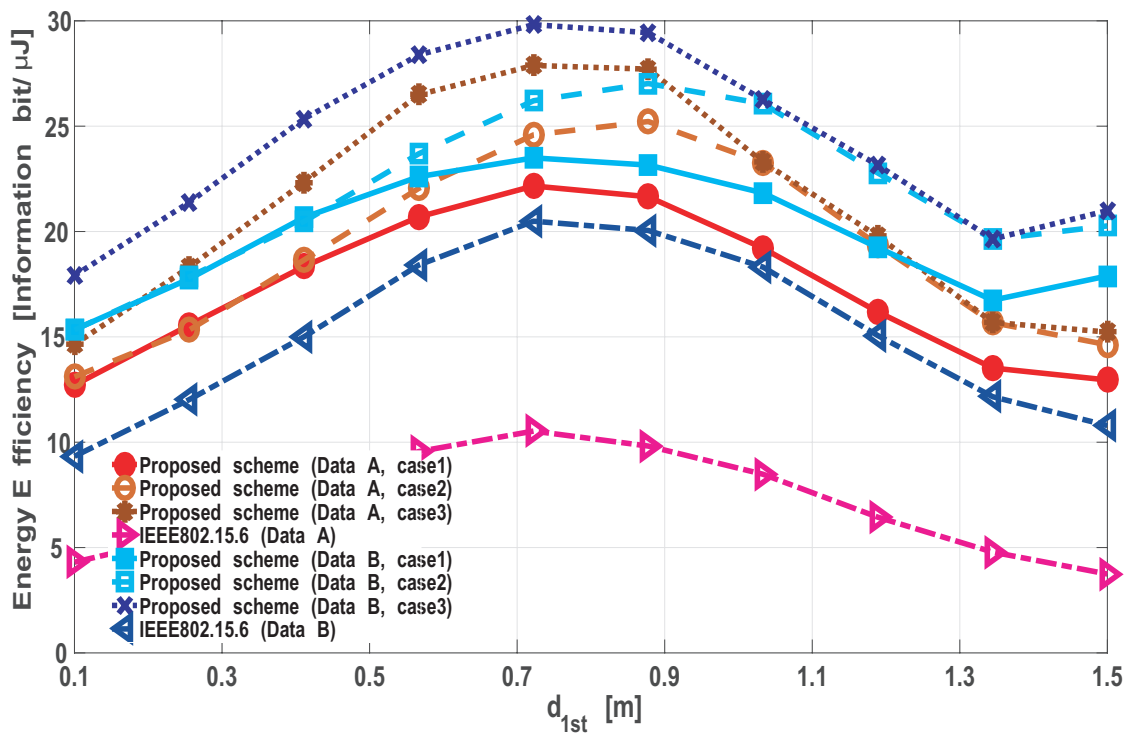
Figure 7.7 Energy efficiency performance in case of a constant d_{2nd}.
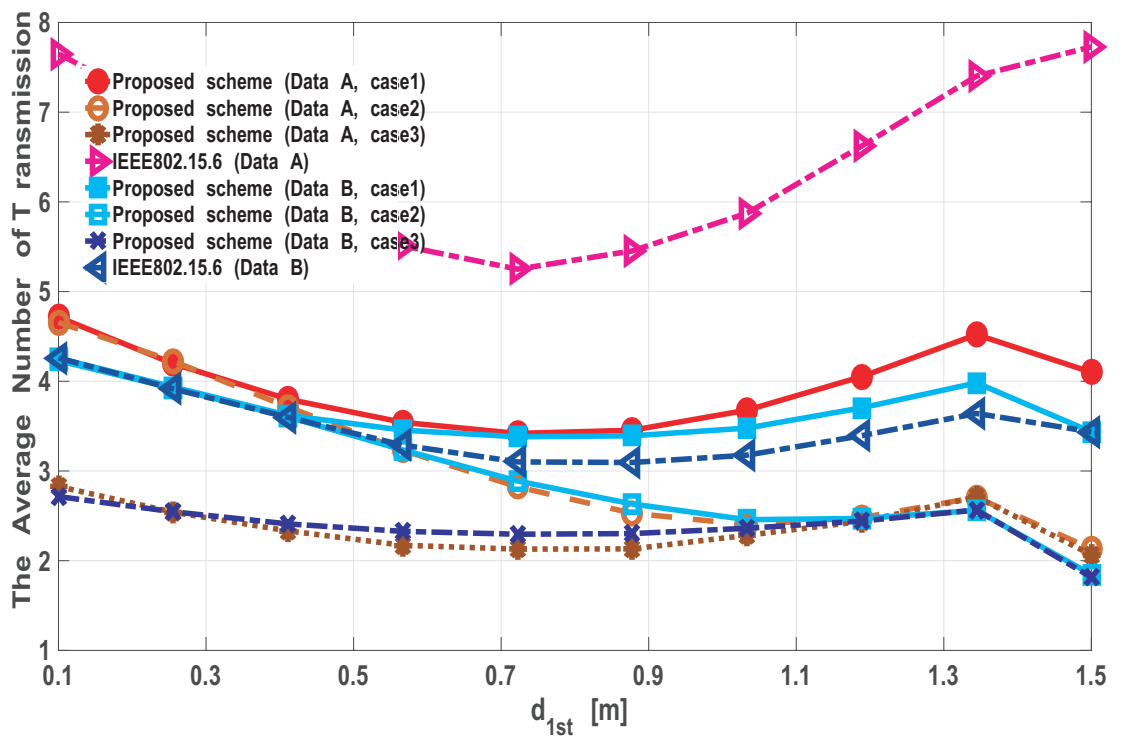
Figure 7.8 The average number of transmission in case of a constant d_{2nd}.

Chapter 8

Performance Analysis and Optimization of Cross-layer Approach

In this chapter, we analyze performance of our QoS control scheme in a cross-layer design for WBANs. A cross-layer approach is one of the most important technique in order to optimize satisfied QoS of various types of data [36],[43]-[47]. In this study, we focus on cross-layer design between PHY and MAC layers. Then, both schedule access and random access protocols are considered at the MAC layer in this chapter.

8.1   MAC protocol

In previous chapters, a schedule-based access protocol is only assumed as a MAC protocol. However, IEEE802.15.6 adopts a hybrid MAC protocol that combines a random and a scheduled access protocol. So, we analyze our error control scheme in a cross layer (PHY and MAC layer) about each access protocol. In this study, we focus on slotted ALOHA as a random access protocol, because slotted ALOHA is adopted in UWB-PHY of IEEE802.15.6 and Smart BAN [22],[24]. Then, TDMA (Time Division Multiple Access) is considered as a scheduled access protocol. In addition, this paper assumes a beacon mode with super frames, defined in IEEE802.15.6 [22].

Figure 8.1 shows an example of behavior of our scheme in the case of a random access protocol. If a collision with other data packets happens, the same data at previous transmission is sent to a WBAN hub. On the other hands, if a bit error is detected because of noise or fading, elements of the encoded data (code word) are transmitted in order to increase an error correcting capability. Then,

if data is transmitted successfully, next data is sent. By the way, it is assumed that a collision does not happen in the case of a scheduled access protocol.
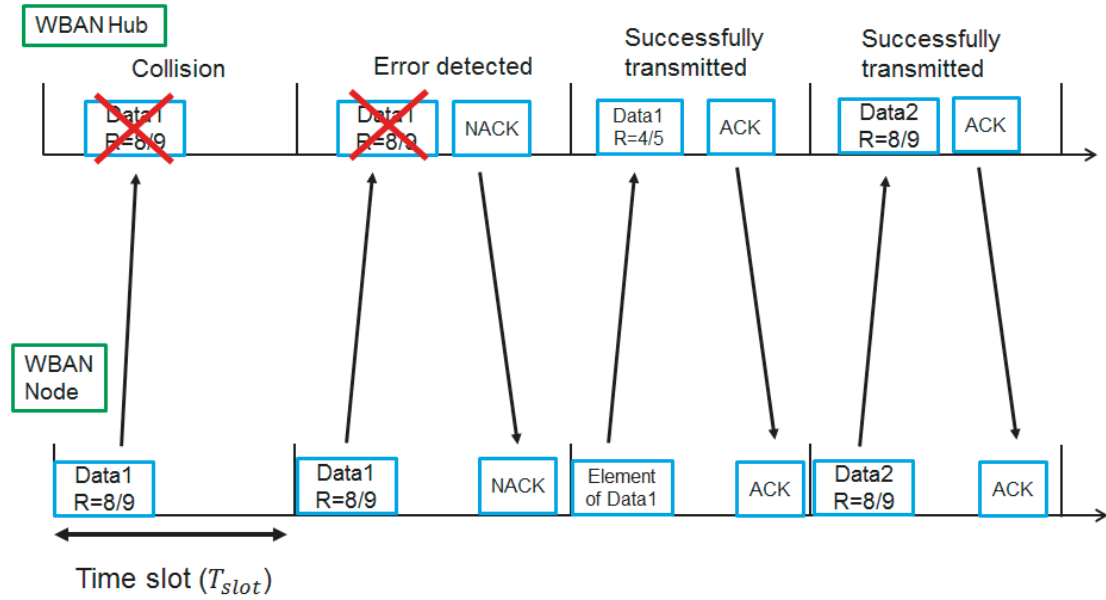
Figure 8.1 Example of behavior of our scheme in a random access protocol.

8.2 Theoretical analysis in cross-layer approach

In this section, we describe a theoretical analysis in a cross-layer approach.

8.2.1 PHY layer

The probability of successful transmission at ith transmission in a PHY layer is defined as follows:

$$P_{succ,i}^{PHY} = 1 - PEP_i \tag{8–1}$$

$$PEP_i = 1 - (1 - BEP_i)^{L_{info}} \tag{8–2}$$

$$BEP_i \leq \frac{1}{k_i} \sum_{d=d_{free}}^{\infty} c_d P_d \tag{8–3}$$

$$P_d = \sum_{t=0}^{d} {}_{d-1-t}C_t \left(1 - P_e\right)^t P_e^d \tag{8–4}$$

$$P_e = \frac{1}{2} e^{-E_s/N_0}. \tag{8–5}$$

In this case, differential binary phase shift keying (DBPSK) modulation is assumed. Then, L_{info} is the length of information bits and E_s/N_0 is the energy per symbol to noise power spectral density. In addition, d_{free} is the free distance of the code, and then c_d is the total number of information bit errors produced by the incorrect paths of the Hamming weight.

8.2.2 MAC layer

Next, the probability of successful transmission at ith transmission in a MAC layer is defined as follows:

$$P_{succ,i}^{MAC} = N_{node}p_y \left(1 - p_y\right)^{N_{node}-1} \tag{8–6}$$

$$p_y = G/N_{node}. \tag{8–7}$$

Here, N_{node} is the number of nodes, p_y is the probability of packet transmission in a slot and G is normalized offered load. Then, the slotted ALOHA best case scenario is considered as well as the reference [36]. Therefore, in the case that $G = 1$, $P_{succ,i}^{MAC}$ can be modified as follows:

$$P_{succ}^{MAC} = \left(1 - \frac{1}{N_{node}}\right)^{N_{node}-1}. \tag{8–8}$$

8.2.3 Cross-layer design

Based on the above, the average number of packet transmission N_{tx} and the probability of successful transmission P_{succ} in the case of a finite transmission are described as examples of a cross-layer design like following equations:

$$N_{tx} = \sum_{i=1}^{q-1} i[\sum_{j=1}^{i} {}_{i-1}C_{j-1}\left(1 - P_{succ}^{MAC}\right)^{i-j}\left(P_{succ}^{MAC}\right)^j P_{succ,j}^{PHY} \prod_{k}^{j-1}\left(1 - P_{succ,k}^{PHY}\right)]$$

$$+q\sum_{j=1}^{q} {}_{q-1}C_{j-1}\left(1 - P_{succ}^{MAC}\right)^{q-j}\left(P_{succ}^{MAC}\right)^{j-1} \prod_{k}^{j-1}\left(1 - P_{succ,k}^{PHY}\right) \tag{8–9}$$

$$P_{succ} = \sum_{i=1}^{q}\sum_{j=1}^{i} {}_{i-1}C_{j-1}\left(1 - P_{succ}^{MAC}\right)^{i-j}\left(P_{succ}^{MAC}\right)^j P_{succ,j}^{PHY} \prod_{k}^{j-1}\left(1 - P_{succ,k}^{PHY}\right) \tag{8–10}$$

Then, average delay time in scheduled access and random access case are expressed as follows:

$$\overline{T_{delay}} = \begin{cases} N_{tx}N_{node}T_{slot} \ (Scheduled \ access) \\ \sum_{i=1}^{\lceil N_{tx} \rceil} \frac{\frac{1}{CP_i}+1}{2}T_{slot} \ (Random \ access). \end{cases} \tag{8–11}$$

Here, T_{slot} is a slot length, CP_i is the contention probability defined in IEEE802.15.6. In this chapter, we assume that user priority is five, hence, $3/8 \leq CP_i \leq 3/16$. Then, T_{slot} is expressed like following equations:

$$T_{slot} = \lceil T_{TOT,q} + pSIFS + T_{ACK} \rceil. \tag{8–12}$$

Here, pSIFS is the duration between the end of duration of data transmission and the beginning of ACK transmission.

8.3 Results

In this section, the proposed scheme and the standard scheme are analyzed. The main parameters are listed in Table 8.1. In this analysis about the standard scheme, data is transmitted using the default mode with ordinary ARQ.

Figures 8.2-8.5 show performances as a function of E_s/N_0 in case that N_{node}=5. Figure 8.2 shows the average number of transmission. In the case of a random access protocol, the performance in a small L_{info} is slightly better because the $P_{succ,i}^{PHY}$ is better and P_{succ}^{MAC} is constant. Then, in the same case, the average number of transmission dose not converge on $N_{tx} = 1$ in high SNR conditions. This is because collision with other packets influences N_{tx}. By the way, our proposed scheme has the better performance than the standard scheme. The reason is that the error correcting capability of our proposed scheme is improved every retransmission in the case of no collision. Because of that, N_{tx} gradually decreases in a scheduled access protocol.

Figure 8.3 shows the probability of unsuccessful transmission (1-P_{succ}). Basically, the same things can be said in the case of the average number of transmission. In a random access protocol case, an error floor region appears, whereas that does not in a scheduled access protocol case because a collision does not occur. Then, our proposed system obtains over 6dB gain than the standard scheme in a scheduled access protocol case.

Table 8.1 Parameters

Parameter	Detail
Channel model	AWGN
Bandwidth	499.2 MHz
Central frequency	3.99 GHz
Modulation	DBPSK
FEC	r_i=8/9 ∼ 1/16, K=3
(Proposal)	convolutional codes
FEC	(63,51)BCH code
Decoding	Soft decision
(Proposal)	Viterbi decoding
Decoding	Berlekamp-Massey
(Standard)	algorithm
ARQ protocol	Weldon's ARQ
Pulse shape	Gaussian monopulse
L_{info}	150, 255 bytes
L_{ACK}	7 bytes
N_{node}	1 ∼ 10
Uncoded data rate, R	7.8 Mbps
T_{slot}	2.0 ms (Proposal)
	1.0 ms (IEEE802.15.6)

Figure 8.4 shows the average delay time. Under low and high SNR conditions, a randam access case has better performance than a scheduled access case about the proposed scheme.   The reason is that in a scheduled access case when a certain node is transmitting data, other nodes do not transmit own data. However, under middle SNR conditions, a scheduled access protocol is better because of no collision and the error correcting capability at the reagion.

Figure 8.5 shows the minimum q while satisfying $P_{succ} \geq 0.9$ in case that L_{info}=255bytes. In this figure, if $P_{succ} < 0.9$, we consider the minimum q as 11 for convenience' sake. Generally, the result of the minimum q is similar to that of N_{tx}. Then, in a random access protocol case, it can be said that q over five and E_s/N_0 over 6dB are required in order to satisfy the condition about our proposed system.

Figures 8.6-8.8 show performances as a function of N_{node} in case that E_s/N_0=6dB. From Fig.8.6-8.7, peformances of N_{tx} and P_{succ} in case of a scheduled access protocol is better than a random access protocol because of no collision.   Then, as N_{node} increases more, those performances become worse in a random access protocol case. On the other hand, in Fig.8.8 whicn shows the average delay time,
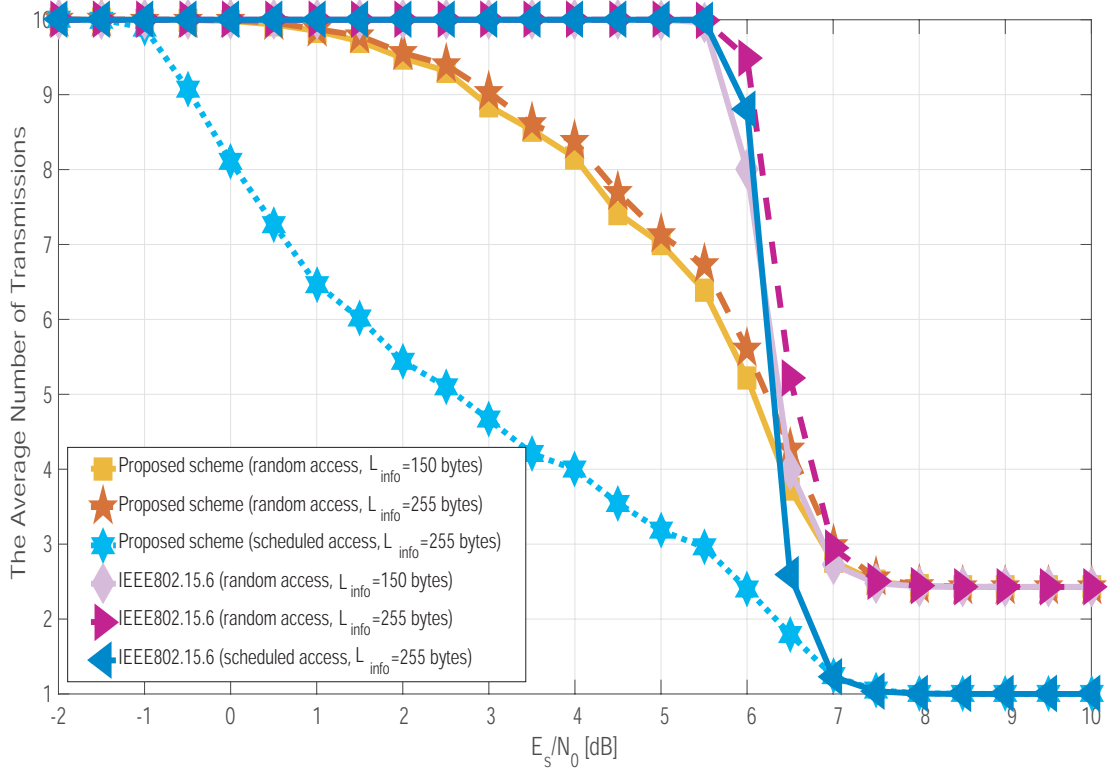
Figure 8.2 The average number of transmission (N_{node}=5, q=10).

it can be said that under small N_{node} conditions a scheduled access protocol has smaller delay time, whereas delay time of a random access protocol is smaller under large N_{node} conditions. This is because the number of time slot assigned to each node becomes small under large N_{node} conditions. Hence, each latency becomes longer under the condition.
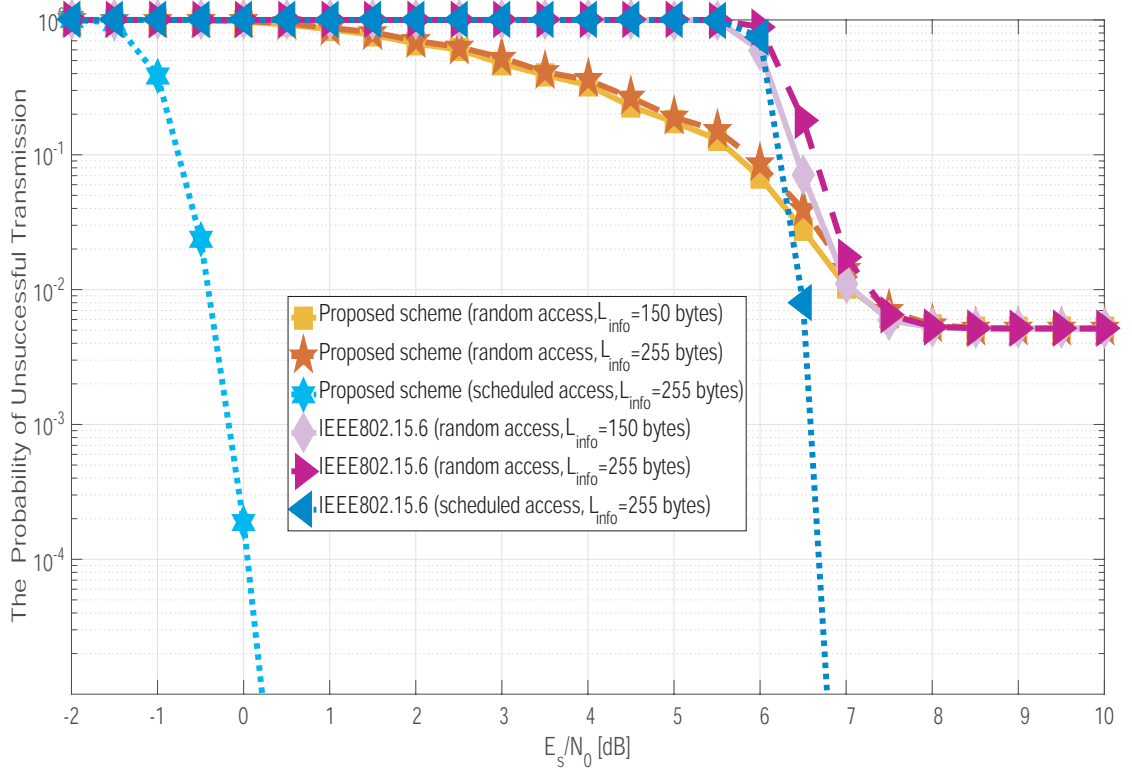
Figure 8.3 The probability of unsuccessful transmission ($1-P_{succ}$, $N_{node}=5$, $q=10$).
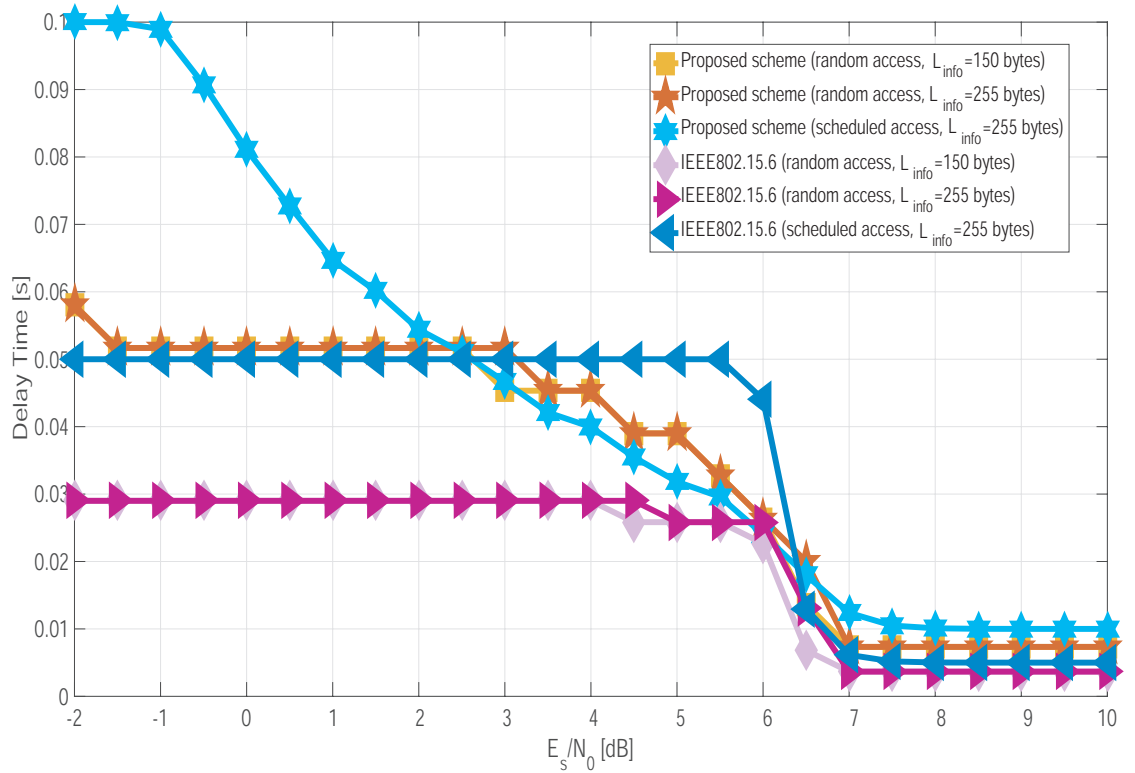
Figure 8.4 The average delay time (N_{node}=5, q=10).
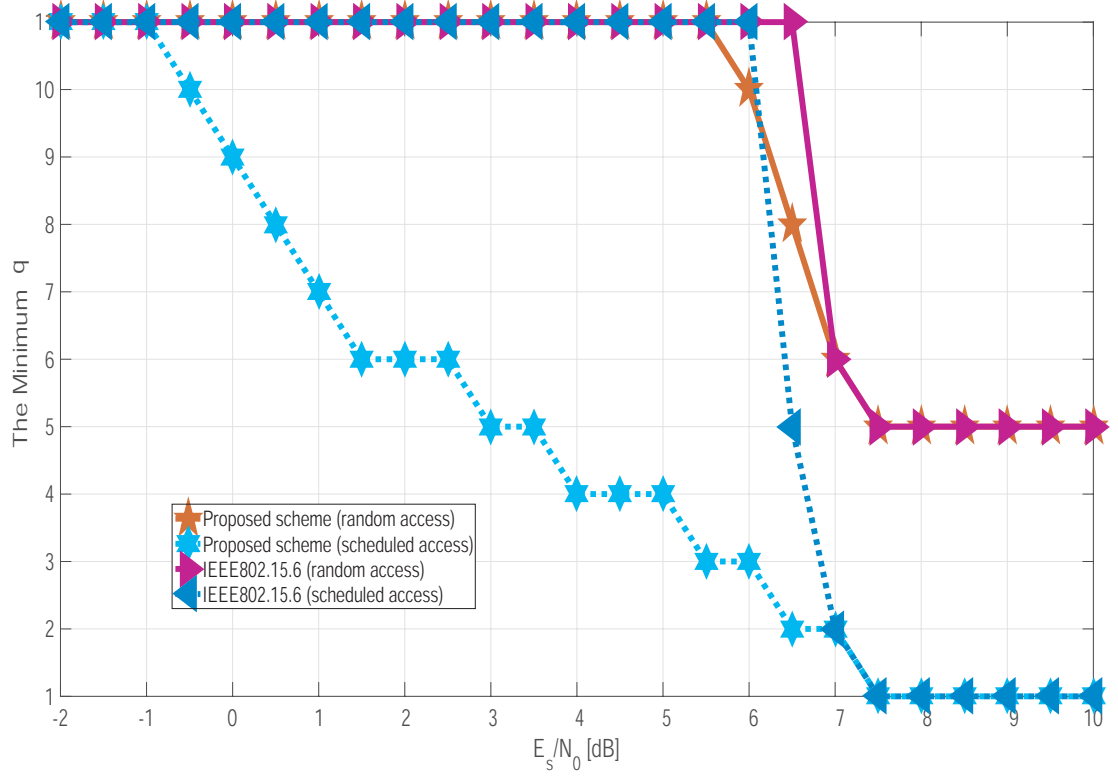
Figure 8.5 The minimum q while satisfying $P_{succ} \geq 0.9$ (L_{info}=255bytes).

Figure 8.6   The average number of transmission (E_s/N_0=6dB, q=10).

Figure 8.7 The probability of successful transmission (E_s/N_0=6dB, q=10).

Figure 8.8   The average delay time (E_s/N_0=6dB, q=10).

Chapter 9

Conclusion

In this thesis, we proposed an optimal QoS control scheme employing a multiplexing layer for priority scheduling and a decomposable error control coding scheme that can adapt to varying channel conditions. The multiplexing module co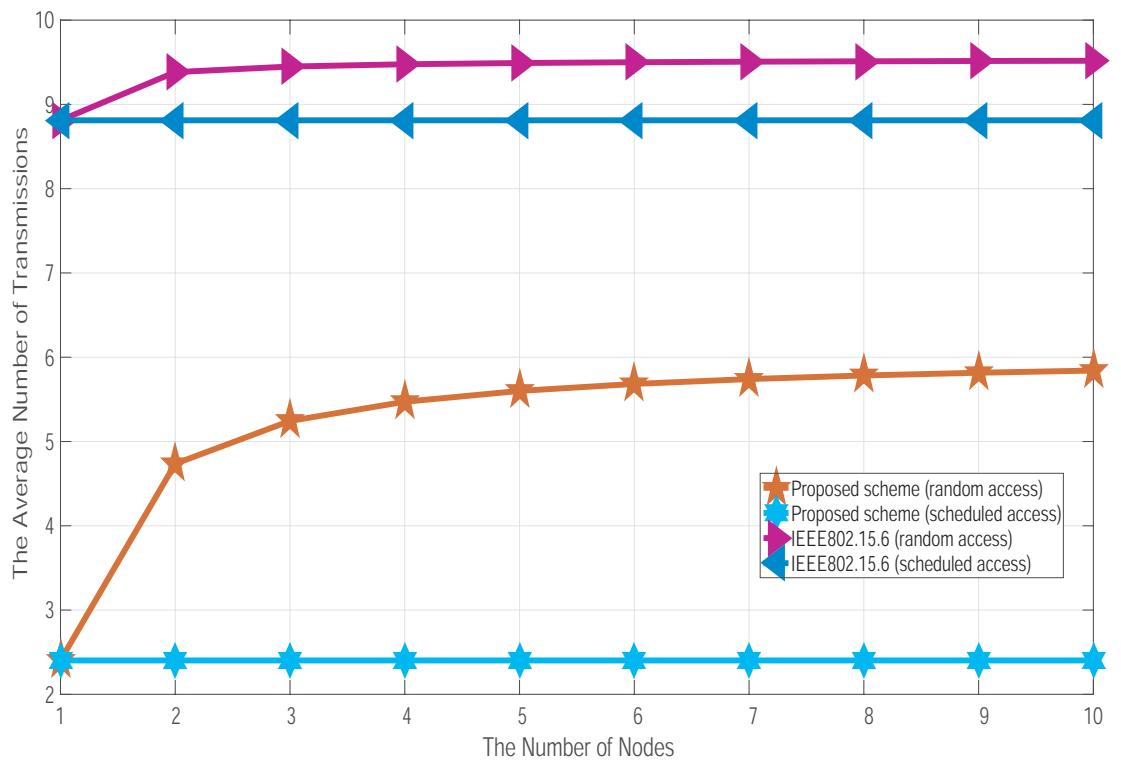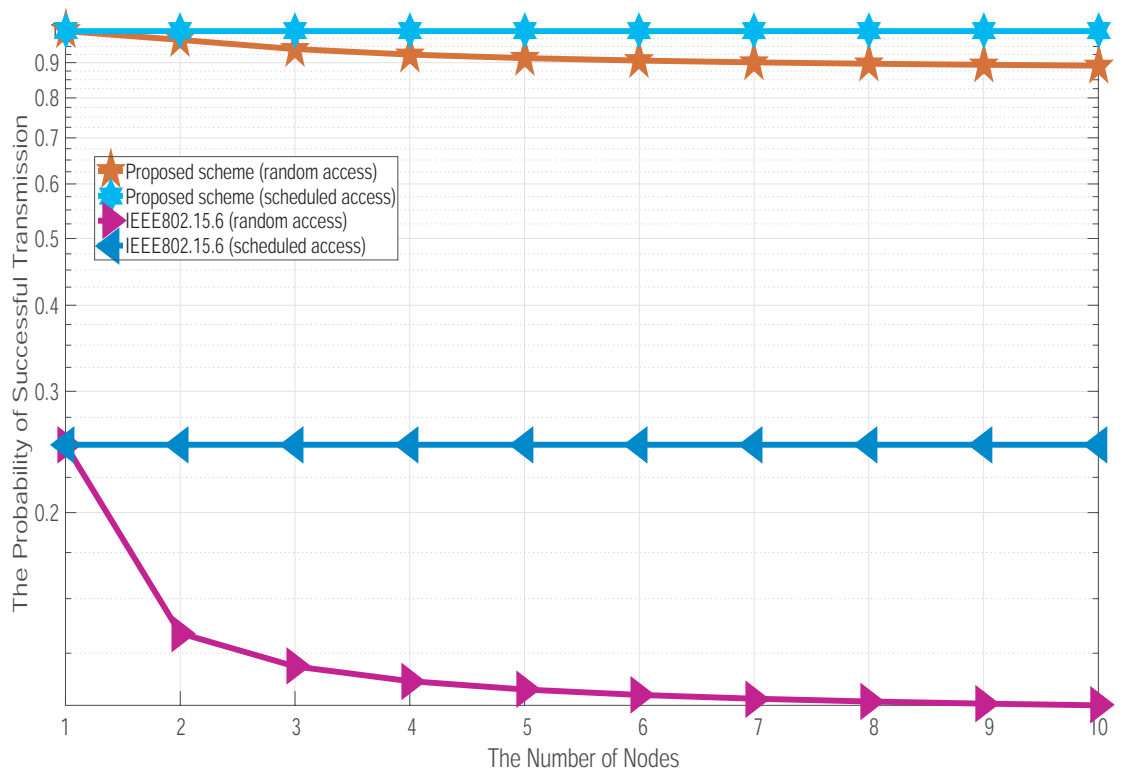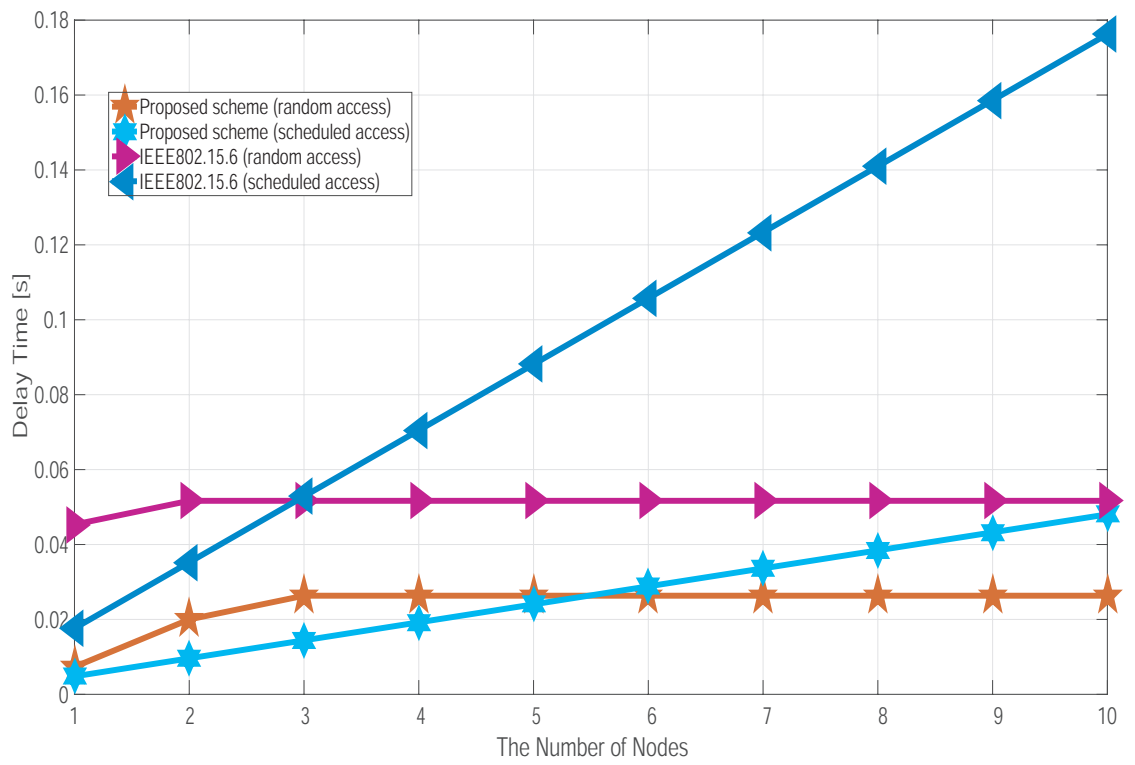ntroled the different types of QoS requirements such as required error ratio and delay according to the following priorities by changing the number of data copies of Weldon's ARQ and combination of decomposable codes.

In Chapter 4 and 5, we presented a theoretical analysis of our proposed scheme to evaluate it under the AWGN channel and the Rayleigh fading channel. We investigated QoS parameters to further optimize our system, showing that our proposed system can achieve optimal performance by arbitrarily selecting parameters of the error-correcting code and Hybrid ARQ. Performance evaluations by theoretical analysis and simulations showed that our proposed scheme has greater flexibility for optimizing QoS parameters according to the required QoS for each input data. Moreover, our evaluations showed that the performance of our proposed scheme is better than that of the conventional scheme.

In Chapter 6, we showed an extended decomposable code and an energy efficiency model. Then, we evaluated our scheme in a multiple WBANs environment as a practical situation. Computer simulations were conducted to evaluate the proposed scheme against performance measures such as RBER and energy efficiency and to compare the results with those from an error control scheme defined in IEEE 802.15.6, using both DBPSK and DQPSK modulation. The results demonstrated that the proposed scheme was able to satisfy the required QoS for each data type, and that the QoS control was more flexible than that of the standard in both the general and worst-case scenarios. The proposed scheme had poorer energy efficiency than IEEE 802.15.6 under high SNR conditions in the general case scenario. However, the IEEE 802.15.6 solution was unable to achieve the required performance under the worst-case scenario. It

can be concluded that the proposed error control coding scheme enables QoS control while maintaining high, or satisfactory, energy efficiency under the different scenarios.

Next chapter presented performance evaluations of an QoS control scheme in the case of a two-hop extension based on IEEE802.15.6. Specifically, PER, the number of transmissions and energy efficiency of our proposed error control system and IEEE Std. 802.15.6 were evaluated in that case. Numeral results showed our proposed scheme had better performances than the standard scheme at many points. Additionally, it was found from those results that both systems had the best performance in case that communication distance on the first hop is equal to that on the second hop.

In Chapter 8, a theoretical analysis of our proposed error control scheme in a cross-layer approach between PHY and MAC layers was presented. Numerical results showed our proposed scheme has better performances than the standard scheme. Then, the case utilizing a schedule access protocol had basically better performances than a random access protocol except delay performance.

As the future work, we are going to consider other error control schemes, for instance error controlling based on turbo coding. This is because the current scheme requires very low coding rate or the large number of retransmissions in a poor SNR condition; therefore large latency and energy consumption are needed. However, in case of turbo codes, it seems that larger error correcting capability is obtained with higher coding rate by adjusting the number of iteration of decoding at a receiver. Hence, it is possible to reduce the number of retransmissions and latency. Then, a dependable MAC protocol for WBANs will also be considered because basic MAC protocols were considered in current work and it was not optimized for WBANs use. In addition, performance of a target WBAN was focused on in this thesis, because the proposed scheme is closed within a WBAN. However, a target WBAN actually interferes with other WBANs in a multiple-WBANs environment. Therefore, we should also consider effective space-time interference countermeasure.

In addition, we are going to consider other application as future directions, for example controlling capsule endoscopy with feedback loop. In the research field, there are many issues, such as optimal error controlling for control signal, effective image coding scheme for a medical image transmitted from capsule endoscope, derivation of channel capacity with feedback which is one of the most difficult problems and so on.

Published Papers

Reviewed Journal Papers

(1) **Kento Takabayashi**, Heikki Karvonen, Tuomas Paso, Hirokazu Tanaka, Chika Sugimoto, Ryuji Kohno, "Performance Evaluation of a QoS-aware Error Control Scheme for Multiple-WBAN Environment," IEEJ Transactions on Electrical and Electronic Engineering, TEEE C, Vol.12, No.S1, pp.-, (2017-6) **Accepted**

(2) **Kento Takabayashi**, Hirokazu Tanaka, Chika Sugimoto, Ryuji Kohno, "Performance Analysis of Multiplexing and Error Control Scheme for Body Area Networks," EURASIP Journal on Wireless Communications and Networking, 2016:70, pp.1-16, DOI: 10.1186/s13638-016-0561-0, (2016-3)

(3) **Kento Takabayashi**, Hirokazu Tanaka, Chika Sugimoto, Ryuji Kohno, "Multiplexing and Error Control Scheme for Body Area Network employing IEEE 802.15.6" IEICE TRANSACTIONS on Communications Vol.E97-B, No.03, pp.564-570, (2014-3)

(4) In addition, two papers are to be submitted.

Reviewed International Conference Papers

(1) **Kento Takabayashi**, Hirokazu Tanaka, Chika Sugimoto, Ryuji Kohno, "Performance Analysis of Cross-layer Approach About Error Control Scheme for WBANs," The 11th International Symposium on Medical Information and Communication Technology (ISMICT 2017), Lisbon, Portugal (2017-2)

(2) Do Thanh Quan, Pham Thanh Hiep, Takumi Kobayashi, **Kento Takabayashi**, Ryuji Kohno, "Proposal Methods for Performance Analysis of WBANs Based on CSMA/CA," The 11th International Symposium on Medical Information and Communication Technology (ISMICT 2017), Lisbon, Portugal (2017-2)

(3) Satoshi Seimiya, **Kento Takabayashi**, Ryuji Kohno, "A Study for the Adaptive Error Correction Using QoS-HARQ Toward Dependable Implant Body Area Network," The 11th International Symposium on Medical Information and Communication Technology (ISMICT 2017), Lisbon, Portugal (2017-2)

(4) **Kento Takabayashi**, Hirokazu Tanaka, Chika Sugimoto, Ryuji Kohno, "Performance Evaluation of Error Control Scheme in Multihop WBAN Based on IEEE802.15.6," The International Symposium on Information Theory and Its Applications 2016 (ISITA 2016), Monterey, California, US, pp.370-374 (2016-10)

(5) Takahiro Goto, **Kento Takabayashi**, Ryuji Kohno, "An Adaptive Error Control Scheme Considering Various Channel Conditions and QoS in Medical and Non- Medical Data for WBAN," 10th International Symposium on Medical Information and Communication Technology (ISMICT 2016), Boston, MA, US, pp.1-3 (2016-3)

(6) **Kento Takabayashi**, Heikki Karvonen, Tuomas Paso, Hirokazu Tanaka, Chika Sugimoto, Ryuji Kohno, "Energy Efficiency Evaluation of ECC Scheme Utilizing Decomposable Codes in IEEE Std 802.15.6 Based WBANs," 10th International Conference on Body Area Networks (BodyNets 2015), Sydney, Australia, pp.110-115 (2015-9)

(7) **Kento Takabayashi**, Hirokazu Tanaka, Chika Sugimoto, Ryuji Kohno, "Error Control Scheme Using Decomposable Codes for Various QoS in Multiple WBAN Environment," 9th International Symposium on Medical Information and Communication Technology (ISMICT 2015), Kamakura, Japan, pp.83-87 (2015-3)

(8) **Kento Takabayashi**, Hirokazu Tanaka, Chika Sugimoto, Ryuji Kohno, "Effective Error Control Scheme with Channel State Information for WBAN," 8th International Symposium on Medical Information and Communication Technology (ISMICT 2014), Florence, Italy, pp.1-5 (2014-4)

(9) **Kento Takabayashi**, Hirokazu Tanaka, Chika Sugimoto, Ryuji Kohno, "Multiplexing and Error Control Scheme with Modified Hybrid ARQ for Body Area Network employing IEEE 802.15.6 in UWB-PHY," The Second

Ultra Wideband for Body Area Networking Workshop (UWBAN-2013), Boston, MA, US, pp.581-587 (2013-10)

(10) **Kento Takabayashi**, Hirokazu Tanaka, Chika Sugimoto, Ryuji Kohno, "An Error Control Scheme with Weldon's ARQ Considering Various QoS in Medical and Non-medical Uses for Wireless BANs," 2013 7th International Symposium on Medical Information and Communication Technology (IS-MICT), Tokyo, Japan, pp.47-51 (2013-3)

Domestic Conference Papers (all in Japanese)

(1) 高林健人、田中宏和、杉本千佳、河野隆二、"標準規格に基づいたマルチホップ WBAN における通信距離に関する性能評価、"第 39 回情報理論とその応用シンポジウム (SITA 2016)、岐阜、pp.152-156 (2016-12)

(2) 清宮聡史、高林健人、河野隆二、"センシング・制御情報の重要度を考慮したカプセル内視鏡カメラの高信頼無線フィードバック制御、"ヘルスケア・医療情報通信技術研究会 (MICT)、東京、116(25)、pp. 23-28 (2016-5)

(3) 高林健人、杉本千佳、河野隆二、"WBAN における緊急情報のためのクロスレイヤ誤り制御方式、"第 38 回情報理論とその応用シンポジウム (SITA 2015)、岡山、pp.197-202 (2015-11)

(4) 後藤高宏、高林健人、河野隆二、"WBAN における異なる誤り原因を考慮した誤り制御のための連接符号、"ヘルスケア・医療情報通信技術研究会 (MICT)、奈良、115(151)、pp. 61-64 (2015-7)

(5) 高林健人、田中宏和、杉本千佳、河野隆二、"複数 WBAN 環境における様々な QoS を考慮した誤り制御法についての一検討、"第 37 回情報理論とその応用シンポジウム (SITA 2014)、富山、pp.595-600 (2014-12)

(6) 高林健人、田中宏和、杉本千佳、河野隆二、"緊急性のある医療用データのためのチャネル情報を用いた誤り制御方式、"ヘルスケア・医療情報通信技術研究会 (MICT)、東京、114(61)、pp.87-92 (2014-5)

(7) 高林健人、田中宏和、杉本千佳、河野隆二、"WBANs のための QoS を考慮した誤り制御方式、"第 35 回情報理論とその応用シンポジウム (SITA 2012)、大分、pp.275-278 (2012-12)

(8) 高林健人、杉本千佳、河野隆二、"無線 BAN のための Decomposable Codes を用いた Hybrid ARQ 方式、"無線通信システム研究会 (RCS)、高知、112(192)、pp.133-138 (2012-08)

IEICE Annual Conference Letters (all in Japanese)

(1) 高林健人、田中宏和、杉本千佳、河野隆二、"IEEE802.15.6 に基づいたマルチホップ WBAN におけるチャネル情報を利用した誤り制御方式の性能評価、"電子情報通信学会ソサイエティ大会、札幌、A-15-1、pp.167 (2016-9)

(2) 清宮聡史、高林健人、河野隆二、"インプラント BAN での無線フィードバックによる誤り制御に向けた一検討、"電子情報通信学会ソサイエティ大会、札幌、B-20-10、pp.439 (2016-9)

(3) 高林健人、田中宏和、杉本千佳、河野隆二、"複数 WBAN 環境における緊急情報のための誤り制御方式に関する一検討、"電子情報通信学会ソサイエティ大会、仙台、B-8-7、pp.117 (2015-9)

(4) 高林健人、田中宏和、杉本千佳、河野隆二、"無線 BAN のための異なる QoS を考慮した多重化・誤り制御方式に関する一検討、"電子情報通信学会ソサイエティ大会、福岡工業大学、BS-9-2、pp.S141-S142 (2013-09)

(5) 高林健人、田中宏和、島圭介、杉本千佳、河野隆二、"無線 BAN のための QoS を考慮した誤り制御方式に関する一検討、"電子情報通信学会総合大会、岐阜大学、BS-8-4、pp.S7-S8 (2013-03)

(6) 高林健人、杉本千佳、河野隆二、"WBANs のための Decomposable Codes を用いた Hybrid-ARQ 方式、"電子情報通信学会ソサイエティ大会、富山大学、A-6-9、pp.108 (2012-09)

Bibliography

[1] Chen, M., Gonzalez, S., Vasilakos, A., Cao, H., Leung, V. C. M., "Body Area Networks: A Survey. Mobile Networks and Applications," Springer 16(2), pp.171-193 (2010)

[2] Acampora, G., Cook, D.J. Rashidi, P. Vasilakos, A.V., "A Survey on Ambient Intelligence in Healthcare," Proceedings of the IEEE 101(12), pp.2470-2494 (2013)

[3] Hayajneh, T., Almashaqbeh, G., Ullah, S., Vasilakos, A.V., "A survey of wireless technologies coexistence in WBAN: analysis and open research issues," Wireless Networks, Springer 20(8), pp.2165-2199 (2014)

[4] Fortino, G., Fatta, G. D., Pathan, M., Vasilakos, A.V., "Cloud-assisted body area networks: state-of-the-art and future challenges," Wireless Networks, Springer 20(7), pp.1925-1938 (2014)

[5] Zhou, J., Cao. Z, Dong, X., Lin, X., Vasilakos, A.V., "Securing m-healthcare social networks: challenges, countermeasures and future directions," Wireless Communications, IEEE 20(4), pp.12-21 (2013)

[6] Zhou, J., Cao, Z., Dong, X., Xiong, N., Vasilakos, A.V., "4S: A secure and privacy-preserving key management scheme for cloud-assisted wireless body area network in m-healthcare social networks," Information Sciences, Elsevier 314(2015), pp.255-276 (2014)

[7] He, D., Chen, C., Chan, S., Bu, J., Vasilakos, A.V., "ReTrust: Attack-Resistant and Lightweight Trust Management for Medical Sensor Networks," Transactions on Information Technology in Biomedicine, IEEE 16(4), pp.623-632 (2012)

[8] Zhang, Z., Wang, H., Vasilakos, A.V., Fang H., "ECG-Cryptography and Authentication in Body Area Networks," Transactions on Information Technology in Biomedicine, IEEE 16(6), pp.1070-1078 (2012)

[9] Lin, D., Labeau, F., Vasilakos, A.V., "QoE-based optimal resource allocation in wireless healthcare networks: opportunities and challenges," Wireless Networks, Springer 21(8), pp.2483-2500 (2015)

[10] Cao, H., Leung, V,. Chow, C., Chan, H., "Enabling technologies for wireless body area networks: A survey and outlook," Communications Magazine, IEEE 47(12), pp.84-93 (2009)

[11] Viswanathan, H., Chen, B., Pompili, D., "Research challenges in computation, communication, and context awareness for ubiquitous healthcare," Communications Magazine, IEEE 50(5), pp.92-99 (2012)

[12] Bachmann, C., Ashouei, M., Pop, V., Vidojkovic, M., Groot, H.D., Gyselinckx, B., "Low-power wireless sensor nodes for ubiquitous long-term biomedical signal monitoring," Communications Magazine, IEEE, 50(1), pp.20-27 (2012)

[13] Caldeira, J.M.L.P., Rodrigues, J.J.P.C., Lorenz, P., "Toward ubiquitous mobility solutions for body sensor networks on healthcare," Communications Magazine, IEEE, 50(5), pp.108-115 (2012)

[14] Boulis, A., Smith, D., Miniutti, D., Libman, L., Tselishchev, Y., "Challenges in body area networks for healthcare: the MAC," Communications Magazine, IEEE, 50(5), pp.100-106 (2012)

[15] Wong, A., Dawkins, M., Devita, G., Kasparidis, N., Katsiamis, A., King, O., Lauria, F., Schiff, J., Burdett, A., "A 1V 5mA multimode IEEE 802.15.6/bluetooth low-energy WBAN transceiver for biotelemetry applications," Proceedings of Solid-State Circuits Conference Digest of Technical Papers (ISSCC), 2012 IEEE International, pp.300-302, (2012)

[16] Suzuki, T., Tanaka, H., Minami, S., Yamada, H., Miyata, T., "Wearable Wireless Vital Monitoring Technology for Smart Health Care," Proceedings of 7th International Symposium on Medical Information and Communication Technology (ISMICT), pp.1-4, Tokyo, Japan (2013)

[17] Riccardo Cavallari, Flavia Martelli, Ramona Rosini, Chiara Buratti, and Roberto Verdone, "A Survey on Wireless Body Area Networks: Technologies and Design Challenges," IEEE Communications Surveys & Tutorials, IEEE, 16(3), pp.1635-1657, (2014)

[18] Samaneh Movassaghi, Mehran Abolhasan, Justin Lipman, David Smith, and Abbas Jamalipour, ″Wireless Body Area Networks: A Survey,″ IEEE Communications Surveys & Tutorials, IEEE, 16(3), pp.1658-1686, (2014)

[19] Maulin Patel, Jianfeng Wang, ″Applications, challenges, and prospective in emerging body area networking technologies,″ IEEE Wireless Communications, IEEE, 17(1), pp.80-88, (2010)

[20] Muhammad Mahtab Alam, Elyes Ben Hamida, ″Surveying Wearable Human Assistive Technology for Life and Safety Critical Applications: Standards, Challenges and Opportunities,″ Sensors, MDPI, 14(5), pp.9153-9209, doi:10.3390/s140509153, (2014)

[21] 李 還幇, ″医療ヘルスケアのためのボディエリアネットワーク - 標準規格の策定と開発事例 -,″ 特技懇, No. 271, pp.53-60,(2013)

[22] IEEE Standard for Information technology - Telecommunications and information exchange between systems - Local and metropolitan area networks-Specific requirements: Part 15.6, ″Wireless Medium Access Control (MAC) and Physical Layer (PHY) Specifications for Wireless Personal Area Networks (WPANs) used in or 12 around a body,″ IEEE (2012)

[23] IEEE Standard for Local and metropolitan area networks Part 15.4, ″Low-Rate Wireless Personal Area Networks (LR-WPANs), Amendment: Alternative Physical Layer Extension to support Medical Body Area Networks (MBANS) services operating in the 2360-2400 MHz band,″ IEEE (2011)

[24] ETSI TC Smart BAN, ″Smart Body Area Network (SmartBAN); Low Complexity Medium Access Control (MAC) for SmartBAN″, TS 103 325 V1.1.1 (2015)

[25] Shu Lin, Daniel, J. Costello, Jr., ″Error Control Coding: Fundamentals and Applications,″ Perntice-Hall, (1983)

[26] M.W. El Bahri, H. Boujernaa, M. Siala, ″Performance comparison of type I, II and III hybrid ARQ schemes over AWGN channels,″ Proceedings of IEEE International Conference on Industrial Technology 2004 (IEEE ICIT '04, 2004), pp.1417-1421 Vol.3, (2004)

[27] Antonio Maria Cipriano, Paul Gagneur, Guillaume Vivier, Serdar Sezginer, "Overview of ARQ and HARQ in Beyond 3G Systems," 2010 IEEE 21st International Symposium on Personal, Indoor and Mobile Radio Communications Workshops, pp.424-429 , Istanbul, Turkey (2010)

[28] TSG-RAN Working Group 1 Meeting No.18, "Proposal of bit mapping for type-III HARQ," Boston, USA (2001)

[29] Obinata, Y., Yamasue, K., Pham, T. H., Nemoto, A., Sugimoto, C. and Kohno, R., "Application of High-band UWB Body Area Network to Medical Vital Sensing in Hospital," Proceedings of The Second Ultra Wideband for Body Area Networking Workshop (UWBAN-2013), pp.594-599, Boston, MA, US (2013)

[30] Weldon, E., Jr., "An Improved Selective-Repeat ARQ Strategy," IEEE Transactions on Communications, IEEE 30(3), pp.480-486 (1982)

[31] Viterbi, A.J., "Convolutional Codes and Their Performance in Communication Systems" IEEE Transactions on Communication Technology, IEEE 19(5), pp.751-772 (1971)

[32] Haccoun, D., Begin, G., "High-Rate Punctured Convolutional Codes for Viterbi and Sequential Decoding," IEEE Transactions on Communications, IEEE 37(11), pp.1113-1125 (1989)

[33] Franger, P., Orten, P., Ottosson, T., "Convolutional codes with optimum distance spectrum," IEEE Commun. Lett., IEEE 3(11), pp.317-319 (1999)

[34] Yazdandoost , K. Y., Sayrafian-Pour, K., "Channel Model for Body Area Network (BAN)" IEEE P802.15Working Group for Wireless Personal Area Networks (WPANs), IEEE P802.15-08-0780-10-0006.14 (2009)

[35] D.G. Daut, J.W. Modestino, L. Wismer, "New short constraint length convolutional code constructions for selected rational rates," IEEE Transactions on Information Theory, IEEE, 28(5), pp.794-800 (1982)

[36] H. Karvonen, J. Iinatti, M. Hämäläinen, "A cross-layer energy efficiency optimization model for WBAN using IR-UWB transceivers," Springer Telecommunication Systems, Springer, 58(2), pp.165-177 (2015)

[37] N. Abughalieh, K. Steenhaut, A. Nowé, and A. Anpalagan, "Turbo codes for multi-hop wireless sensor networks with decode-and-forward mechanism" Eurasip J. Wireless Communications and Networking, Springer, 204(1) (2014)

[38] P11073-00101/D02J. Health informatics - Point-of-care medical device communication - Technical report - Guidelines for the use of RF wireless technology, IEEE (2007)

[39] J. Ryckaert, C. Desset, A. Fort, M. Badaroglu et al, "Ultra-Wide-Band Transmitter for Low-Power Wireless Body Area Networks: Design and Evaluation" IEEE Trans. Circuits Syst. I, Reg. Papers, IEEE, 52(12), pp.2515-2525 (2005)

[40] Z. Zou, D. Sarmiento Mendoza, P. Wang, Q. Zhou et al, "A Low-Power and Flexible Energy Detection IR-UWB Receiver for RFID and Wireless Sensor Networks," IEEE Trans. Circuits Syst. I, Reg. Papers, IEEE, 58(7), pp.1470-1482 (2011)

[41] Benoit Latre, Bart Braem, Ingrid Moerman, Chris Blondia, Elisabeth Reusens, Wout Joseph, Piet Demeester, "A Low-delay Protocol for Multihop Wireless Body Area Networks," Proceedings of 4th Annual International Conference on Mobile and Ubiquitous Systems: Networking & Services 2007 (MobiQuitous 2007), Philadelphia, PA, USA, pp.1-8 (2007)

[42] Shariar Imtiaz, Md. Mosaddek Khan, Md. Mamun-or-Rashid, Md. Mustafizur Rahman, "Improved Adaptive Routing for Multihop IEEE 802.15.6 Wireless Body Area Networks," International Journal of Intelligent Systems & Applications, MECS Publisher, 5(12), pp.64-71 (2013)

[43] Vinay Verma, Savita Shiwani, "A Novel approach for Optimizing Cross Layer among Physical Layer and MAC Layer of Infrastructure Based Wireless Network using Genetic Algorithm," International Journal of Advanced Research in Computer Engineering & Technology, Index Copernicus International, 2(7), pp.2292-2296 (2013)

[44] Ian F. Akyildiz, Mehmet C. Vuran, Ozur B. Akan, "A Cross-Layer Protocol for Wireless Sensor Networks," Proceedings of 2006 40th Annual Conference on Information Sciences and Systems, Princeton, New Jersey, USA, pp.1102-1107 (2006)

[45] Qian Gao, Gang Zhu, Siyu Lin, Shichao Li, Lei Xiong, Weiliang Xie, Xiaoyu Qiao, "Robust QoS-Aware Cross-layer Design of Adaptive Modulation Transmission on OFDM Systems in High-Speed Railway," IEEE Access, IEEE, 4, pp.7289-7300 (2016)

[46] Nikola Zogovic, Goran Dimic, Dragana Bajic, "PHY-MAC Cross-Layer Approach to Energy-Efficiency and Packet-Loss Trade-off in Low-Power, Low-Rate Wireless Communications," IEEE Communications Letters, IEEE, 17(4), pp.661-664 (2013)

[47] Taniya Shafique, Muhammad Zia, Huy-Dung Han, Hasan Mahmood, "Cross-Layer Chase Combining With Selective Retransmission, Analysis, and Throughput Optimization for OFDM Systems," IEEE Transactions on Communications, IEEE, 64(6), pp.2311-2325 (2016)